NOVA SCHOOL OF SCIENCE & TECHNOLOGY

DEPARTMENT OF PHYSICS

MAFALDA HELENA DE ALBUQUERQUE MARTINS PEREIRA PIRES

Bachelor of Science in Biomedical Engineering

CHANGES IN HEART RATE DYNAMICS WITH AGE AND DISEASE: TRADITIONAL *VERSUS* NEWER ANALYSES

MASTER IN BIOMEDICAL ENGINEERING

NOVA University Lisbon
February, 2022

NOVA SCHOOL OF
SCIENCE & TECHNOLOGY

DEPARTMENT OF
PHYSICS

CHANGES IN HEART RATE DYNAMICS WITH AGE AND DISEASE: TRADITIONAL *VERSUS* NEWER ANALYSES

MAFALDA HELENA DE ALBUQUERQUE MARTINS PEREIRA PIRES

Bachelor of Science in Biomedical Engineering

Advisers: Carla Maria Quintão Pereira
Assistant Professor, NOVA University Lisbon
Madalena Damásio Costa
Assistant Professor, Beth Israel Deaconess Medical Center

MASTER IN BIOMEDICAL ENGINEERING

NOVA University Lisbon
February, 2022

Changes in Heart Rate Dynamics with Age and Disease: Traditional *versus* Newer Analyses

This document was created with the (pdf)LaTeX processor, based on the NOVAthesis template (v6.7.0), developed at the Dep. Informática of FCT-NOVA by João M. Lourenço.

I dedicate this dissertation to my parents,
grandparents, brother, and Manuel.

Acknowledgements

The past ten months have been packed full of learning experiences. It would have been impossible to complete this dissertation without the careful and patient guidance of my advisers. Thus, I would like to express my deepest and most sincere gratitude to Professor Carla Quintão and Professor Madalena Costa, who have dedicated many hours to guide me and ensure that I was on the right track.

I would like to further thank Professors Cláudia Quaresma, Ricardo Vigário and Ary Goldberger who were always available to discuss my work and provide key suggestions to improve it.

In addition, I would like to thank my mother who taught me to be persistent and to determinedly follow my objectives, and my father who always motivated me to be curious, inciting me to contemplate and reflect. I deeply thank my brother for encouraging me to be confident and for always having relevant advice to give.

I would also like to thank my friends and extended family for the support they have provided me during the writing of this dissertation.

I want to especially thank Manuel, who has always looked after me.

Abstract

One of the greatest achievements of humanity was the tremendous increase in lifespan. However, this increase has not been followed by a similar increase in healthspan. To expand healthspan, new biomarkers of aging and disease are being developed to improve the knowledge regarding the aging process and the emergence of diseases.

A highly accessible source of non-invasive biomarkers is the dynamics of heart rate. The analysis of this dynamics provides indirect access to the state of the autonomic nervous system, the integrity of the heart's main pacemaker – the sinoatrial node –, and the interactions between the two. The Heart Rate Variability (HRV) temporal and frequency approaches correspond to the traditional and most widely used methods to measure heart rate dynamics. However, they have failed to permeate clinical practice due to inconsistent results among high-risk groups, such as in the elderly and in patients with cardiovascular diseases. Phase-Rectified Signal Averaging (PRSA) and Heart Rate Fragmentation (HRF) are two newer approaches developed to address some of the major problems that are associated with the HRV approach.

In this dissertation, we investigate the changes in heart rate dynamics with age, with the severity of atrial fibrillation (AF), and with prevalent congestive heart failure (CHF), using HRV, PRSA, and HRF indices. We also provide an in-depth revision on the physiological mechanisms linking changes in these dynamical indices and the referred contexts.

We found HRF indices to be more associated with the aging process and AF severity than PRSA and HRV indices. Whereas, PRSA and HRV indices were slightly more associated with CHF. Nonetheless, when HRF indices were added to PRSA and HRV linear regression models of CHF, the performance of the resulting models improved.

We also provide an estimate of the minimum electrocardiogram duration for computation of HRF indices, which we found to be 2 to 10 minutes.

Keywords: heart rate variability, heart rate fragmentation, phase-rectified signal averaging, autonomic nervous system, sinoatrial node

Resumo

Uma das maiores conquistas da humanidade foi o tremendo aumento da esperança média de vida (*lifespan*), contudo a esperança média de vida saudável (*healthspan*) não acompanhou este aumento. Para aumentar o *healthspan* têm sido desenvolvidos biomarcadores que visam alargar o conhecimento dos processos de envelhecimento e de aparecimento de doenças. Uma fonte de biomarcadores não-invasivos é a dinâmica da frequência cardíaca. A análise desta dinâmica permite aceder ao estado do sistema nervoso autónomo, à integridade do pacemaker principal do coração – o nó sinusal –, e à interação entre ambos. A abordagem tradicional e mais amplamente utilizada para medir a dinâmica da frequência cardíaca corresponde às medidas temporais e de frequência da Variabilidade da Frequência Cardíaca (VFC). No entanto, estas falharam na obtenção de translação clínica devido aos seus resultados inconsistentes em grupos de alto risco, como idosos e doentes cardiovasculares. Novas abordagens como a Média do Sinal com Retificação de Fase (MSRF) e a Fragmentação da Frequência Cardíaca (FFC) pretendem resolver alguns dos problemas associados ao uso de VFC.

Nesta dissertação, é apresentado um estudo das alterações da dinâmica da frequência cardíaca com a idade, a severidade da fibrilação auricular (FA) e a insuficiência cardíaca (IC), através dos índices de VFC, MSRF e FFC. Paralelamente, é apresentada uma revisão detalhada dos mecanismos fisiológicos subjacentes às alterações dos índices dinâmicos nos contextos referidos.

A partir dos resultados obtidos, concluiu-se que os índices FFC estão mais associados ao processo de envelhecimento e à severidade da FA do que os índices VFC e MSRF. Contudo, os índices VFC e MSRF mostraram-se mais associados à presença de IC. Ainda assim, a adição de índices FFC melhorou o desempenho de modelos de regressão linear de IC que recorrem a índices VFC e MSRF. Foi também obtida uma estimativa da duração mínima necessária de sinais eletrocardiográficos para o uso dos índices FFC, concluindo-se que são necessários entre 2 a 10 minutos.

Palavras-chave: variabilidade da frequência cardíaca, fragmentação da frequência cardíaca, Média do Sinal com Retificação de Fase, sistema nervoso autónomo, nó sinoatrial

Contents

List of Figures **x**

List of Tables **xii**

Abbreviations **xiv**

1 Introduction **1**
1.1 Context and Motivation 1
1.2 Problem Statement and Proposed Approach 2
1.3 Document Structure 5

2 Background Concepts **6**
2.1 Major Cardiovascular Physiological and Electrophysiological Concepts 6
2.1.1 Electrical Propagation of a Normal Heartbeat 6
2.1.2 The Electrocardiogram 8
2.1.3 Sinus Rhythm and the Sinoatrial Complex Dominance 8
2.1.4 The Regulation of the Cardiovascular System 8
2.1.5 Autonomic Regulation of the Cardiovascular System 13
2.1.6 Heart Rate Changes Coupled with Respiration: The Respiratory Sinus Arrhythmia 16
2.2 Major Concepts of Heart Rate Dynamics Analysis 16
2.2.1 Heart Rate Variability 17
2.2.2 Heart Rate Fragmentation 20
2.2.3 Phase Rectified Signal Averaging Approach - Acceleration and Deceleration Capacities of the Heart 25
2.3 Statistical Concepts 26
2.3.1 Likelihood, Likelihood Function, Log-Likelihood, and Likelihood Ratio 27
2.3.2 Regression Analysis 28
2.3.3 Measures of the Dependence between two Variables 33

2.3.4 Summary of some Important Statistical Tests 33

3 General Methods **36**
3.1 Databases 36
3.2 Methods 36
3.2.1 An Example of Application of HRF and PRSA Indices 37

4 Changes in Heart Rate Dynamics with Cross-sectional Age **42**
4.1 Conceptual Introduction 42
4.2 Related Work 43
4.3 Methods 44
4.3.1 Databases 44
4.3.2 Heart Rate Dynamical Analysis 45
4.3.3 Statistical Analysis 46
4.4 Results 47
4.4.1 Changes in Heart Rate Dynamics with the Participants' Age in the NSRdb Population 47
4.4.2 Changes in Heart Rate Dynamics with the Participants' Age in the Fantasia Population 53
4.4.3 Changes in Heart Rate Dynamics with the Participants' Age in the AAdb Population 57
4.5 Discussion 59

5 Changes in Heart Rate Dynamics with Disease **64**
5.1 Changes in Heart Rate Dynamics with Atrial Fibrillation Severity 64
5.1.1 Conceptual Introduction 64
5.1.2 Related Work 66
5.1.3 Methods 67
5.1.4 Results 69
5.1.5 Discussion 69
5.2 Changes in Heart Rate Dynamics with Congestive Heart Failure 73
5.2.1 Conceptual Introduction 73
5.2.2 Related Work 73
5.2.3 Methods 74
5.2.4 Results 75
5.2.5 Discussion 78

6 Changes in Heart Rate Dynamics From Early Childhood to Late Adulthood **80**
6.1 Introduction 80
6.2 Related Work 81
6.3 Methods 82
6.3.1 RR Interval Time Series from Healthy Subjects Database 82

6.3.2 The Normal Sinus Rhythm RR Intervals Database 82
6.3.3 Heart Rate Dynamical Analysis 83
6.3.4 Specific Hypotheses 83
6.3.5 Statistical Analysis 83
6.4 Results 84
6.5 Discussion 87

7 Estimation of the Minimum Time Required to Measure Heart Rate Fragmentation Indices **91**
7.1 Introduction 91
7.2 Methods 93
7.2.1 Population - Fantasia Database 93
7.2.2 Heart Rate Fragmentation Analysis 93
7.2.3 Statistical Procedures 93
7.3 Results 94
7.4 Discussion 95

8 Conclusion **100**
8.1 Future Work 102

Bibliography **104**

List of Figures

2.1 Conduction system within the heart and a segment of an ECG during a normal heartbeat. 7
2.2 Generic efferent pathway of the autonomic nervous system. 11
2.3 Representation of the sympathetic division of the autonomic nervous system. 12
2.4 Representation of the parasympathetic division of the autonomic nervous system. 14
2.5 Effect of respiratory sinus arrhythmia on ventilation-perfusion matching in the lungs. 17
2.6 Example of a power Fourier spectrum of a heartbeat intervals time series. . 19
2.7 Example of fluent and a fragmented heart rate time series. 22
2.8 Comparison between acceleration capacity from different PRSA signals. . . 27

3.1 Example of a heart rate time series eligible for heart rate fragmentation analysis obtained from an ECG excerpt. 38
3.2 Illustration of the main features of the heart rate time series used in HRF analysis. 39
3.3 Selection of accelerative anchors and definition of segments used for the computation of a PRSA signal. 40
3.4 Example of a PRSA signal. 41

4.1 Scatter plots of heart rate dynamical indices vs. cross-sectional age, in the 24-hour period of the NSRdb Population. 51
4.2 Scatter plots of heart rate dynamical indices vs. cross-sectional age, in the AAdb Population. 60

5.1 Comparison between a normal heart and associated ECG with those of AF patients. 65
5.2 Scatter plots of heart rate dynamical indices vs. percent time in atrial fibrillation. 70

6.1 Scatter plots of heart rate dynamical indices vs. cross-sectional age, from early childhood to infancy. 85
6.2 Scatter plots of heart rate dynamical indices vs. cross-sectional age, from early childhood to late adulthood. 88

7.1 Evolution of two HRF indices in a young and an old subject, using different window resolutions. 92
7.2 Schematic representation of the statistical procedure used to estimate the minimum time required to measure HRF indices. 94
7.3 Schematic representation of the procedure used to estimate the uncertainty and stability of HRF indices. 95
7.4 Probability associated with the separation of young adulthood from late adulthood using HRF indices along different window lengths. 96
7.5 Evolution of HRF measurements uncertainty for different window lengths. 97
7.6 Evolution of the coefficient of variation of HRF indices for different window lengths. 98

List of Tables

2.1 Schematic representation of the 81 different dynamical words of HRF analysis. 24

4.1 Age distribution of the population present in the AAdb database. 46
4.2 Comparison of heart rate dynamical indices between young and old participants in the 24-hour period of the NSRdb population. 48
4.3 Comparison of heart rate dynamical indices between young and old participants in the awake period of the NSRdb population. 49
4.4 Comparison of heart rate dynamical indices between young and old participants in the sleep period of the NSRdb population. 50
4.5 Comparison between heart rate dynamics in awake and sleep periods in old and young participants of the NSRdb population. 52
4.6 Comparison of the change in heart rate dynamics from wake to sleep period between older and younger subjects in the NSRdb population. 53
4.7 Correlation coefficients for the relationships between heart rate dynamical indices and cross-sectional age in the 24-hour period of the NSRdb population. 54
4.8 Correlation coefficients for the relationships between heart rate dynamical indices and cross-sectional age in the awake period of the NSRdb population. 55
4.9 Correlation coefficients for the relationships between heart rate dynamical indices and cross-sectional age in the sleep period of the NSRdb population. 56
4.10 Comparison of heart rate dynamical indices between young and old participants included in the Fantasia database. 57
4.11 Logistic linear regression analysis of the relationship between heart rate dynamical indices and old age for the Fantasia population. 58
4.12 Comparison between logistic models of age using a HRV variable and these same models where an HRF variable is added for the participants included in the Fantasia database. 59
4.13 Correlation coefficients for the polynomial linear regression models used to describe the relationship between age and heart rate dynamical indices in the AAdb population. 61

5.1 Summary of the arrhythmias observed in the population of the LTAFdb Database. 68
5.2 Comparison of heart rate dynamical indices between low burden and high burden atrial fibrillation. 71
5.3 Correlation coefficients for the relationships between heart rate dynamical indices and percent time in atrial fibrillation. 72
5.4 Comparison of heart rate dynamical indices between healthy subjects and congestive heart failure patients. 76
5.5 Logistic linear regression analysis of the relationship between heart rate dynamical indices and presence of congestive heart failure. 77
5.6 Comparison between logistic models of congestive heart failure using a HRV or a PRSA variable and these same models where an HRF variable is added. 78
5.7 Comparison between logistic models of congestive heart failure using both HRV and PRSA variables and these same models where an HRF variable is added. 79

6.1 Age Distribution of the population included in the NSRdb and RRHSdb Databases. 83
6.2 Evaluation of the independence of HRF indices from mean heart rate when predicting age in early childhood using linear regression models. 84
6.3 Correlation coefficients for the relationships between heart rate dynamical indices and cross-sectional age from birth to infancy in the population RRHdb database. 86
6.4 Polynomial linear regression analysis for the relationship between age and heart rate dynamical indices from birth to late adulthood. 89

Abbreviations

AAdb	Autonomic Aging Database
AC	Acceleration Capacity
ACh	acetylcholine
AF	Atrial Fibrillation
ALS	Average Length of acceleration/deceleration Segments
ANS	Autonomic Nervous System
AUC	Area Under the Curve
AVN	Atrioventricular Node
CHF	Congestive Heart Failure
CHFdb	Congestive Heart Failure Database
CV	Coefficient of Variation
DC	Deceleration Capacity
ECG	Electrocardiogram
GLM	Generalized Linear Model
HF	High Frequency
HR	Heart Rate
HRF	Heart Rate Fragmentation
HRV	Heart Rate Variability
LF	Low Frequency
LTAFdb	Long Term AF Database
MAP	Mean Arterial Blood Pressure

NE	norepinephrine
NN	Normal-to-Normal
NSRdb	Normal Sinus Rhythm RR Intervals Database
NT-proBNP	N-Terminal Pro-B-Type Natriuretic Peptide
NTS	Nucleus Tractus Solitarius
PAS	Percentage of NN intervals in Alteration Segments
PIP	Percentage of Inflection Points
PIP_H	Percentage of Hard Inflection Points
PIP_S	Percentage of Soft Inflection Points
PNN50	Percentage of differences between adjacent NN intervals that are greater than 50 ms
PNNLS	Percentage of NN intervals in Long accelerative/decelerative Segments
PNNSS	Percentage of NN intervals in Short accelerative/decelerative Segments
PNS	Parasympathetic Nervous System
PRSA	Phase-rectified Signal Averaging
PSD	Power Spectral Density
RAAS	renin-angiotensin-aldosterone system
RMSSD	Root Mean Square of Successive Differences
ROC	Receiver Operating Characteristic Curve
RR	R peak-to-R peak
RRHdb	RR Intervals Time Series From Healthy Subjects Database
RSA	Respiratory Sinus Arrhythmia
SAN	Sinoatrial Node
SD	standard deviation
SDANN	Standard deviation of the average NN intervals calculated over 5-minute windows
SDNN	Standard deviation of NN intervals
SDNNI	Average of the standard deviation of NN intervals calculated over 5-minute windows
SDSD	Standard Deviation of Successive Differences
SNS	Sympathetic Nervous System
ULF	Ultra Low Frequency
VLF	Very Low Frequency

1

Introduction

1.1 Context and Motivation

In 2020, there were 727 million persons aged 65 years or over in the world [1]. In the next three decades, the United Nations foresees that the number of older persons worldwide will more than double, reaching over 1.5 billion in 2050 [1], a little less than one fifth of the current world population. Although the lifespan has, and is, increasing dramatically, the healthspan, or also called Healthy Life Expectancy (HALE), is not following this increase. It is estimated that the healthspan in Europe is 68 years, and the lifespan is 78 years, consequently, around 13% of life is estimated to be lived in disability [2]. Indeed, from the fifth decade of life, advancing age is associated with an exponential increase in burden from many different chronic conditions [3]. Thus, there is a clear need to expand healthspan, which will require a deeper understanding and characterization of the aging process and the advent of diseases.

Aging is associated with a decrease of the reparative and regenerative potential in tissues and organs, which leads to cumulative damage and reduction of systems' ability to adapt [4]. This disruption of resilience mechanisms and reduction of physiologic reserve is typically accompanied with disease. Chronological age is a major risk factor for functional impairments, chronic diseases and mortality. However, chronological age is not a reliable measure of aging, since deficits can accumulate at different rates and have different origins. Thus, individuals of the same age may diverge markedly in their age-related decline [5]. For example, there are individuals that appear frail and require assistance in daily routines already in their 70's, whereas others remain independent of assistance and seem to escape major physiological deterioration until very extreme ages [6].

The massive changes that occur during fetal and postnatal growth are followed by a period of relative "stability" during which alterations in physical and cognitive function are only apparent with high sensitive tools or stress tests. In this plateau phase most individuals are free of diseases [3], [7]. Nevertheless, age-related physiological changes accumulate from early life (in early child development and early adulthood), affecting

organ systems years before diseases diagnosis [3]. In fact, early in life, homeostatic and compensatory mechanisms are highly effective, but begin to fade later in life, and unrepaired damage accumulates beyond functional threshold [7].

Therefore, the quest to increase healthspan is tightly tied to the (1) understanding of aging beyond chronological age, which demands for measures of biophysiological changes that capture the disruption of resilience and cumulative damage, and (2) the search for aging measures sensitive enough to detect the onset of diseases and accelerated aging years before the establishment of clinical evident deterioration [3], [4], [7]–[9].

Candidate biomarkers of aging and disease are numerous and diverse, ranging from simple measures of functional frailty [10], e.g., walking speed and grip strength, to measures of organ-specific functions, e.g., mean arterial pressure and lung volumes [3], to more sophisticated measures of molecular and epigenetic changes, e.g., the patterns of DNA methylation and telomere's length [11]. However, some of these biomarkers are either not sensible enough to be useful in examining changes in young- or middle-aged adults, and therefore not ideal for use in prevention, or not easily obtainable, rendering it difficult to continuously track changes.

No single biomarker is likely to be accurate enough to measure biological aging and the risk for diseases, given the multifactorial nature of aging and diseases [12]. The most compelling approach is the use of combinations of biomarkers that capture different properties of aging and age-related diseases, better accounting for the complexity of these processes [3], [13]. Hence, the search for new biomarkers that capture different properties of aging and disease is of utmost importance.

The silent incursion of disease and deterioration begin early in life, and there is increasing evidence that tracking changes in early childhood development is not only important to prevent infant mortality [14], [15], but also to predict diseases and early aging in adulthood [14]–[16]. This conceptual framework is embodied in the theory named developmental origins of health and disease (DOHaD) [17], [18], whose first demonstration was made by proving the correlation between birth weight and the future incidence of ischemic heart diseases. Thus, the use of biomarkers should also be mobilized for the detection of silent abnormalities in early childhood.

1.2 Problem Statement and Proposed Approach

For the purposes of detecting accelerated aging, diseases, and also early childhood development disturbances, new biomarkers are needed. One of the best systems to non-invasively probe for steady disruption and changes in physiological resilience is the Autonomic Nervous System (ANS), which is the special nerve supply of the peripheral nervous system responsible for regulating involuntary physiologic processes including heart rate, blood pressure, and respiration. This system comprises two major divisions, the sympathetic and parasympathetic subsystems. The sympathetic division is mainly

responsible for mobilizing bodies' resources for dealing with challenges of all sorts. Conversely, parasympathetic activity predominates during states of relative quiescence, so that energy resources previously expended can be restored. This continuous neural regulation of the expenditure and replenishment of the body's resources is crucial for the overall physiological balance of bodily functions called homeostasis [19].

In elderly people, autonomic functions are relatively well maintained at rest, but upon internal and external changes subjects often demonstrate inability to respond properly [20]. The incidence of many diseases increases with age, and chronic diseases are often accompanied by ANS dysfunction [20]. In early childhood, the ANS is still maturing, being highly vulnerable to adverse environmental and physiological contexts [15]. Indeed, there is evidence suggesting that adverse early exposure in the neonatal period can affect ANS maturation and function, leading to infant mortality, psychological and mood disorders, and cardiovascular diseases in adulthood [14].

A valuable and non-invasive way to measure the state of the ANS, as well as its interaction with the heart's main pacemaker – the Sinoatrial Node (SAN) – is to monitor the dynamics of the rate at which the heart beats, i.e., the dynamics of the Heart Rate (HR) time series, or conversely the dynamicas of heart interbeat intervals. HR time series exhibit quasi-periodic patterns at different time-scales that reflect ANS modulation of HR. The propriety of these time series that most widely-used analytical tools attempt to quantify is the amplitude of beat-to-beat variation in HR, i.e., Heart Rate Variability (HRV) [21]. Of note, the abbreviation HRV is also used to refer the set of traditional indices used to quantify this propriety. These traditional HRV indices include time and frequency domain metrics that will be discussed in Section 2.2.1. However, despite decades of use in research studies, HRV metrics have not gained clinical traction. In fact, analyses performed under the current HRV framework, particularly in high-risk groups (e.g., those with advanced age and/or cardiovascular disease) have yielded inconsistent results [22]–[25].

Normally higher HRV is associated with greater physiological reserve, however, multiple studies have shown that both high and low HRV predicted cardiac mortality in the elderly. This finding has been described as the "HRV Paradox" [22], [26]. The resolution of this paradox was attained by Costa, Davis, and Goldberger [23] who developed a new approach to the analysis of HR dynamics [23], [24]. The metrics and construct of their use was termed Heart Rate Fragmentation (HRF) and its focus is on quantifying non-physiological high-frequency dynamical patterns that give a non-smooth/fragmented appearance to the HR time series. These patterns were shown to spuriously inflate traditional short-term HRV measures. HRF indices, are based on the assessment of the frequency of the change in HR acceleration sign.

Recently, Costa et al. published results from the analysis of two separate databases demonstrating the translational value of using HRF indicators as biomarkers of aging and disease. Specifically, the authors reported that HRF (1) increased with cross-sectional age in healthy subjects and those with coronary artery disease [23], [24], (2) was predictive of

major adverse cardiovascular events and Atrial Fibrillation (AF) [25], (3) added predictive value to well-known cardiac risk models [25], [27], and (4) was associated with diminished cognitive performance (assessed at the same time as HRF) and with the degradation of cognitive function at a future time (relative to the moment when HRF was measured) [28].

Beyond HRF analysis, other approaches have emerged to resolve other aspects of traditional HRV, one of which is the Phase-rectified Signal Averaging (PRSA) approach.

A major challenge in HRV traditional analysis is to capture the amplitude of quasi-periodic patterns in the HR time series since constant perturbations, e.g., postural changes, lead to phase de-synchronization of these rhythmic oscillations. Baeur et al. [29] have proposed a signal analysis procedure PRSA that effectively eliminates the nonstationarities created by random perturbations, thus allowing the sublimation of periodicities. They have further proposed two measures to quantify the amplitude of periodicities related to acceleration and deceleration events, namely Acceleration Capacity (AC) and Deceleration Capacity (DC) [30], [31], as an attempt to distinguish between sympathetic and parasympathetic modulations of HR. The PRSA approach has proven valuable in predicting mortality after myocardial infarction [30], in monitoring fetal distress [32]–[34], and as an independent risk factor for dilated cardiomyopathy and Congestive Heart Failure (CHF) [35], [36].

It should be noted that both PRSA and HRV traditional indices are based on the quantification of the **amplitude** of HR variations, whereas HRF indices are based on change in HR acceleration **sign**.

In the present dissertation, we explore and compare HRV, HRF, and PRSA approaches to probe HR dynamics in various contexts, as means to gain insight into cardiac neuroautonomic function, pacemaker integrity, and their changes with: (1) two cardiovascular diseases – AF and CHF – , and (2) with cross-sectional age from early childhood to senescence. We also address (3) some of the technical aspects of HRF measurement. More specifically, the main contributions of this dissertation are:

1. An evaluation of the changes in HR dynamics with cross-sectional age, from young adulthood to late adulthood, using three Electrocardiogram (ECG) and interbeat intervals databases, comprising recordings obtained under different conditions.

2. A study of the proprieties of HR dynamics observed during normal sinus rhythm in patients with different degrees of AF burden. The latter is defined as the amount of time in AF out of the total monitored time.

3. An evaluation of the changes in HR dynamics associated with prevalent CHF.

4. Description and quantification of cross-sectional changes in HR dynamics from birth to late adulthood, with a closer look at the evolution of this dynamics from birth to infancy.

5. Comprehensive comparison between the performances of different HR dynamical indices: HRV metrics, AC and DC capacities, and HRF metrics.

6. An estimation of the minimum time needed to measure HRF indicators, in order to use them as aging biomarkers in supine position in an awake state.

1.3 Document Structure

The remaining of this document is structured as follows:

- Chapter 2 summarizes the fundamental knowledge needed for understanding the following chapters in this dissertation. The first part of the Chapter is dedicated to cardiovascular physiological and electrophysyological concepts, attempting to answer the following main questions: How a heartbeat emerges?; Why HR fluctuates over time?; How the ANS functions and how it influences HR dynamics?. The second part of this Chapter introduces the main concepts underlying HR dynamical analysis, with special focus on the three types of approaches used in this dissertation, namely traditional HRV, HRF, and AC/DC capacities. The third part of the Chapter is dedicated to the presentation of the main statistical concepts that were used to draw inferences about the changes in HR dynamical indices.

- Chapter 3 describes the databases and the methods used for HR dynamical analysis and the preprocessing of interbeat interval time series required to obtain the HR dynamical indices computed in this dissertation.

- Chapters 4, 5, 6, and 7 present the results of the analyses carried out to address, respectively, the changes in HR dynamics: with (1) age from young adulthood to late adulthood; in (2) two diseases, namely with AF severity and with CHF; (3) with age from birth to infancy and from birth to late adulthood; and (4) the estimation of the minimum time needed to measure HRF indices. Each of these Chapters are self-contained, providing a brief introduction describing the physiological basis for the changes in HR dynamics (conceptual introduction); a summary of the work previously done regarding the evaluation of the changes in HR dynamics (related work) with special emphasis on traditional HRV, HRF, and PRSA measures; the specific hypotheses being tested; the HR dynamical indices used from HRV, HRF and PRSA approaches; the statistical analysis performed; and the results achieved, as well as their discussion.

- Chapter 8 concludes the dissertation, providing a summary of our main results and contributions, and a discussion for the direction of future work.

2

Background Concepts

2.1 Major Cardiovascular Physiological and Electrophysiological Concepts

The normal heart contracts spontaneously approximately once per second, with each contraction being derived from electrical currents that transverse the heart in an exceptionally coordinated and synchronized fashion. These electrical currents originate from the chain of depolarizations that are produced by three different type of cardiac cells: pacemaker cells, specialized conduction tissue, and the working cardiac muscle.

Pacemaker cells are like oscillators capable of spontaneously generating electrical stimuli in a repetitive way, i.e., they are endowed with *automaticity*. The main pacemaker cells of the heart are the ones present in the Sinoatrial Node (SAN).

The specialized conduction tissue, e.g., His-Purkinje system, functions like wires that transmit the electrical signal; and the working heart muscle cells, e.g., ventricular and atrial cells, convert the transmitted electrical signal to mechanical contraction.

Normally, a heartbeat is initiated by the pacemaker cells of the SAN, thus its activity determines the rate at which the heart pumps blood through the vascular system. SAN activity, and, thereby, HR, is modulated by an interplay of influences from the brain, the mechanics of respiration and circulation, and circulating neurohormones, both of which are mainly mediated by the two branches of the ANS, the parasympathetic (or vagal) and sympathetic branches [37], [38]. These influences are responsible for the variations in HR that occur over a range of time scales (seconds to hours). Effectively, HR dynamics provides a "window" for assessing the state of the ANS and the integrity of the SAN through the use of various time series analysis methods.

2.1.1 Electrical Propagation of a Normal Heartbeat

The sequence of events that underlie a heartbeat, under healthy conditions, are enumerated below and can be visually followed by the left side of Figure 2.1 [37], [39]–[41]:

1. Action potentials generated in the pacemaker cells of the SAN spread throughout

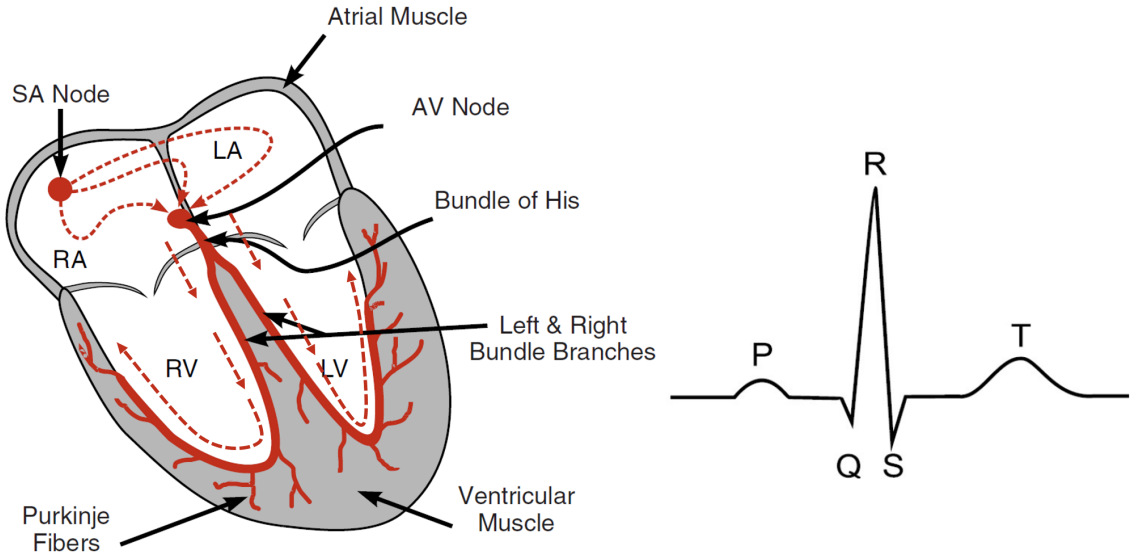

Figure 2.1: Conduction system within the heart and a segment of an ECG during a normal heartbeat. The dotted red arrows indicate the direction of electrical propagation in the heart. Adapted from [39].

the atria;

2. As the wave of action potentials depolarizes the atrial muscle it elicits the contraction of cardiomyocytes, giving rise to atrial contraction;

3. The action potentials are conducted to the ventricles through the Atrioventricular Node (AVN), which typically is the only pathway available for the passage of action potentials to the ventricles;

4. The action potentials leaving the AVN enter the base of the ventricles at the bundle of His, which divides into two main branches, one for each ventricle. Each of these branches is further ramified, giving rise to an extensive system, the His-Purkinje fibers, that conducts the action potentials at high velocity throughout the ventricles;

5. This branched conducting system transmits the electrical signals to ventricular muscle cells generating ventricular contraction.

The AVN is a specialized conduction tissue, that has the important function of slowing the impulse conduction between the atria and the ventricles [39]. This delay in the AVN is fundamental to ensure that atrial contraction occurs before ventricular contraction. Furthermore, in the context of supraventricular tachyarrhythmia (e.g., AF) it limits the occurrence of ventricular tachycardia, which could drastically reduced cardiac output[1] due to inadequate time for ventricular filling.

[1] Cardiac output corresponds to the volume of blood eject by the left ventricle per unit time.

2.1.2 The Electrocardiogram

The Electrocardiogram (ECG) traces the depolarization and repolarization events originated in the heart. During a heartbeat, as cardiac cells depolarize and repolarize, electrical currents spread throughout the body. Thus, if electrodes are placed on the skin on opposite sides of the heart, the electrical potentials generated by these currents can be recorded producing what is called the ECG signal [39].

The normal ECG signal, which is shown in the right side of Figure 2.1, is composed of a sequence of three complexes: P wave, QRS complex, and T wave [37], [41].

The P wave corresponds to the depolarization of the atrial myocardium, triggered by the electrical impulses generated in the SAN, and indicates the start of atrial contraction. The QRS complex represents the depolarization of the ventricular myocardium and indicates the start of ventricular contraction. The T-wave corresponds to the repolarization of the ventricular myocardium, which is a necessary recovery process for the myocardium to be able to depolarize and contract in the next heartbeat. The end of the T-wave coincides with the end of the ventricular contraction.

2.1.3 Sinus Rhythm and the Sinoatrial Complex Dominance

The SAN is composed of multiple intranodal pacemaker cells and several exit conduction pathways for the atria that provide physiological redundancy. Thus, if for some reason a portion of the pacemaker cells are compromised or a portion of the intranodal pathways are blocked, other available pacemaker cells or conducting pathways of the SAN are available, allowing for the maintenance of heart contraction [42], [43]. Even if none of the SAN cells are capable to initiate a heartbeat in a timely way, other heart cells, such as those in the AVN and Purkinje Fibers, can also trigger a heartbeat. The fact that all cardiac cells possess automaticity (though with very different intrinsic rates) provides further physiological redundancy.

It is important to note that, under healthy conditions, the heartbeat is initiated by the SAN, whereby the heart is said to be in sinus rhythm. Cells outside the SAN usually do not trigger a heartbeat, despite possessing automaticity, because the SAN cells have a faster intrinsic firing rate that suppresses the firing of the other heart cells. For this reason, the SAN is said to be the dominant pacemaker complex.

Nevertheless, sporadic (typically physiologic – ectopic beats) or consistent (typically non-physyiological – arrhythmias) suppression of SAN primacy may be present due to SAN failure or/and to abnormal increased automaticity in other heart cells.

2.1.4 The Regulation of the Cardiovascular System

The primary drive of cardiovascular regulation is the maintenance of adequate blood pressure in tissues under varying metabolic demands of the body. These demands are constantly varying due to ever-changing external and internal conditions, such as in

exercising and change in position from lying down to standing up. The control of arterial blood pressure, which is made through its various determinants – HR, stroke volume, and systemic vascular resistance –, is accomplished by the ANS, as well as by circulating hormones, whose release is also mainly mediated by the ANS. The main hormones that participate in the regulation of arterial pressure include the catecholamines released by the adrenal gland, the angiotensin from the renin-angiotensin-aldosterone system (RAAS), and the antidiuretic hormone [39], [40], [44].

The ANS and the hormonal factors operate on different time scales, typically, the ANS influences occur over shorter time periods [39], [45].

2.1.4.1 The Three Determinants of Arterial Blood Pressure

To appreciate the fluctuations in HR due to autonomic control, HR should be also percieved as one of the main determinants of arterial blood pressure. Usually, Mean Arterial Blood Pressure (MAP) is used as surrogate of arterial blood pressure. The determinants of arterial blood pressure include heart rate (HR), stroke volume (SV), which is the volume of blood ejected by the left ventricle, and systemic vascular resistance (SVR), which corresponds to the resistance to blood flow offered by all of the systemic vasculature. These three factors relate with MAP according to the follow equation [39]:

$$MAP = HR \times SV \times SVR \tag{2.1}$$

The main factors that affect stroke volume are ventricular afterload, preload and inotropy, i.e., ventricular contraction force [39].

Afterload is the amount of pressure that the heart needs to exert to eject the blood during ventricular contraction. Afterload is typically increased when aortic pressure and systemic vascular resistance are increased, for example, due to aortic valve stenosis and ventricular dilation. When afterload increases there is a decrease in stroke volume.

Preload refers to the amount of blood arriving to the ventricles immediately before ventricular contraction. Preaload increases stroke volume through the Frank-Starling mechanism, i.e., greater volume induces greater stretch of cardiac muscle, which, in turn, increases contraction force. Increased preload could be due to increased total blood volume or increased central venous pressure, i.e., the pressure in the thoracic vena cava near the right atrium. An increase in central venous pressure entails an increase in pressure in veins, which, in turn, increases the amount of blood returning to the heart and, thereby increasing preload.

The main factor affecting systemic vascular resistance is vessel diameter, whereby vasoconstriction/vasodilation increases/decreases it.

2.1.4.2 The Autonomic Nervous System

The ANS is the portion of the peripheral nervous system that innervates the smooth musculature of all organs, the heart, and the glands to mediate the regulation of the

internal *milieu* [46]. As mentioned in Section 1.2, the ANS has two main divisions the Parasympathetic Nervous System (PNS) and the Sympathetic Nervous System (SNS). Both of these divisions are associated with a set of afferent fibers that provide sensory input for the central nervous system and efferent fibers, arising from the central nervous system that provide motor output to target organs and tissues [47].

How is the Activity of the Autonomic Nervous System Controlled? The output of the ANS is regulated by what are called autonomic reflexes. In these reflexes subconscious sensory signals from chemical and mechanical sensors in organs enter the afferent autonomic pathways that go through the autonomic ganglia and end up in two main regions of the central nervous system, namely, the brain stem and/or the hypothalamus. These brain structures then coordinate efferent (also subconsciously) signals to target tissues and organs.

Higher level brain areas, such as the cerebral cortex and limbic system, can also provide afferent signals to the brain stem and the hypothalamus, triggering autonomic responses. Through these pathways, emotional stimuli, such as recalling a bad event, may induce somatic symptoms in many organs, including tachycardia and sweating [48].

General Structure The efferent pathways of the ANS consist of two type of neurons that transmit impulses from brain centers to effector tissues: the preganglionic, with cell bodies on the central nervous system, and postganglionic neurons, with cell bodies in autonomic ganglia located near target tissues or organs. As illustrated in Figure 2.2, generally, a preganglionic neuron arises from a lateral horn of the gray matter in the spinal cord or from the brain stem and synapses with a postganglionic neuron in ganglia located near target tissues. Normally, all preganglionic fibers are cholinergic, meaning that they synapse with postganglionic fibers through the release of acetylcholine (ACh). The postganglionic fibers of the PNS are also cholinergic, but SNS ones are adrenergic, meaning that they cause changes in effector tissues through the release of norepinephrine (NE).

The most remarkable features of the ANS its celerity and intensity in inducing changes in tissues. For instance, within 10 to 15 seconds the arterial pressure can be doubled [40]. This is possible because postganglionic fibers do not terminate in a single protrusion-like synaptic knob nor do they synapse directly with the cells of tissues (see Figure 2.2). Instead, the axons of postganglionic fibers with beading-like structures, i.e., *varicosities*, wrap around tissues, whereby neurotransmitters are released over a large surface area of the effector tissue [47].

Brief Anatomy of the Sympathetic and Parasympathetic Nervous Systems To follow the description of the SNS and PNS, detailed below, see Figures 2.3 and 2.4, respectively.

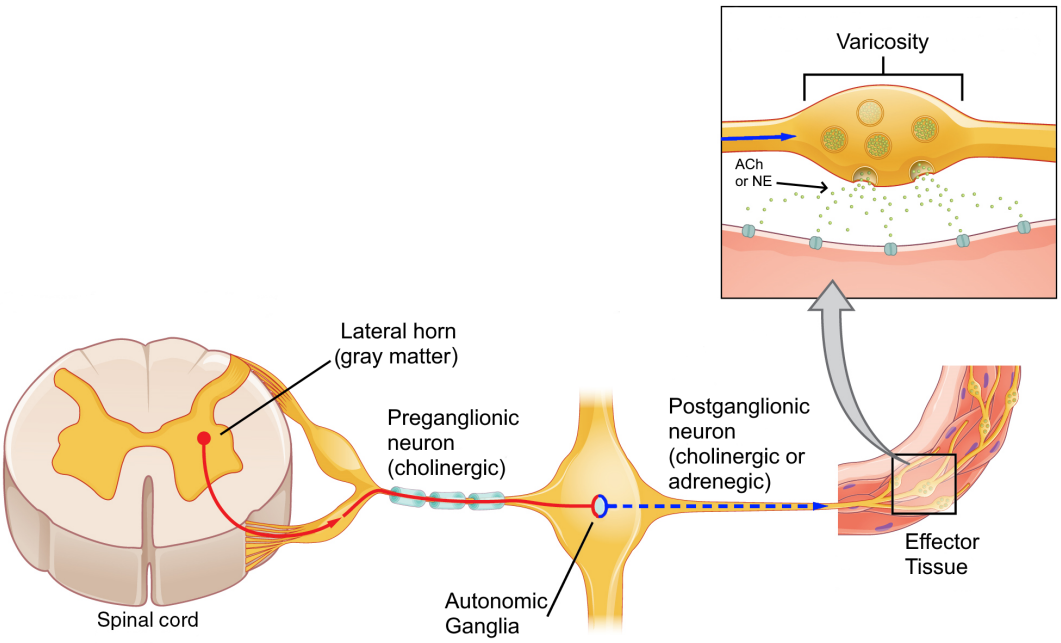

Figure 2.2: Representation of an efferent pathway of the autonomic nervous system. Adapted from [49].

The preganglionic neurons of the SNS arise from the thoracic and lumbar regions of the spinal cord segments (T_1 trough L_2) [40], [44]. These neurons synapse with postganglionic ones in the sympathetic ganglion chains, which run parallel to the spinal cord on either side. One preganglionic neuron may synapse with many postganglionic neurons, with around a 1:20 ratio [47], in different locations of the ganglion chains. This allows extremely coordinated and concurrent stimulation by the SNS of many organs and tissues of the body. Other SNS preganglionic fibers travel more peripherally and synapse with postganglionic neurons in sympathetic collateral ganglia. Preganglionic fibers may also travel to the adrenal medulla, which releases cathecolamines to the blood stream. The SNS innervates most of the smooth muscle of blood vessels in the entire body, all sweat glands, and many structures of the head, e.g., eye, salivary glands, and muscus membranes of the nasal cavity, of the thoracic organs, e.g., heart and lung, and the organs within the abdominal and pelvic cavities, e.g., stomach, intestines, pancreas, spleen, adrenal medulla, and urinary bladder [40].

The preganglionic neurons of the PNS arise from several nuclei of the brainstem and from the lowermost part of the spinal cord (segments S_2 trough S_4) [40], [44]. These neurons synapse with postganglionic neurons within terminal ganglia that are embedded within or close to the effector tissue. The portion of the preganglionic neurons leaving the brainstem exits the central nervous system through cranial nerves such as the occulomotor nerve (III), innervating the pupillary sphincter and ciliary muscles of the eye; facial nerve (VII), innervating lacrimal, nasal, and submandibular glands; glossopharyngeal nerve (IX), innervating the parotid gland; and the vagus nerve (X), which innervates the organs

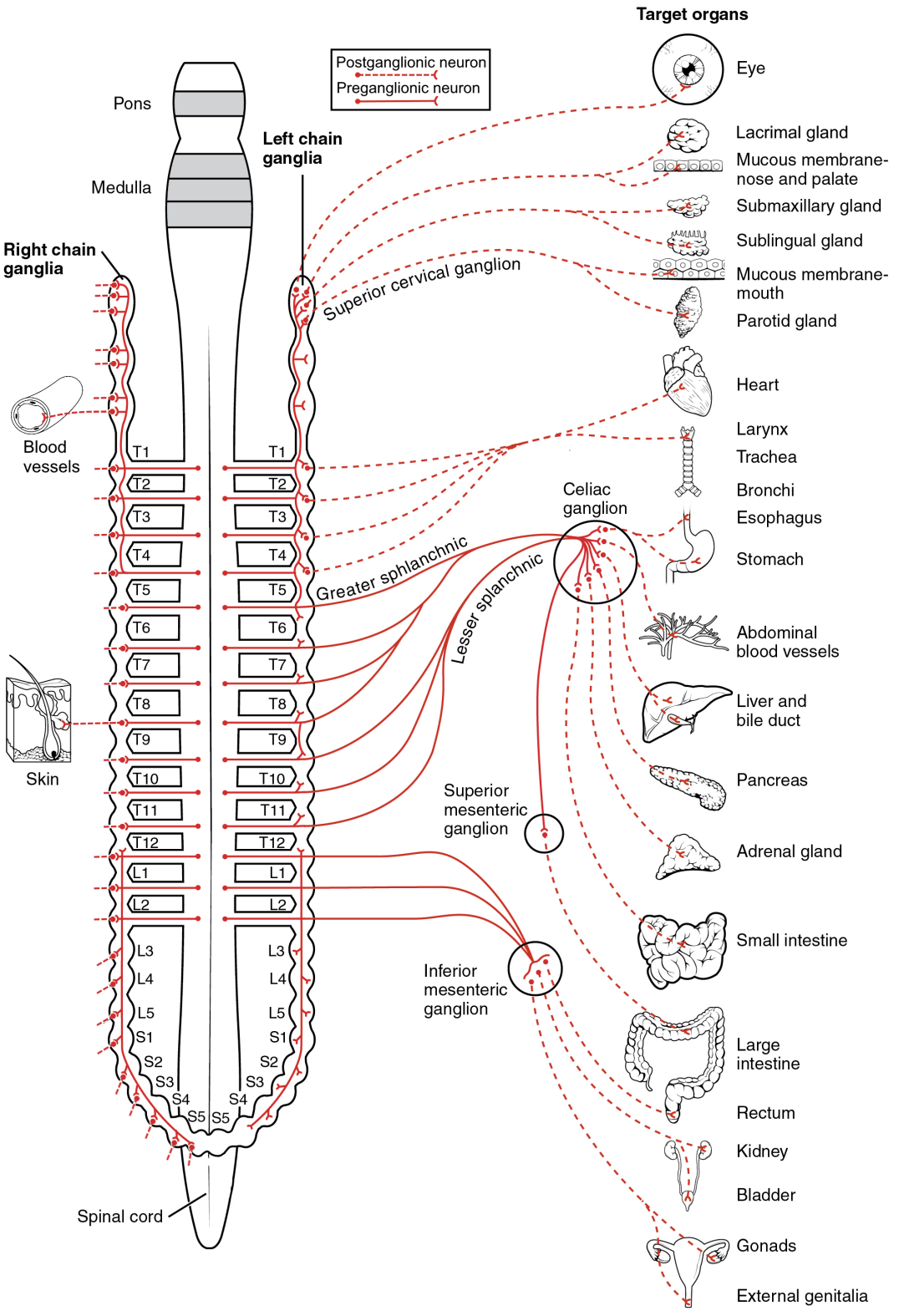

Figure 2.3: Representation of the sympathetic division of the autonomic nervous system. Adapted from [49].

of the thorax and the abdomen, including the heart, lungs, stomach, pancreas, small intestine, upper half of the large intestine, and liver.

As visible from the number of organs it innervates, the vagus nerve has great physiological significance. In fact, it comprises around 75% of parasympathetic fibers [40]. The sacral preganglionic neurons of the PNS exit the central nervous system and join together to form the pelvic nerves, which innervate the viscera of the pelvic cavity. As opposed to the SNS, in the PNS preganglionic neurons synapse with postganglionic neurons in a 1:1 ratio [47]. Therefore, the effects of the PNS tend to be more discrete and localized, with only specific tissues being stimulated at any given moment, whereas SNS tends induce whole-body responses.

Balance Between Parasympathetic and Sympathetic Activities In a healthy individual both PNS and SNS are tonically active, providing some degree of nervous input to a given tissue at all times. Thus, the nervous input can both increase or decrease, by changing the frequency of neuronal activation. Typically, the two branches have antagonic effects on organs. Sympathetic activity usually prepares the body for strenuous physical activity by increasing the perfusion of well-oxygenated and nutrient-rich blood to tissues that are in most need in these situations, such as the working skeletal muscles. Conversely, the parasympathetic activity predominates during quiet and resting condition, allowing for the recovery after energy expenditure by conserving and storing energy.

Nevertheless, although their opposing effects, it should be noted that there has been increasing evidence that the PNS and SNS do not relate to each other in a zero-sum manner. In fact, PNS increased activity may be associated with increased, decreased or no change in the activity of the SNS. As an example, following aerobic exercise, typically PNS activation occurs while SNS activity remains elevated [50].

2.1.5 Autonomic Regulation of the Cardiovascular System

In the autonomic regulation of the cardiovascular system the SNS typically acts to increase arterial blood pressure by inducing vasoconstriction, an increase in HR (chronotropy), as well as an increase in both contractility (inotropy) and conduction velocity (dromotropy) in cardiac tissue. Conversely, the PNS acts to decrease arterial blood pressure by inducing a decrease in HR, as well as a decrease in both inotropy and dromotropy. However, it should be noted that as vagal fibers are mainly distributed to the atria and not much to the ventricles (where the power of contraction occurs), PNS control is mainly through changes in chronotropy [40].

The control of ANS regulation of cardiovascular function is mainly accomplished by the Nucleus Tractus Solitarius (NTS) of the medulla oblongata, i.e., the inferior part of the brain stem, and the hypothalamus. Generally, the NTS receives afferent information from baroreceptors, chemoreceptors, respiratory stretch receptors, as well as from higher brain areas. Then, the NTS integrates these afferent signals and sends stimulus through

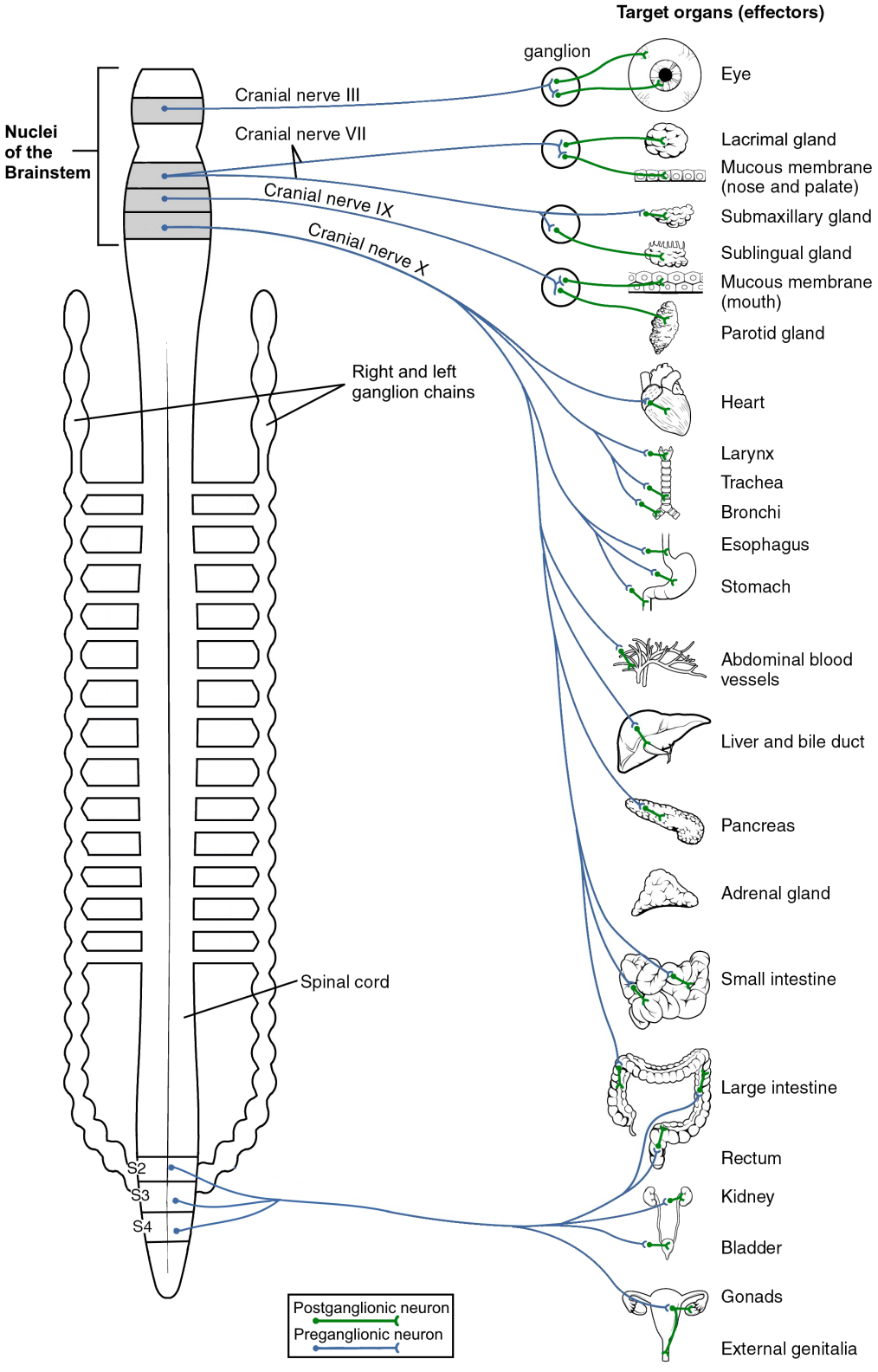

Figure 2.4: Representation of the parasympathetic division of the autonomic nervous system. Adapted from [49].

the sympathetic thoracic nerves and through the vagus nerve of the PNS. To induce their responses in the heart, the postganglionic PNS and SNS nerves innervate the SAN, AVN, conduction pathways, and myocardial cells [39].

2.1.5.1 The Action of the Autonomic Nervous System in the Sinoatrial Node Activity

Without autonomic innervation of the SAN, the heart would beat at the intrinsic firing rate of the SAN, approximately 100 times per minute. However, as is known, at rest HR is much lower, being approximately 60 bpm. This derives from the predominant activity of the PNS over the SAN at rest, which is known as the *vagal tone*. Another important observation is that the SAN response time to sympathetic stimulation is much longer when compared to the parasympathetic stimulation. A change in the level of PNS activity will affect HR with a delay of approximately 0.5 s, while the SNS is associated with a delay of approximately 3 s [51]. Thus, the PNS acts on HR in a beat-to-beat basis. This is the case because the SAN is rich in acetylcholinesterase, ensuring that ACh is rapidly hydrolyzed [21], furthermore, the signaling mechanisms are based on conformational changes of membrane potassium channels [22]. In contrast, the sympathetic activation causes effects through several phosphorylation enzymatic processes in the intercellular transduction mechanisms, which renders sympathetic latency in the SAN much higher.

Moreover, the parasympathetic branch can slow the heart to 20 or 30 bpm or even briefly stop it [52], whereas the changes elicited by the SNS stimulation are more progressive, typically, in this case the HR only achieves a steady level after 20 s – 30 s [53].

As we have previously stated, the SAN is composed of multiple pacemaker cells, it has been shown that a predominance in PNS activation causes more inferior located cells to start the heartbeat, whereas SNS activation causes more superior located cells to initiate the heartbeat [54].

2.1.5.2 The Major Autonomic Reflexes of Cardivascular Regulation

The *baroreflex* [39] is the main cardioautonomic reflex by which arterial pressure is maintained to ensure adequate organ perfusion. In this reflex, the NTS receives afferent information from arterial baroreceptors located in strategic places like the aortic arch. The arterial baroreceptors are stimulated by stretching of the vessel walls produced by increases in arterial blood pressure. Thus, if arterial blood pressure decreases from normal values, arterial baroreceptors stimulation lowers, consequently, the NTS increases sympathetic outflow, which increases systemic vascular resistance by vasoconstriction and increases chronotropy and inotropy in the heart. If, instead, there is a rise in arterial pressure beyond normal values, an increased parasympathetic outflow coordinates opposite changes in the heart, i.e., decreased HR and atrial inotropy.

The *Bainbridge reflex* [55] is another special cardioautonomic reflex. This is a compensatory reflex resulting in an increase in HR following an increase in cardiac preload. In

this reflex the NTS receives afferent information from stretch receptors present in atrial tissue.

2.1.6 Heart Rate Changes Coupled with Respiration: The Respiratory Sinus Arrhythmia

The Respiratory Sinus Arrhythmia (RSA) is the physiological phenomenon whereby HR increases during inspiration and decreases during expiration [56]. These changes can be quite marked, up to 10 bpm–20 bpm [41]. Since these HR changes occur on less than ~ 4 seconds, they are attributed to vagal modulation.

These HR changes result in the time matching between maximal alveolar ventilation and maximal perfusion within each respiratory cycle, whereby unnecessary heartbeats during expiration are suppressed. Thus, this mechanism has been recognized as a physiological mechanism to ensure optimal ventilation-perfusion matching in the lungs [22], [37], [56]–[58]. This effect is illustrated in Figure 2.5.

Although it has long been recognized, the autonomic reflexes underlying this phenomenon are not yet clear. It has been proposed that the balance between Bainbridge reflex and baroreflex create the RSA [55]. During inspiration there is a decrease in intrathoracic pressure and a subsequent expansion of the lungs. This results in reduced right atrial pressure which leads to increased venous return. This rise is sensed by the atrial stretch receptors that then induce HR increase through the Bainbridge reflex. The increased cardiac filling during inspiration elicits an increase in stroke volume, an thereby arterial blood pressure rises due to both increased HR and stroke volume. This rise stimulates baroreceptors, triggering a vagal outflow to the SAN through the baroreflex, leading to a a decrease in HR during expiration.

The lungs-inflation reflex was also proposed to mediate the RSA. This reflex is typically triggered to prevent the over-inflation of the lungs. Lungs' inflation activates pulmonary stretch receptors that send inhibitory signals to the NTS that elicit a decrease in PNS outflow to heart, thereby increasing HR [59], [60].

2.2 Major Concepts of Heart Rate Dynamics Analysis

The interplay between internal (to the body) and external perturbations to cardiovascular function and the dynamic response of the ANS, give rise to quasi-periodic fluctuations in HR at different time scales [61]–[63]. Perturbations may result from changes in posture and the mechanical effects associated with the respiratory cycle, or even from internal changes as subtle as the slight adjustments in local vascular resistance in different tissues [61], [64].

HR dynamics analysis is based on the quantification of information encoded in the temporal fluctuations of HR. This quantification is made by analyzing the series of the time intervals between heartbeats. It should be noted that, typically, only heartbeats

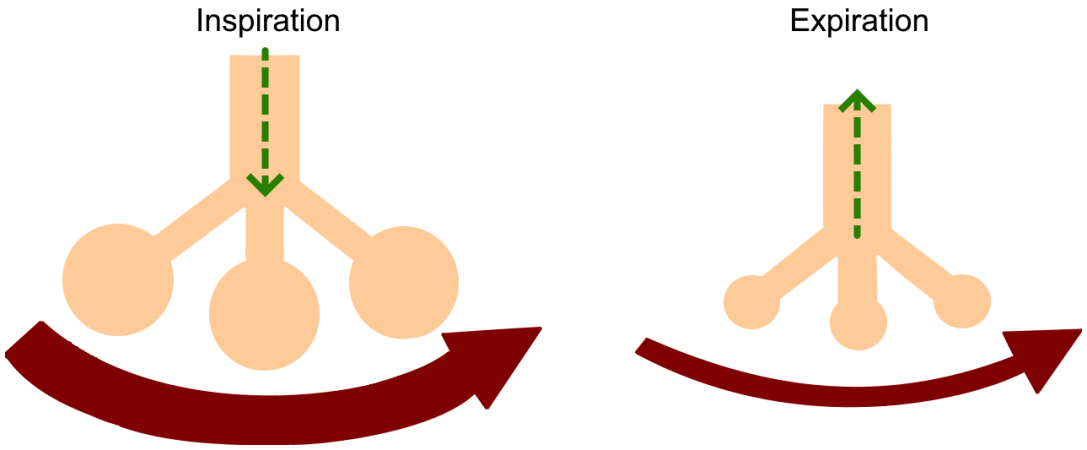

Figure 2.5: Schema of the effects of RSA on the ventilation-perfusion matching in the alveoli. Horizontal red arrows and vertical green arrows indicate the volume of blood flow and the direction of gas flow to the alveoli, respectively. RSA improves respiratory gas exchange efficiency through matching between alveolar ventilation and capillary perfusion throughout the respiratory cycle. Adapted from [57].

that arise from the firing of the SAN are considered. Heartbeats derived from abnormal pacemakers are excluded. Generally, this time series is obtained by computing the time difference between the R waves of the QRS complex of the ECG. When abnormal beats are removed this series is named Normal-to-Normal (NN) time series and defined as $\{NN_i\} = \left\{t_{N_i} - t_{N_{i-1}}\right\}$, where t_{N_i} represents the time occurrence of the i^{th} sinus beat. When non-sinus beats are not removed the series is called R peak-to-R peak (RR) time series and defined as $\{RR_i\} = \left\{t_{R_i} - t_{R_{i-1}}\right\}$, where t_{R_i} represents the time occurrence of the i^{th} a heartbeat.

For communication (and sometimes visualization) purposes, HR time series will be referred instead of the NN time series. However, HR dynamical analysis were obtained from the NN time series and not the HR time series, which is inversely related to the former.

2.2.1 Heart Rate Variability

HRV metrics quantify the amplitude of the variations in the NN time series [21]. The working hypothesis underlying HRV analysis is that reduced values of HRV measures constitute a sign of degraded neuro-autonomic control. It should also be noted that higher values of HRV are typically associated with increased vagal activity rather than sympathetic one, specially under resting conditions [21].

Some studies found HRV analysis to have diagnostic and prognostic ability as a clinical tool to evaluate cardioautonomic abnormalities in contexts such as in anticipation of fetal distress [65], mortality after myocardial infarction [66], and detection of neuropathy in diabetic patients [67], [68].

There are two primary approaches for the analysis of HRV: time domain and frequency domain [21], [37], [61], [69].

The time domain approach is based on the application of basic statistical operations, such as mean and variance, to the NN interval time series or to the time series of the differences between consecutive NN intervals, the so-called increment NN interval time series, i.e., $\{\Delta NN_i\} = \{NN_i - NN_{i-1}\}$. From this perspective, the time domain metrics are insensitive to the order of the data points in a time series.

The frequency domain approach employs power spectral analysis of the NN time series, allowing not only the quantification of the amplitude of HR fluctuations, but also the identification of the specific oscillatory frequencies at which they occur.

Although excluded from the analyses present in this dissertation, beyond the two standard approaches to measure HRV, there are different kinds of approaches that have been extensively used. These approaches are motivated by the recognition that the NN time series displays apparently complex, i.e., fractal-like, behavior [69]. The quantification of this type of behavior in the NN time series is accomplished by complexity measures that, typically, derive from the evaluation of two proprieties of its temporal structure: the amount of regularity (or conversely unpredictability) and the presence of correlations across multiple time scales [70]. The former propriety is mainly quantified by entropy methods, such as Approximate Entropy [71] and Sample Entropy [72], and the latter is mainly quantified by fractal analysis methods, such as Detrended Fluctuation Analysis [73].

2.2.1.1 Different Periodic Components Identified by Frequency Domain Analysis

In traditional HRV analysis, the power of the Fourier spectrum of NN intervals over four frequency bands is independently computed: 1) between 0.15 and 0.4 Hz, quantifying oscillatory patterns with periods ranging from 2.5 s to 7 s; 2) between 0.04 and 0.15 Hz, quantifying oscillatory patterns with periods ranging from 7 s to 15 s; 3) between 0.0033 and 0.04 Hz, quantifying oscillatory patterns with periods ranging from 15 s to 5 min; and above 0.0033 Hz, quantifying oscillatory patterns with periods above 5 min. The power in these different bands are called High Frequency (HF), Low Frequency (LF), Very Low Frequency (VLF), and Ultra Low Frequency (ULF), respectively. They are computed for relatively short segments of NN interval time series, typically 5 minutes, or for the entire duration of a recording.

The HF band is mainly attributed to the previously described RSA mechanism, which is modulated by PNS activity [74], since the time the scale at which the PNS branch operates is much shorter than that of the sympathetic branch.

The LF band has been mainly attributed to intrinsic oscillations resulting from the negative feedback loop of the baroreflex, the so-called the *Mayer Waves* [75]. The frequency of the Mayer waves is determined by the time delay of this control loop [37], [62]–[64], which depends on both the PNS and SNS activity [76].

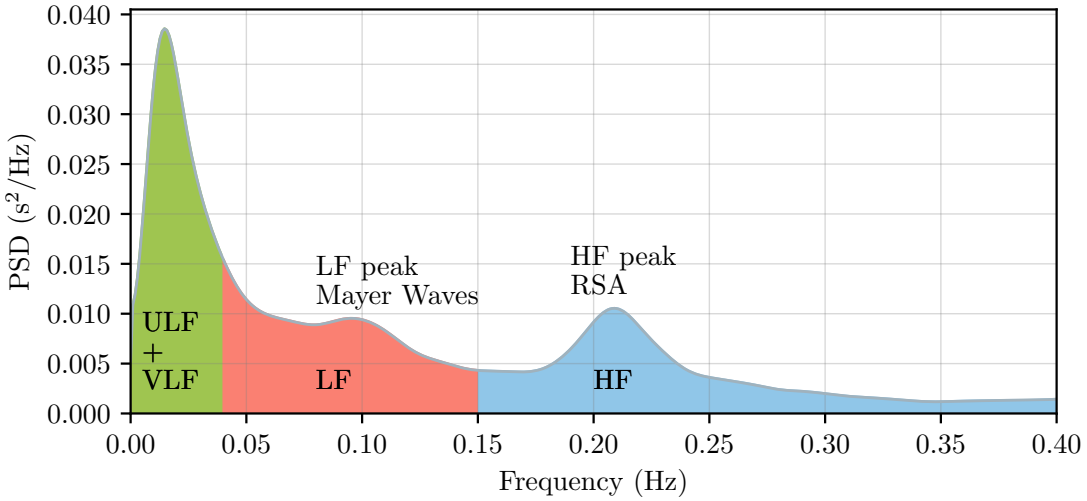

Figure 2.6: Example of a Power Spectral Density (PSD) of a 24-hour long NN time series belonging to a healthy young subject of the Normal Sinus Rhythm RR intervals database [78]. PSD was estimated using Fast Fourier transform with the Welch's method, using the *pyhrv* Python package [79].

The exact physiological mechanisms underlying very low and ultra low frequencies are not yet established, but they are thought to be related to day-night periodicities and changes due to the RAAS system, thermoregulation, and the peripheral vasomotor tone [62], [63].

Another striking observation, derived from the frequency domain analysis, is that the power spectrum of the human HR, measured over 24 h, exhibits a power-law, i.e., $1/f$, spectral behavior. This means that the variance of human HR tends to increase when examined on longer and longer time scales [77]. This propriety is typically evaluated with the application of complexity measures.

Figure 2.6 shows a power spectrum of a 24-hour NN time series obtained from a healthy young subject. In this spectrum, a peak in the HF band is apparent at a frequency of ~ 0.21 Hz (~ 5 s), which may be due to the RSA phenomenon; as well as peak in the LF band at a frequency of ~ 0.10 Hz (~ 10 s), which may reflect the Mayer waves. In this Figure is also visible the $1/f$ behavior of the power spectrum.

2.2.1.2 Heart Rate Variability Time Domain Measures

Time domain measures of HRV are generally based on the analysis of descriptive statistics applied to either the NN time series or to the NN increments time series [21]. These variables may be derived from analysis of the entire ECG recording or be calculated using smaller segments of it, typically, 5 min windows [21]. Windowed measures have the benefit of allowing the comparison of HRV to be made during varying activities. There are many time domain measures. We will highlight only a subset of those most widely used:

1. Standard deviation of NN intervals (SDNN): a measure which reflects all periodicities of the NN time series. Thus, when calculated over a 24 h period, SDNN merges high to very low frequency variations. However, about 30 % – 40 % of the variation captured by the SDNN measure is considered to be related to day-night changes [62], i.e, ultra low frequency variations.

2. Standard deviation of the average NN intervals calculated over 5-minute windows (SDANN): a measure which estimates changes in the NN time series due to periodicities longer than 5 min. It is similar to SDNN, but allows for comparisons between series of different lengths.

3. Average of the standard deviation of NN intervals calculated over 5-minute windows (SDNNI): a measure which correlates with both very low and low frequency HR variations.

4. Root Mean Square of Successive Differences (RMSSD) and Percentage of differences between adjacent NN intervals that are greater than 50 ms (PNN50) measures which associate with high frequency oscillations of the HR.

2.2.2 Heart Rate Fragmentation

As previously mentioned, higher short-term (high frequency) HRV, predominantly caused by the vagally-mediated RSA mechanism, is associated with better health. However, some studies have shown that higher short-term HRV is not always an indication of health. Instead, it may be associated with poorer clinical outcomes in the elderly and in cardiovascular diseases [22]–[27], [80]–[82]. This has been reported as the "HRV paradox".

In healthy young subjects, changes in vagal tone regulate the coupling between breathing and SAN depolarization (i.e., RSA). However, with progressive aging and emergence of cardiovascular diseases, beat-to-beat oscillations at a rate higher than that of PNS modulation often develop, giving rise to a type of abnormal, nonrespiratory sinus arrhythmia, which have been reported in diverse terms, e.g., sinus extrasystoles, sinus alternans, erratic heart rate, and complex HRV [22], [80]. All of these abnormal rhythms share the common trait of causing an appearance of peak and valley in the NN time series (sometimes at every beat), albeit the visible normal sinus rhythm on the ECG. Because these frequent abrupt reversals occur at a frequency higher than the changes mediated by the PNS, they tend to inflate HRV measures.

Recently, Costa et al. [23], [24] created the concept of Heart Rate Fragmentation (HRF) as a dynamical biomarker of disease that joins all mentioned abnormal HR patterns, which have been widely neglected in HRV analysis. They defined the fragmentation phenomenon as:

Frequent changes in heart rate acceleration sign, giving rise to an excessive inter-beat fluctuation at a rate higher than that attributable to healthy vagal tone modulation of the sinoatrial node.

An important note is that HRF is not an episodic phenomena; consequently, it can not be readily identified and filtered out with the aim of allowing a more reliable HRV traditional analysis [80]. Moreover, fragmented patterns in the NN time series are not random, instead, they present a short-term anticorrelated nature, which makes them more predictable than either uncorrelated or long-range correlated patterns. Thus, nonlinear methods might not be successful in capturing HRF [80].

Figure 2.7 shows an extremely fluent (top) and a highly fragmented (bottom) HR time series. The former corresponds to a healthy young subject and the latter to a patient with AF. It should be highlighted that both time series are obtained from ECGs that show a clear normal sinus rhythm. It is remarkable that in the most fragmented time series HR acceleration sign changes every beat (almost). Furthermore, the fragmented series is associated with higher RMSSD than the fluent one. Thus, this Figure illustrates how a fragmented series might be associated with high HRV.

2.2.2.1 Heart Rate Fragmentation Measures

Typically, the differences between a fluent rhythm and a fragmented one are not as apparent in the NN time series shown in Figure 2.7; thus, some statistical and symbolic metrics were defined to quantify the fragmentation propriety [23], [24].

To compute these metrics the increments time series, $\{\Delta NN_i\}$, is used to analyze the changes in HR acceleration sign. HR deceleration, acceleration, and no-change intervals (in seconds) are defined as $\Delta NN_i \geq \frac{1}{S_f}$, $\Delta NN_i \leq -\frac{1}{S_f}$, and $-\frac{1}{S_f} < \Delta NN_i < \frac{1}{S_f}$, respectively, where S_f is the sampling frequency of the ECG signal (in Hz). Sequences of HR accelerations/decelerations are termed accelerative (decelerative) segments. The length of a segment is given by the number of ΔNN intervals it contains.

HRF can be evaluated using the following statistical indexes [23], [27]:

1. Percentage of Inflection Points (PIP) is defined as the combined percentage of transitions from HR acceleration/deceleration to HR deceleration/acceleration, i.e., hard inflection points (H), and from HR acceleration/deceleration to no-change in HR and vice-versa, i.e., soft inflection points (S). A given NN_i interval is an inflection point if $\Delta NN_i \times \Delta NN_{i+1} \leq 0$ and $\Delta NN_i \neq \Delta NN_{i+1}$. The Percentage of Soft Inflection Points (PIP_S) or the Percentage of Hard Inflection Points (PIP_H) can also be considered.

2. Average Length of acceleration/deceleration Segments (ALS) is defined as the number of ΔNN intervals in accelerative/decelerative segments over the number of different segments.

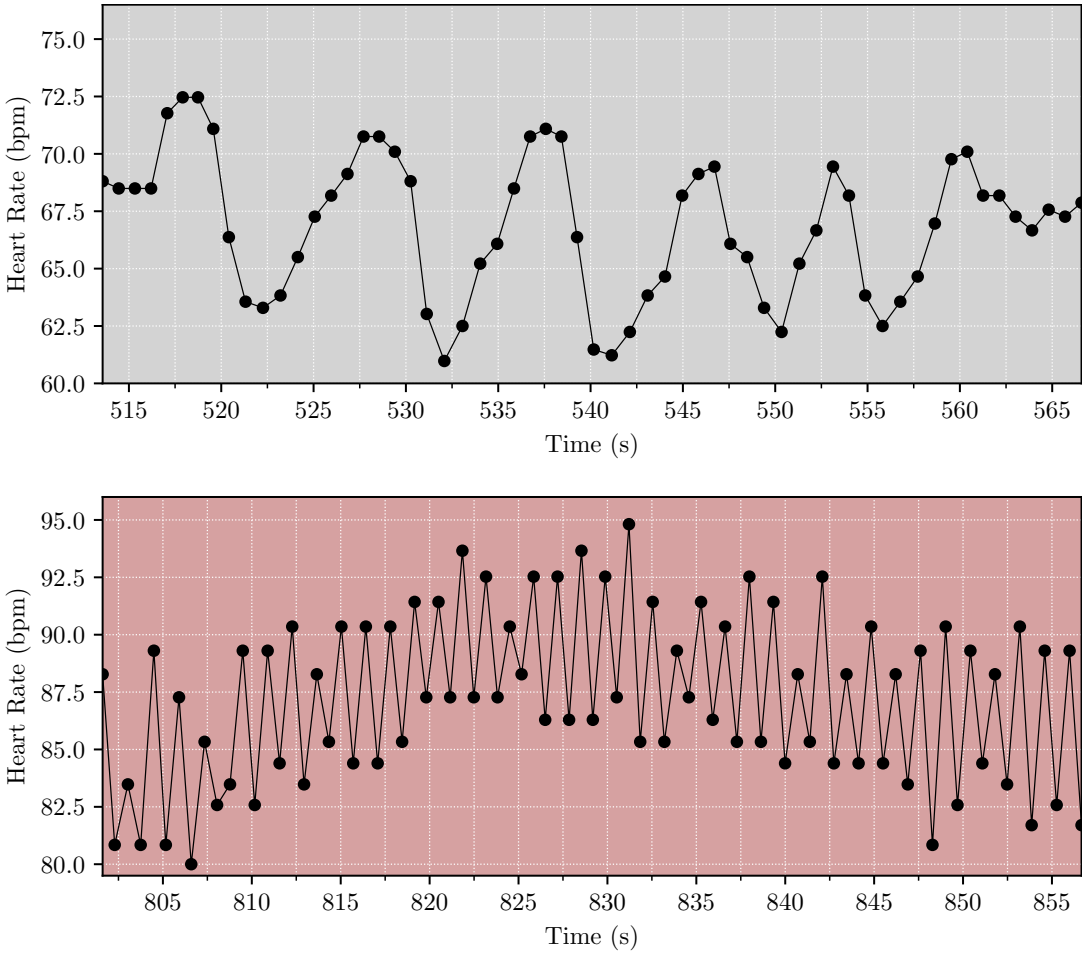

Figure 2.7: In the top row, it is presented a fluent HR time series, with a prominent periodicity with a cycle-length around 5 to 10 s, which might reflect the RSA mechanism. In the bottom row, it is presented a highly fragmented HR time series. The fluent series belongs to a healthy young subject from the Fantasia database [83] and the fragmented series belongs to a subject with AF from the Long-term AF database [84]. It should be noted that the fluent and fragmented series are associated, respectively, with a RMSSD of ~ 20 ms and ~ 37 ms.

3. Percentage of NN intervals in Short accelerative/decelerative Segments (PNNSS) is defined as the number of ΔNN intervals in short (< 3) accelerative/decelerative segments over the total number of ΔNN intervals in accelerative/decelerative segments of any length.

4. Percentage of NN intervals in Long accelerative/decelerative Segments (PNNLS) is defined as the number of ΔNN intervals in long (≥ 3) accelerative/decelerative segments over the total number of ΔNN intervals in the time series.

5. Percentage of NN intervals in Alteration Segments (PAS) is the percentage of sequences of, at least, four NN intervals, where the HR acceleration changes sign every beat. Such sequences follow an "ABAB" pattern, where "A" and "B" represent increments of opposite sign.

An illustrative example of the application of these metrics is given in Section 3.2.
Some features of the mentioned metrics include [23]:

- Higher values of PIP, PIP_S, PIP_H, PNNSS, PAS, and lower values of PNNLS, and ALS indicate a more fragmented (less fluent) time series. However, it should be noted that as PAS corresponds to a very particular pattern of fragmentation, i.e., alternation, a highly fragmented series might show low levels of PAS.
- Independence relatively to the mean HR (except for PAS) and to the amplitude of the NN time series.
- Reduced influence of nonstationarities.

To get a better insight into the temporal structure of fragmentation, Costa et al. [24] also created a symbolic analysis in which the NN time series is mapped to three symbols according to the following rules:

- "-1" signifies $\Delta NN_i < -1/S_f$
- "0" signifies $-1/S_f < \Delta NN_i < 1/S_f$
- "1" signifies $\Delta NN_i > 1/S_f$

These symbols are grouped into words (W) of length 4 increments (5 intervals), allowing the definition of 81 different words. Thus, each word corresponds to a time scale within short-term variations of the RSA mechanism.

A word is characterized by the number of inflection points it contains (j) and by their type of inflections, namely hard (H), i.e., transitions from "1" to "-1" or from "-1" to "1", soft (S), i.e., transitions from "-1" to "0", "0" to "-1", "1" to "0", and "0" to "1", or mixed (M). All possible words are presented in Table 2.1.

Word groups are labeled as:

- W_0 if there are no inflection points.
- W_j^H if it contains j hard infection points.
- W_j^S if it contains j soft infection points.
- W_j^M if it contains j inflection points of more than one type (soft and hard).
- W_j if it contains j inflection points independent of the type of inflection.

To measure the degree of HRF the percentage of each word group is computed in relation to the number of total words in the NN time series.

Typically, the least fragmented word groups correspond to W_0 and W_1^H, and the more fragmented correspond to W_3^M, W_2^M, W_H^3, and W_S^3. The other word groups – W_1^S, W_2^H, W_S^2 – have not yet a clear meaning regarding their degree of fragmentation.

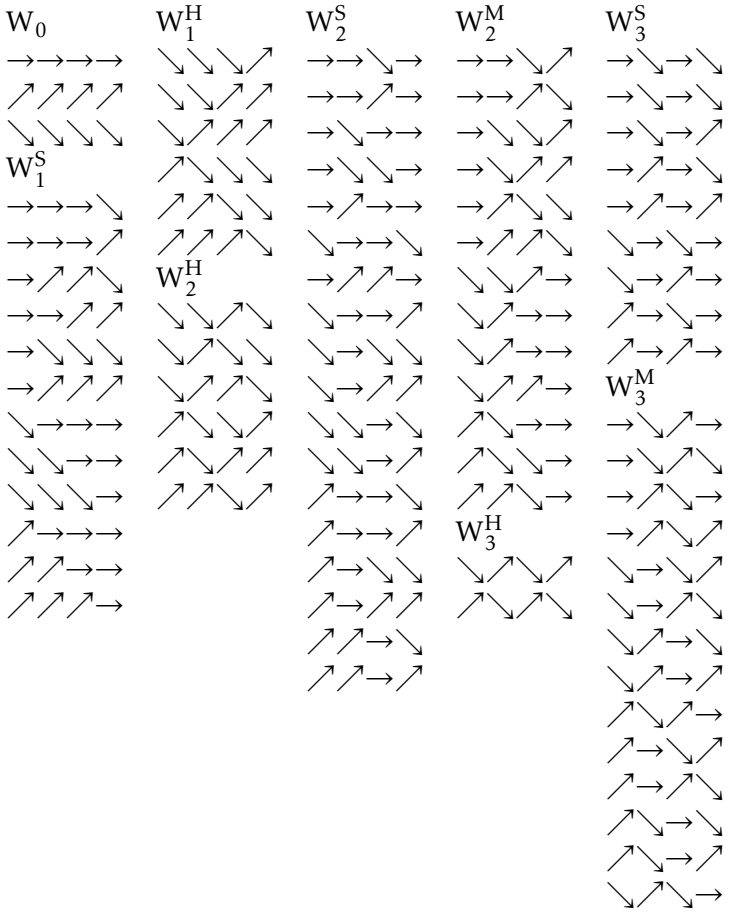

Table 2.1: Schematic representation of the 81 different dynamical words of length 4 increments used in HRF analysis. Each set of 4 arrows represents a word. The symbols "↗", "↘", and "→" represent HR acceleration, deceleration, and no change, respectively. Adapted from [27].

2.2.2.2 Physiological Origins of Heart Rate Fragmentation

The specific electrophysyiologic substrates of HRF are not yet fully understood. However, it is speculated that more than one mechanism may be contributory. These mechanisms include [23], [27], [80], [82]: (1) subtle atrial bigeminy[2] originating near or even within the SAN; (2) SAN modulated parasystole in which two pacemaker sites within the SAN complex show bidirectional coupling and appear to "compete" for the control of the heartbeat; (3) perturbations of internal pacemaker "clocks", i.e., intrinsic rates; and (4) transitory blockage of SAN intranodal pathways.

All of these possible mechanisms, and others that may cause HRF, in a broad sense, are thought to derive from abnormalities in the "autonomic-SAN-atrial network", that is from impairment of autonomic modulations, SAN complex, and from alterations in the proprieties (conduction and automaticity) of the atrial syncytium.

[2]Atrial bigeminy is a cardiac arrhythmia where sinus beats are consistently alternated by premature atrial contractions.

2.2.3 Phase Rectified Signal Averaging Approach - Acceleration and Deceleration Capacities of the Heart

As an effort for better quantification of periodicities in the NN time series, as well as with the aim of separating between sympathetic and parasympathetic modulations of the SAN activity, Bauer et al. [29]–[31] proposed a method for assessment of deceleration-related and acceleration-related HR dynamics. This is accomplished by employing the signal processing technique of PRSA to the NN time series.

It can be said that the NN time series consists of periodic patches that are interrupted by nonstationarities. This pertains because internal and external perturbations are constantly influencing the SAN activity causing interruptions of the periodic behavior, e.g., posture changes might interrupt the prevalent high frequency rhythm of the RSA fluctuations. These interruptions lead to phase de-synchronization of the rhythmic oscillations.

The PRSA technique compresses the NN time series into a smaller signal containing only the most prevalent quasi-periodicities.

We now describe how the PRSA signal is obtained and how acceleration/decelaration-related HR dynamics are quantified separately.

In the *first step*, a subset of NN intervals from the NN time series are selected as anchor points, according to a certain propriety. To quantify acceleration/deceleration, increasing/decreasing events are selected as anchor points. This selection may take into consideration T values of the time series; thus, to test if a NN interval, NN_i, is a deceleration anchor the following comparison is made:

$$\frac{1}{T}\sum_{j=0}^{T-1} NN_{i+j} > \frac{1}{T}\sum_{j=1}^{T-1} NN_{i-j} \tag{2.2}$$

conversely, the test for an acceleration anchor corresponds to:

$$\frac{1}{T}\sum_{j=0}^{T-1} NN_{i+j} < \frac{1}{T}\sum_{j=1}^{T-1} NN_{i-j} \tag{2.3}$$

The quasi-periodic oscillations of the NN time series will cause anchor points predominantly in the phase of steepest ascent or decent. The T parameter sets an upper frequency limit for the periodicities that can be detected, i.e., functions as a low-pass filter.

In the *second step*, windows of length $2L$ are defined around each anchor point. Denoting the positions of all selected anchor points by i_v, $v = 1,...,M$, where i represents the index of the anchor point and v the window number. The intervals included in the window number v, corresponding to the anchor point i_v, will be:

$$NN_{i_v-L}, NN_{i_v-L+1}, ..., NN_{i_v}, NN_{i_v+L-2}, NN_{i_v+L-1} \tag{2.4}$$

Anchor points close to the beginning or the end, where no full surroundings of length $2L$ exist, are neglected. L is typically chosen as the period of slowest oscillation that it is intended to be detected, i.e., coherence time.

In the *third step*, two PRSA signals are obtained (one for acceleration anchors and another for deceleration ones), denoted as $\overline{NN_{PRSA}}(k)$, by averaging over all windows,

$$\overline{NN_{PRSA}}(k) = \frac{1}{M}\sum_{v=1}^{M} NN_{i_v+k} \text{ for } k = -L, -L+1, ..., 0, ..., L-2, L-1 \tag{2.5}$$

With this average, non-periodic components that are not phase synchronized with the anchor points, i.e., nonstationarities, will cancel out, given their random nature. Thus only events that have a fixed phase with the anchor points will "survive".

Finally, in the *fourth step*, acceleration and deceleration capacities are computed using the four central points of the PRSA curve as follows[3]:

$$AC(DC) = \frac{1}{4}(\overline{NN_{PRSA}}(0) + \overline{NN_{PRSA}}(1) - \overline{NN_{PRSA}}(-1) - \overline{NN_{PRSA}}(-2)) \tag{2.6}$$

Typically, AC and DC are calculated using $T = 1$, this ensures that high frequency oscillations are well captured.

An example of computation of these PRSA indices will be shown in Section 3.2

AC and DC measures estimate the average capacity of the heart to quickly decelerate/accelerate the HR. Thus, lower AC and DC are associated with poorer health. The authors of these analysis method argued that AC and DC quantify sympathetic and parasympathetic activity separately. However, one might argue that this is an oversimplified assertion, since decreasing events of HR may be caused by both increased parasympathetic activity or decreased sympathetic activity.

Figure 2.8 shows three PRSA signals computed for acceleration anchor points, using windows of length 128 and $T = 1$, as well as the absolute value of AC associated with the PRSA signal. The top plot is representative of a healthy subject with an elevated AC, whereas the other two plots are representative of individuals with poorer health, with lower AC values. Note that a PRSA signal associated with a low AC may be due to a short distance between $\overline{NN_{PRSA}}(0)$ and $\overline{NN_{PRSA}}(-1)$ (middle plot) or/and due to $\overline{NN_{PRSA}}(1)$ being higher than $\overline{NN_{PRSA}}(-2)$ (bottom) plot.

This approach has proven to be useful to predict mortality after myocardial infarction [30], monitoring fetal distress [32]–[34], and as an independent risk factor for dilated cardiomyopathy and heart failure [35], [36].

2.3 Statistical Concepts

We will now present the main concepts underlying the statistical analysis performed in the present dissertation. We will (1) describe the main concepts related with likelihood,

[3] Technically, this expression corresponds to a quantification of the amplitude of the PRSA signal by Haar wavelet analysis, where the scale of 2 is used [31].

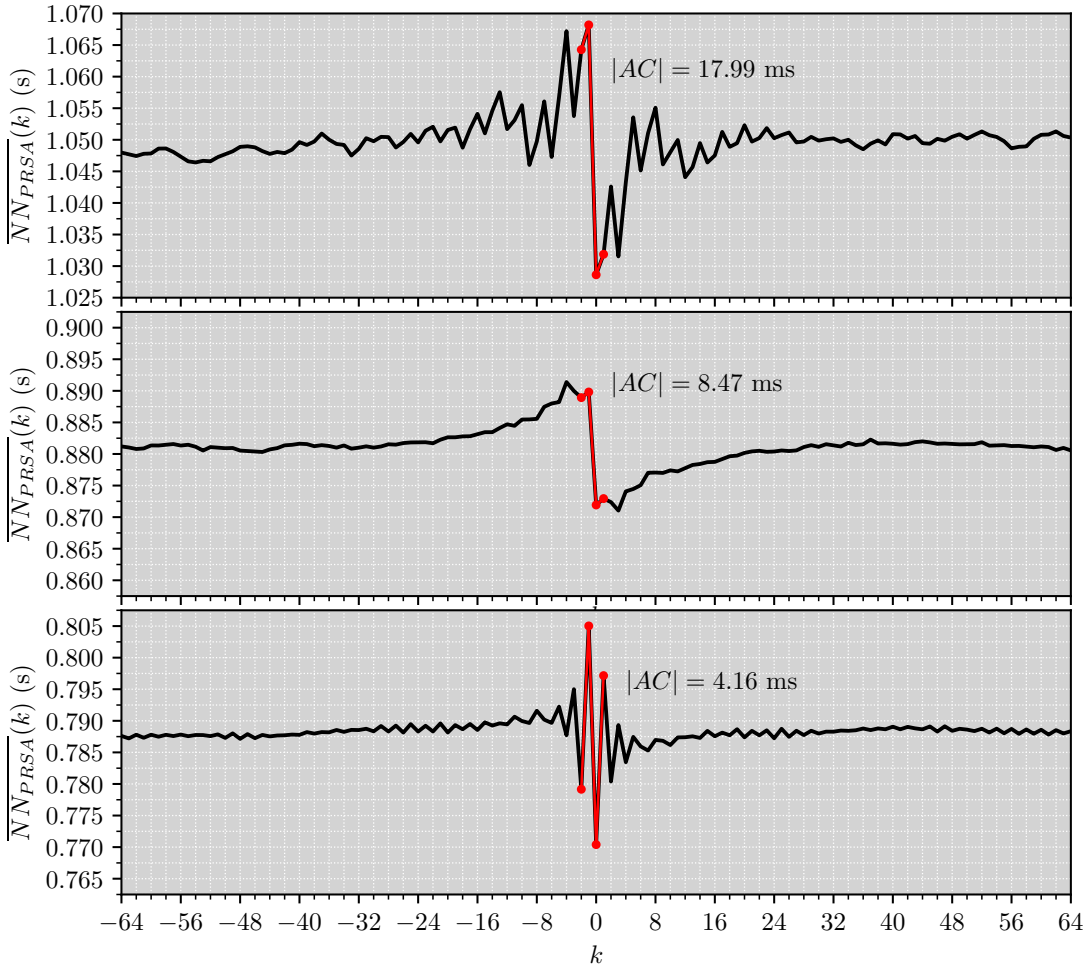

Figure 2.8: PRSA signals, computed for acceleration anchor points, and respective AC indices from NN time series belonging to a young healthy subject (top), an old healthy subject (middle), both from the fantasia database [83], and a patient with AF (bottom) from the long-term AF database [84]. The PRSA signal were obtained using segments of length 128 and the selection of anchor points was made using $T = 1$. In red are highlighted the points used for computation of AC index.

which will be needed for the comprehension of the logistic linear regression analysis and the likelihood ratio test; (2) present the simple and logistic linear regression models as cases of the generalized linear model; (3) explain two measures of correlation, namely, Pearson Product-Moment Correlation Coefficient and Spearman Rank Correlation Coefficient; and (4) present the main statistical hypothesis tests used to compare between two populations, as well as a statistical test used to compare between models.

2.3.1 Likelihood, Likelihood Function, Log-Likelihood, and Likelihood Ratio

A stochastic process may be described by a discrete random variable Y, whose possible values are associated with a probability distribution function characterized by certain assumed parameters θ_0, $P(Y;\theta = \theta_0)$. Assuming this distribution, one might find the

probability of Y taking a certain value y_i, that is $P(Y = y_i; \theta = \theta_0)$.

Computing the likelihood is the reverse of computing the probability. Instead of calculating the probability of a certain observation from a probability distribution with known parameters, $P(Y = y_i|\theta = \theta_0)$, one might want to find the most plausible parameters for a given set observed values of Y. The likelihood of a parameter $\theta = \theta_0$ is defined for fixed values of Y, and corresponds to:

$$L(\theta_0; y) = P(Y = y|\theta = \theta_0) \tag{2.7}$$

For a given set of values of Y, likelihood can be calculated for all possible values for the parameters of the assumed distribution. This corresponds to a likelihood function,

$$L(\theta) = L(\theta; y) \tag{2.8}$$

For the random variable Y with observed values $y_1, y_2, ..., y_n$ the likelihood function is defined as the joint probability distribution function of observing $y_1, y_2, ..., y_n$ for every possible value of θ [85], that is,

$$\begin{aligned} L(\theta) &= P(Y = y_1, Y = y_2, ..., Y = y_n; \theta) \\ &= P(Y = y_1; \theta)P(Y = y_2; \theta)...P(Y = y_n; \theta) \\ &= \prod_{i=1}^{n} P(Y = y_i; \theta) \end{aligned} \tag{2.9}$$

The first equality comes from the definition of joint probability, the second one comes from the fact that Y is a random variable, thus $y_1, y_2, ..., y_n$ are independent random samples.

In most cases, for various reasons, but often for computational convenience, the log-likelihood function $l(\theta)$ is used instead, since it transforms the products in sums,

$$l(\theta) = \sum_{i=1}^{n} \log P(Y = y_i; \theta) \tag{2.10}$$

It should be noted that the exact value of any likelihood is meaningless. Usually, the likelihood ratio (LR), which is the ratio between two likelihoods,

$$LR = \frac{L(\theta_1)}{L(\theta_0)} \tag{2.11}$$

is used to make inferences.

2.3.2 Regression Analysis

Regression analysis is used to evaluate the relationship between a response variable Y, i.e., dependent variable, and one or more explanatory variables $X_1, ..., X_k$, i.e., independent variables. Typically, the response variable corresponds to the quantity we are trying to

predict or whose variation we are trying to explain; the explanatory variables correspond to the quantities we are using to predict or explain the variation of the response variable.

For a given set of observed explanatory variables $(x_1,...,x_k)$, for stochastic processes, the response variable Y is not fixed, that is Y is a random variable with an associated probability distribution. In board terms, regression analysis traces this conditional distribution of Y – or some aspect of it, generally its mean, – as a function of the explanatory variables $X_1,...,X_k$ [86], that is:

$$p(y|x_1,..,x_k) = f(x_1,..,x_k) \tag{2.12}$$

Here, $p(y|x_1,...,x_k)$ represents the probability distribution of observing the specific value y of the response variable Y, given (conditional on) a set of specific values $(x_1,...,x_k)$ of the explanatory variables $(X_1,...,X_k)$.

The most common method of regression analysis is linear regression analysis, which assumes a linear relationship between some parameter of the distribution of Y and the explanatory variables. However, depending on the type of the response variable we are studying, the distribution assumed for Y may vary, as well as the way this distribution relates to a linear combination of the explanatory variables.

2.3.2.1 The Generalized Linear Model

The most generalized form of linear regression analysis is described by the **Generalized Linear Model (GLM)**. We will start by presenting the GLM and then from this model particularize for the two types of linear regression used in the present dissertation, namely, simple linear regression and logistic linear regression.

The GLM consists of three components [86]:

1. A *random component* that specifies the conditional distribution of the response variable Y, given the values of the explanatory variables; e.g., normal distribution or binomial distribution.

$$Y \sim \text{some distribution} \tag{2.13}$$

2. A *linear predictor* or *systematic component* which refers to a linear combination of the explanatory variables.

$$\eta = \beta_0 + \beta_1 X_{i1} + \beta_2 X_{i1} + ... + \beta_k X_{ik} \tag{2.14}$$

3. A *link function*, f, which specifies $\theta = f(\eta)$ connecting the chosen parameter θ of the distribution of Y with the X's of the linear predictor η. This is the link between the random component and the systematic component.

In simple linear regression $Y \sim$ Normal distribution, the parameter θ corresponds to the mean value of this distribution and the link function is the identity.

In logistic linear regression, $Y \sim$ Bernoulli distribution, the parameter θ corresponds to the probability of success associated with the Bernoulli distribution.

2.3.2.2 Simple Linear Regression

When the response variable of interest is said to be quantitative, i.e., numerical, the first and most used approach is simple linear regression. This type of linear regression assumes that each y_i of the response variable Y follows a normal distribution with a variance equal for all y_i and that the mean value of each y_i, $\mathrm{E}(Y|x_i)$, corresponds to a linear combination of the explanatory variables.

$$\mathrm{E}(Y|x_i) = \beta_0 + \beta_1 x_1 + ... + \beta_k x_k \tag{2.15}$$

Thus, in the light of the GLM the random component in simple linear regression is assumed to be normally distributed with equal variance, σ^2, for all realizations of Y; and the link function is the identity.

Consequently, in simple linear regression:

$$Y \sim N(\beta_0 + \beta_1 x_1 + ... + \beta_k x_k, \sigma^2) \tag{2.16}$$

It should be noted that the explanatory variables themselves can be transformed, e.g., X^2 or $log(X)$. Thus, the response variable Y can be modeled by a n^{th} degree polynomial.

To find the regression coefficients, $\beta_0, \beta_1, ..., \beta_k$, usually the method *Ordinary Least-Squares Fit* is used. This method finds the combination of regression coefficients that minimize all of the squared distances between the observed values of y_i and the predicted values of y_i, $\hat{y_i}$. That is,

$$\min_{\beta_0,\beta_1,...,\beta_k} : \sum_{i=1}^{n} [y_i - (\beta_0 + \beta_1 x_{i1} + ... + \beta_k x_{ik})]^2 \tag{2.17}$$

where $\min_{\beta_0,\beta_1,...,\beta_k}$ means minimize over $\beta_0, \beta_1, ..., \beta_k$, n is the number of observed values, and i represents the n^{th} observation.

To measure the goodness of the fit of a simple linear regression model typically correlation coefficient [86]. The correlation coefficient, denoted as r, is defined as ratio of the variation explained by the model to the total variation in the observed response variables.

Total variation corresponds to the sum of squared distance between each observed response, y_i, and the mean of all observed y_i, $\overline{Y}$ – typically called Total Sum of Squares (TSS),

$$TSS = \sum_{i=1}^{n} (y_i - \overline{Y})^2 \tag{2.18}$$

Conversely, the variation not explained by the model corresponds to the sum of squared distances between each estimate response, $\hat{y_i}$ and the observed value y_i – typically called Residual Sum of Squares (RSS),

$$RSS = \sum_{i=1}^{n} (y_i - \hat{y_i})^2 \tag{2.19}$$

Thus, the variation that is explained by the model corresponds to difference between TSS and RSS, and the correlation coefficient (r) can be defined as:

$$r = \sqrt{\frac{TSS - RSS}{TSS}} \tag{2.20}$$

Some times the square of r is used, being called coefficient of variation and represented by R^2.

2.3.2.3 Logistic Regression

When the response variable of interest is binary, e.g. healthy *versus* non-healthy, logistic linear regression is generally used. In this context, each response variable can either take the value one for success or zero for failure.

$$y_i = \begin{cases} 1 \text{ if success} \\ 0 \text{ if failure} \end{cases} \tag{2.21}$$

A binary random variable is typically associated with a Bernoulli distribution, thus:

$$Y \sim \text{Bernoulli}(p) \tag{2.22}$$

where p represents the probability of success.

As a probability $p \in [0,1]$. For the linear predictor $\eta = \beta_0 + \beta_1 X_{i1} + ... + \beta_k X_{ik}$, which can yield any real value, $\eta \in [-\infty, +\infty]$, to be bounded between one and zero, it has to be transformed with a link function f that maps $[-\infty, +\infty] \rightarrow [0,1]$. In logistic regression this link function corresponds to the logistic function,

$$f(\eta) = \frac{e^{\eta}}{1 + e^{\eta}} \tag{2.23}$$

which is a sigmoid function.

Thus, in logistic regression the response variable Y relates with the set of explanatory variables as follows:

$$Y = P(Y = 1|X) = p = \frac{e^{\beta_0 + \beta_1 X_1 + ... + \beta_k X_k}}{1 + e^{\beta_0 + \beta_1 X_1 + ... + \beta_k X_k}} \tag{2.24}$$

To find the regression coefficients and for interpretation purposes of these coefficients, the inverse of f is applied on the response variable, thus,

$$f^{-1}(p) = \log\left(\frac{p}{1-p}\right) = \beta_0 + \beta_1 X_1 + ... + \beta_k X_k \tag{2.25}$$

$\log(p/(1-p))$ has a meaningful interpretation, it corresponds to the log-odds, where the odds corresponds to $(p/(1-p))$.

Thus, it follows that the regression coefficients can be interpreted as the increase in log-odds per unit increase of the value associated with the explanatory variable. As

increases in terms of log-odds are difficult to interpret, odds ratio are used instead. Odds in this regression model is obtained by the following equation:

$$odds = \frac{p}{1-p} = e^{\beta_0+\beta_1 X_1+...\beta_k X_k} \tag{2.26}$$

For a given explanatory variable used, odds ratio corresponds to the magnitude of change in the odds of success with the unit increase in that explanatory variable, holding all others constant. Thus, the odds ratio associated with a given explanatory variable X_1, can be computed as follows:

$$\text{odds ratio} = \frac{odds(X_1+1)}{odds(X_1)} = \frac{e^{\beta_0+\beta_1(X_1+1)+...\beta_k X_k}}{e^{\beta_0+\beta_1(X_1)+...\beta_k X_k}} = e^{\beta_1} \tag{2.27}$$

The best set of regression coefficients $\beta_0, \beta_1, ..., \beta_k$ is obtained through *maximum likelihood estimation* [86]. Briefly, this method finds the set of regression coefficients that maximizes the log-likelihood function associated with the observed set of response-explanatory pairs – $\{(y_1, x_1, ..., x_k), ..., (y_n, x_1, ..., x_k)\}$ –, that is,

$$\underset{\beta_0,\beta_1,...,\beta_k}{argmax} : \sum_{i=1}^{n} \log P(Y = y_i|X, \beta) \tag{2.28}$$

By inputting different values of observed explanatory variables, $x_1, ..., x_k$, in the constructed logistic regression model, one obtains the probability of these explanatory variables being associated with a successful event, $P(y_i = 1|x_1, ..., x_k; \hat{\beta})$. However, typically, a binary outcome, i.e., $\hat{y_i} = 0$ or $\hat{y_i} = 1$, is what is being pursuit when using a logistic regression. The transition from an estimated probability to an estimated discrete binary outcome is usually attained by applying a threshold, c, to the probability obtained. For example, one might say that for an estimated probability above 0.5, $P(y_i = 1|x_1, ..., x_k; \hat{\beta}) > 0.5$, the event associated with the set of used explanatory variables is a success, $\hat{y_i} = 1$, whereas below or equal to 0.5 is a failure, $\hat{y_i} = 0$.

To evaluate the performance of the logistic model constructed, the estimated response binary outcomes, $\hat{y_i}$, are compared with observed responses, y_i. This is done by computing the Area Under the Curve (AUC) of the Receiver Operating Characteristic Curve (ROC) [87]. The ROC curve is obtained by plotting, for all possible threshold values, c, the proportion of correctly estimated successes – true positive rate (TPR) – that corresponds to:

$$TPR = \frac{\text{number of } \hat{y_i} = 1 \text{ when the corresponding } y_i = 1}{\text{number of } y_i = 1} \tag{2.29}$$

against the proportion of correctly estimated failures – true negative rate (TNR) – that corresponds to:

$$TNR = \frac{\text{number of } \hat{y_i} = 0 \text{ when the corresponding } y_i = 0}{\text{number of } y_i = 0} \tag{2.30}$$

Thus, the ROC curve summarizes the goodness of the fit of the logistic regression across all possible threshold values. Typically, the higher the area under this curve, i.e., AUC, the better it performs.

2.3.3 Measures of the Dependence between two Variables

2.3.3.1 Pearson Product-Moment Correlation Coefficient

The most commonly used measure to evaluate the dependence between two variables, X and Y, is the Pearson product-moment correlation coefficient, r_p. The Pearson coefficient measures the strength of a linear association, being defined as the covariance between X and Y divided by the product of the standard deviation of X and Y:

$$r_p = \frac{\text{cov}(X, Y)}{\sigma_X \sigma_Y} \tag{2.31}$$

From the definition of $\text{cov}(X, Y)$ and standard deviation, it follows that:

$$r_p = \frac{\sum_{i=1}^{n}(x_i - \overline{x})(y_i - \overline{y})}{\sqrt{\sum_{i=1}^{n}(x_i - \overline{x})^2}\sqrt{\sum_{i=1}^{n}(y_i - \overline{y})^2}} \tag{2.32}$$

2.3.3.2 Spearman Rank Correlation Coefficient

When a linear relationship is not assumed between two variables, Y and X, there is a non-parametric version of the Pearson coefficient, the Spearman rank correlation coefficient, that can be used to evaluate the degree of association between Y and X. The Spearman coefficient, r_s, measures how well the relationship between Y and X can be described by a monotonic function.

The Spearman coefficient is equivalent to calculating the Pearson coefficient using the equation 2.31 with the ranks of Y and X, $\text{R}(Y)$, $\text{R}(X)$, instead of their observed values [88]:

$$r_s = \frac{\text{cov}(\text{R}(X), \text{R}(Y))}{\sigma_{\text{R}(X)} \sigma_{\text{R}(Y)}} \tag{2.33}$$

2.3.4 Summary of some Important Statistical Tests

In this section, we will briefly present the main statistical tests performed in the present dissertation, so that the reader may refer to this section for clarification of their use.

2.3.4.1 Tests for Normality and Equal variance

Parametric statistical tests can only be applied when some assumptions of the sampled populations are verified. In particular, most of parametric tests assume that the samples being analyzed are drawn from normally distributed populations and that these distributions share the same variance. An example of a normality test is the Shapiro-Wilk test [89], [90]. An example of a test of equal variance is the Levene's test [91].

2.3.4.2 Independent Two-Sample T-Test

The independent two-sample T-test tests if two samples from different populations are drawn from normal distributions with equal means [92]:

$$H_0 : \mu_1 = \mu_2$$
$$H_1 : \mu_1 \neq \mu_2$$

The test statistics, t, for this test is calculated by taking the difference in the two sample means and dividing by the pooled standard error, that is,

$$t = \frac{\mu_1 - \mu_2}{s_p \sqrt{\frac{1}{n_1} + \frac{1}{n_2}}} \tag{2.34}$$

where s_p is the pooled standard deviation which corresponds to:

$$s_p = \sqrt{\frac{(n_1 - 1)s_1^2 + (n_2 - 1)s_2^2}{n_1 + n_2 - 2}} \tag{2.35}$$

where s_1 is the estimated variance for population 1 and s_2 is the estimates variance for population 2. This test assumes that two populations are both normally distributed and have equal variances.

If the two samples are known to come from the same population a paired T-test (or also called dependent T-test) is used to compare between the mean of the two samples.

2.3.4.3 Paired T-test

The paired T-test is used to evaluate the equality of two dependent samples, i.e., two sets of measures for the same population.

In a paired T-test, the test statistic t, is computed as follows:

$$t = \frac{\mu_1 - \mu_2}{\frac{1}{\sqrt{n}} s_d} \tag{2.36}$$

where s_d corresponds to the estimated standard deviation of the differences between the two sets of measurement, i.e, paired measures.

To perform this test the normality of the differences between paired measures should be ensured.

2.3.4.4 Welch's Test

The Welch's Test is a variant of the independent two-sample T-test for populations samples with unequal variances [92].

The test statistic used in this test is similar to that used in the independent two-sample T-test, it differs in the denominator,

$$t = \frac{\mu_1 - \mu_2}{\sqrt{\frac{s_1^2}{n_1} + \frac{s_2^2}{n_2}}} \tag{2.37}$$

where s_1 is the estimated variance for population 1 and s_2 is the estimates variance for population 2.

2.3.4.5 Wilcoxon Rank-Sum Test

The Wilcoxon Rank-Sum Test [93] evaluates if two samples come from the same population. It can be said to be a non-parametric alternative for the independent two-sample T-test. Given two independent samples, it tests whether one variable tends to have values higher than the other [94]. This, results in testing if the two populations have the same median (η):

$$H_0 : \eta_1 = \eta_2$$
$$H_1 : \eta_1 \neq \eta_2$$

This test is performed by ranking all observations and then finding the sum of the ranks in each sample. If the values in one sample are generally higher than in the other, the rank sums will differ. The test statistic U [93] is a measure of the difference in rank sums that is typically used in this setting.

For paired samples Wilcoxon signed-rank test should be used as an alternative. In this test the sign of the differences between paired measures are evaluated [95].

2.3.4.6 Likelihood Ratio Test

The Likelihood Ratio Test is used to compare between two competing statistical models, one model with restricted parameters and other with unrestricted parameters [92].

Let L_1 represent the maximum value of the likelihood function with an unrestricted set of parameters θ_1. Let L_0 represent the maximum value of the likelihood function with restricted parameters θ_0, i.e., L_0 has less parameters than L_1.

In the likelihood ratio test, the ratio between L_0 and L_1, $\lambda = \frac{L_0}{L_1}$ is computed. If L_0 is higher than L_1, it means that the parameters associated with L_0 are more likely than the parameters associated with L_1. Thus, the extra parameters associated with L_1 do not improve the model used.

To make inferences about the ratio λ, a Chi-Squared test is often used.

3

General Methods

3.1 Databases

In this dissertation, six databases from Physionet were analyzed, namely, Normal Sinus Rhythm RR Intervals Database (NSRdb) [78], Fantasia Database [83], Autonomic Aging Database (AAdb) [96], Long Term AF Database (LTAFdb) [84], Congestive Heart Failure Database (CHFdb) [78], [97], and RR Intervals Time Series From Healthy Subjects Database (RRHdb) [98]. These databases will be appropriately described later in the chapters where their analyses are made, namely: NSRdb, AAdb, and Fantasia databases in Section 4.3; LTAFdb database in Section 5.1.3; CHFdb database in Section 5.2.3; and RRHdb database in Section 6.3. All of these databases contained beat annotations, except for the AAdb database. The annotation of the AAdb was performed in this work as explained in Section 3.2.

The beat annotations indicate the times of occurrence and types of each individual heart beat, i.e., an R-peak in the ECG. The types of beats generally covered by these annotations include normal beats (N), permature ventricular beats (V), permature atrial beats (A), supraventricular premature or ectopic beats (atrial or nodal) (S), and unclassifiable beats (Q). Beyond the type of beat, there were also annotations regarding the change in signal quality in a given set of beats. The CHFdb and LTAFdb databases further contained annotations regarding the onset and termination of arrhythmias. Typically, the beat annotations of these databases were automatically obtained and manually reviewed by the providers of the databases, except for a portion of the CHFdb database.

It should be noted that the study populations underlying these databases had their approval granted by Institutional Review Boards or ethics committees.

3.2 Methods

The work done in the following next four chapters was made using the programming language Python and occasionally Matlab.

For the statistical analysis some specific Python packages were used such as *scipy* [99]

and *statsmodel* [100]. However, likelihood ratio tests were not provided by these packages, thus we implemented this test.

To read the annotations of Physionet databases, the Python *WFDB* [101] package was used. This packages allows the extraction of ECG signals and beat annotations from the different type of files provided by the physionet databases used.

Beat annotations for the AAdb were obtained with the Matlab *ECG-Kit* module [78], [102], using the a Wavelet-Based ECG Delineator [103] implemented in this module.

All HR dynamical indices used in this dissertation were implemented in Python as described in Section 2.2. Namely, we implemented (1) SDNN, SDANN, SDNNI, PNN50, and RMSSD for HRV analysis; (2) both PRSA indices were computed using $T = 1$ and $L = 5$, which best capture high-frequency modulations of HR; (3) all HRF indices, mentioned in Section 2.2.2.1, were implemented, however, the fragmentation word groups with 2 inflection points, as well as the word group W_1^S were disregarded from most of the analyses made, given some ambiguity regarding their classification as fragmented or as fluent indices.

The RR time series for each database were obtained by computing the difference between the time occurrences of heart beats identified by the annotations provided by the databases. To obtain the NN time series from the RR time series all intervals containing abnormal beat annotations, i.e., different than NN, or with lengths lower than 0.3 s (200 bpm) or higher than 2 s (30 bpm) were removed.

For PRSA analysis only NN intervals were eligible for anchors, and the segments surrounding the anchors containing abnormal intervals were discarded from the computation of the PRSA signal.

For HRF analysis any accelerative/decelerative segments containing abnormal intervals were removed.

For computation of SDANN and SDNNI indices, 5-min windows with a step of 30 s were used. Windows containing at least one NN interval were included. These choices were made in order to maximize the number of windows used to compute these metrics.

3.2.1 An Example of Application of HRF and PRSA Indices

We now take a closer look on how HRF and PRSA analyses were implemented using an ECG excerpt from a subject in the Fantasia database with more than 65 years.

In Figure 3.1, we show the excerpt of the ECG (top row), as well as the NN time series (bottom row) with the intervals used for HRF analysis marked with red circles. Note that one of the identified beats is a premature ventricular beat (not a sinus beat). The first and last intervals of the NN time series are not considered for HRF analysis, since we do not have past and forward dynamical information to infer if it corresponds to a inflection point or if it belongs to an accelerative, decelerative, or no change segment. The data points #16 and #17 (the ones out of range) correspond to intervals containing the abnormal beat, that is the beat identified in the ECG with a red cross. These beats are

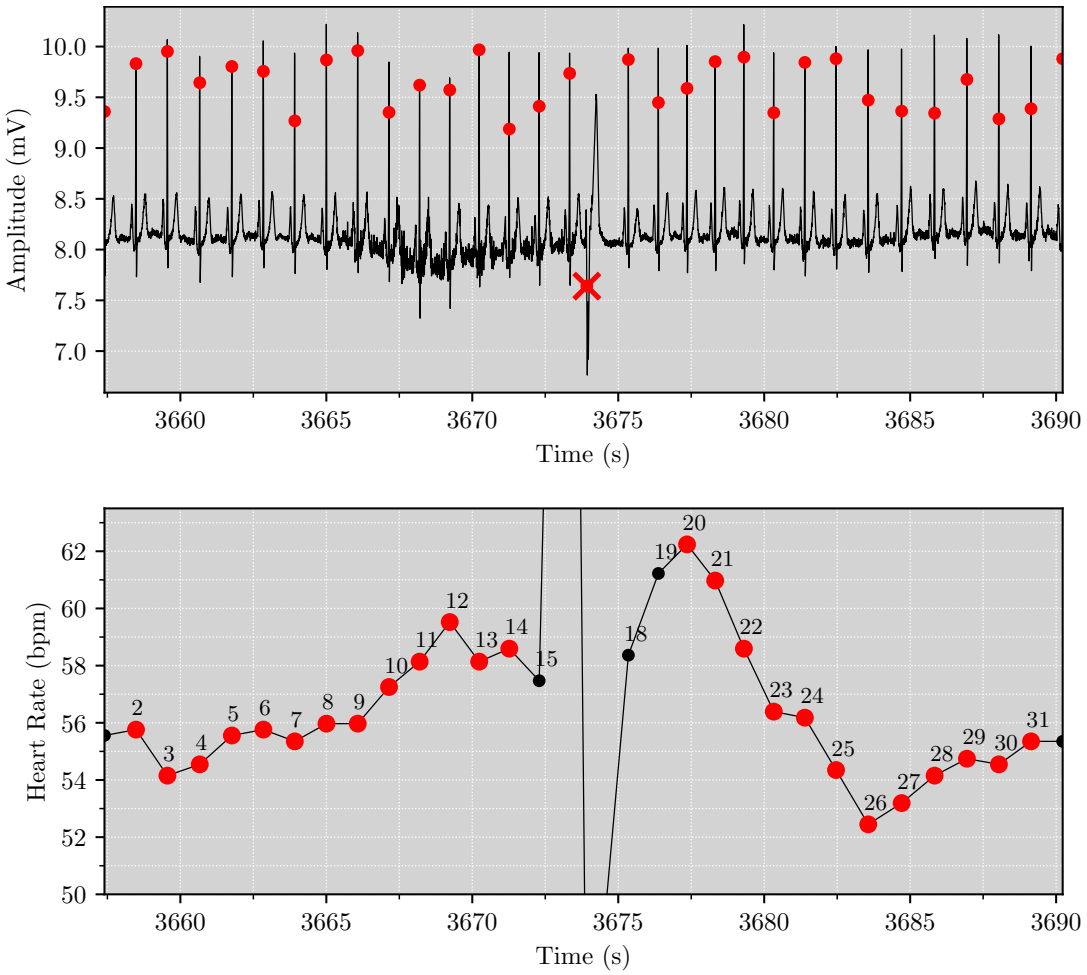

Figure 3.1: Electrocardiogram from a healthy old subject from the Fantasia Database (top). Red circles mark the occurrence of a normal beat, the red cross marks the occurrence of an abnormal beat. RR time series (bottom) with normal intervals eligible for HRF analysis marked with red circles. Each interval is associated with an identification number.

disregarded from the analysis. From interval #14 to interval #15 a decelerative segment is starting, however, as it is interrupted by the abnormal intervals we do not have information about the end of this segment, thus, this interval is excluded; from interval #18 to interval #20 there is an accelerative segment, however, we do not have information about its beginning, thus, these two intervals contained in this accelerative segment are disregarded.

In Figure 3.2, we present the main features of the NN time series used to make HRF analysis. In this excerpt, we highlight the following features:

1. 27 NN intervals and 24 ΔNN intervals were identified. The former are highlighted in red circles, and the later correspond to the lines linking those NN intervals.

2. 14 inflection points were identified (shown as yellow diamonds), from which 3 are soft and 11 are hard.

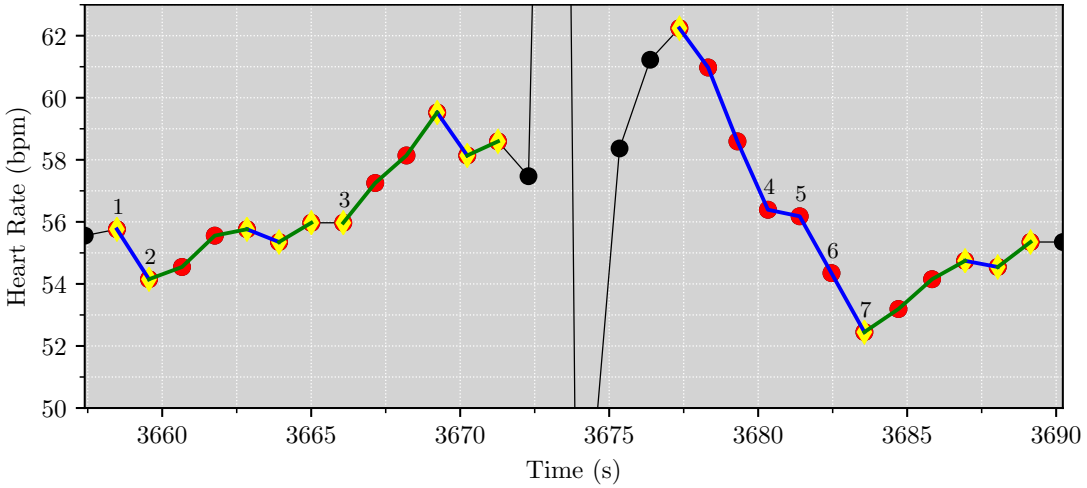

Figure 3.2: Illustration of the main features of the heart rate time series used in HRF analysis. Yellow diamonds highlight inflection points; blue lines indicate decelerative segments; green lines indicate accelerative segments; red circles (superimposed or not with yellow diamonds) indicate heart rates included in HRF analysis. The numbers indicate the beginning of dynamical words contained in the W_1^H word group.

3. 11 accelerative/decelerative segments were identified (marked with green/blue lines) with lengths $\underline{1}$, $\underline{3}$, and $\underline{6}$ being present 7, 3, and 1 times in the series, respectively.

4. 22 ($7\times\underline{1}+3\times\underline{3}+1\times\underline{6}$) ΔNN intervals were identified in the accelerative/decelerative segments.

From these features it is possible to conclude that PIP is 52% (PIP = $(14/27)\times 100$); PIP_S is 11% ($PIP_S = (3/27)\times 100$); PIP_H is 41% ($PIP_H = (11/27)\times 100$); PNNSS is 32% (PNNSS = $((7\times\underline{1})/22)\times 100$); PNNLS is 63 % (PNNLS = $(3\times\underline{3}+1\times\underline{6})/22)\times 100$); and ALS is 2 (ALS = 22/11).

To compute the percentage of the HRF word groups, each sequence of 5 consecutive NN intervals is translated into a word, following the rules mentioned in Section 2.2.2.1, and then the occurrences of words in each respective word group is counted and divided by all possible sequences of 5 consecutive intervals present in the NN time series. Using the NN time series present in Figure 3.1, we exemplify the computation of the percentage of fragmentation word groups using the word group W_1^H. To count as this word group a sequence of 5 consecutive NN intervals has to contain a transition from blue to green (or green to blue); in Figure 3.2, we highlight the begining of these sequences with a number. Given that this NN time series contains 17 sequences of 5 consecutive intervals, and there are 7 W_1^H words, the percentage of this word group is 41% ($(7/17)\times 100$).

To illustrate PRSA analysis, we now present the calculation of the AC index. As discussed in Section 2.2.3, to compute AC, accelerative anchor points must be chosen and the average of segments of a selected length, centered at these anchors, must be computed. Figure 3.3 shows, for the ECG excerpt shown in the top row of Figure 3.1, the 5-beat long

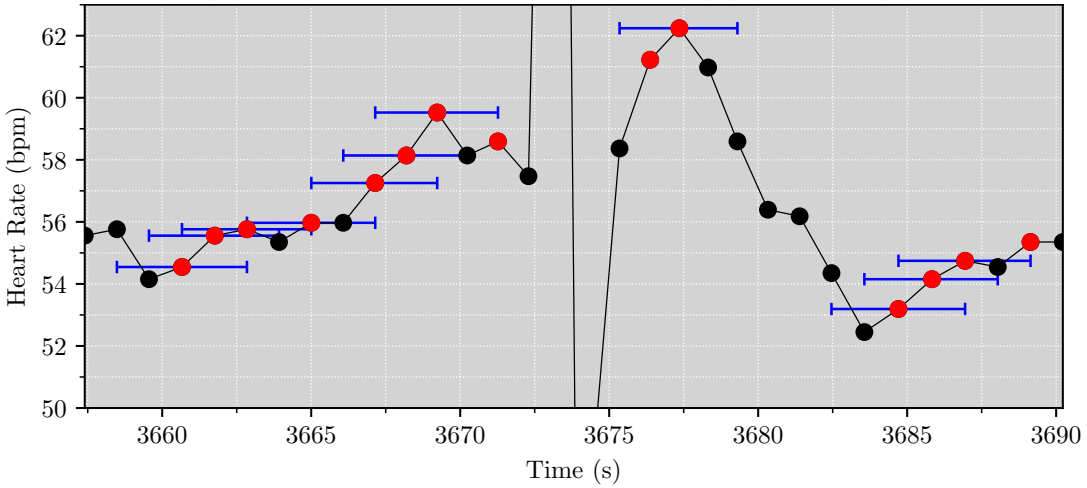

Figure 3.3: Selection of accelerative anchors (marked in red) and definition of segments of length 5 (marked in blue) used for the computation of a PRSA signal.

segments (blue lines) centered at each of the accelerative anchors (red circles). Note that it was not possible to use the last anchor point before the abnormal intervals, as well as the first anchor point after them, since the corresponding segments would contain abnormal intervals.

The PRSA signal, $\overline{NN_{PRSA}}(k)$, is computed by averaging over all the segments present in the NN time series. Note that k denotes the distance to the anchor points in the segments used to compute the PRSA signal. In Figure 3.4, we show the PRSA signal obtained when using segments of length 32. AC is obtained by using the points in the PRSA signal highlighted in red. They correspond to $\overline{NN_{PRSA}}(0)$, $\overline{NN_{PRSA}}(1)$, $\overline{NN_{PRSA}}(-1)$, $\overline{NN_{PRSA}}(-2)$. However, in the present dissertation we used a length of 5, which is associated with a much shorter PRSA signal. This shorter signal can be said to approximate the center region of the PRSA signal computed using larger segments.

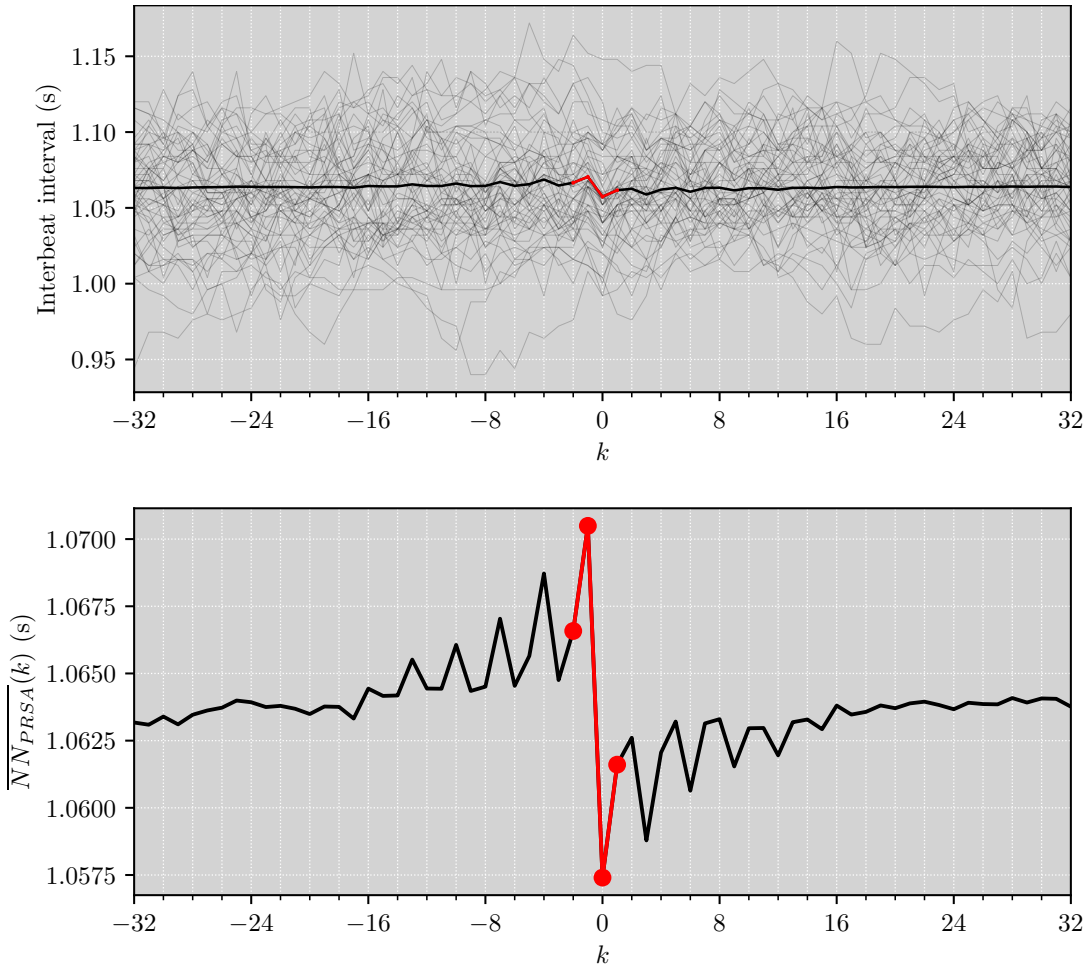

Figure 3.4: Example of a PRSA signal obtained from segments surrounding accelerative anchors. In the plot above are shown all the segments of length 32 used for the computation of the PRSA signal, which in this plot is highlighted with darker black. In the plot below, only the PRSA signal, $\overline{NN_{PRSA}}(k)$, is shown. Points highlighted in red correspond to the values used for AC calculation.

4

Changes in Heart Rate Dynamics with Cross-sectional Age

As discussed in Section 1.1, there is an express need to find aging biomarkers that help detect accelerated aging years before the emergence of functional decline. In this Chapter, we aim to study how HRF, PRSA and traditional HRV indices change with aging from adulthood to late adulthood. Furthermore, we will investigate if HRF analysis adds value to both PRSA and HRV traditional analysis.

4.1 Conceptual Introduction

Normal aging is accompanied by a complex series of changes in the autonomic control of the cardiovascular system. These changes typically entail a heightened cardiac sympathetic tone with parasympathetic withdrawal and a blunted sensitivity of major cardiopulmonary autonomic reflexes [104]–[106], e.g., baroreflex and RSA.

During aging the maximal HR that can be achieved diminishes due to a decrease in the intrinsic firing rate of the SAN [106], [107]. The decrease in SAN automaticity is thought to be caused by atrophy of its pacemaker cells, reduction of its size, infiltration of fatty tissue, and fibrosis [108]. The decrease in adrenergic receptors responsiveness in the SAN are thought to cause a blunted sensitivity of the SAN to SNS stimulation, contributing to a reduction in maximal HR [104], [106].

Nevertheless, resting HR remains fairly constant with aging [106]. This is only possible because there is a concomitant increased outflow of the sympathetic branch to the SAN and a decrease in vagal tone [105], [106], which compensates the diminished intrinsic rate of the SAN cells. In fact, it has been shown that NE levels increase with aging, resulting in elevated basal SNS activation [109].

Regarding the blunted sensitivity of the baroreflex, it has been shown that the response to changes in arterial blood pressure elicit less steep changes in HR, thus implying lower vagal and sympathetic reactivity [110]. Reduced parasympathetic activity is also revealed by reduced RSA oscillations [111], which is estimated to fall approximately 10% per age decade [112].

The decreased sensitivity of those two reflexes reveal the reduction of efficient adaptation to changing conditions as an individual ages.

4.2 Related Work

We now present a brief review of the main findings of the changes in HR dynamics with age.

Reardon and Malik [113] evaluated the changes in HR dynamics using RMSSD. The population in this study included 56 healthy subjects aged between 40 to 102 years and the ECG recordings lasted between 17 to 20 hours. Using Pearson correlation coefficient and the independent two-sample T-test to compare dynamical indices of subjects aged below and above 70 years of age, the authors found that RMSSD was not significantly associated with cross-sectional age. From these results they hypothesized that vagal modulations of HR were maintained with age.

Stein et al [114] used HRV temporal measures such as SDNN, SDANN, SDNNI, RMSSD, and PNN50, as well as the power of each of the traditional HRV frequency bands. These metrics were compared between two groups with 30 subjects each. The mean ± standard deviation (SD) in the "older" and "younger" groups were of 67 ± 3 and 33 ± 4 years, respectively. The metrics were computed for 24-h, as well as the nighttime and daytime periods separately. They found that all these indices decreased with age; however, the reduction was higher for the short-term HRV measures, RMSSD, PNN50, and the HF power.

Umentabi et al. [115] evaluated changes in HR dynamics with age using SDNN, SDANN, SDNNI, RMSSD, and PNN50. The study population included 260 healthy subjects aged between 10 to 99 years. Measures were computed over 24-h ECG recordings. All five measures were shown to decrease with age. However, PNN50 and RMSSD were shown to be more correlated, and decline more rapidly, with age until the sixth decade, beyond which these metrics stabilized. SDNN and SDANN were shown to be the ones more weakly correlated with aging. The SDNNI was shown to gradually and more linearly decline with age, in a more correlated manner with age than SDANN and SDNN.

Costa, Davis and Goldberger [23] evaluated changes in HR dynamics using HRF, namely PIP, PNNSS, ALS, and PAS, as well as standard time and frequency domain indices of short-term HRV, namely Standard Deviation of Successive Differences (SDSD), PNN50, PNN20, and HF power, detrended fluctuation analysis and sample entropy. The study population included 24-hour ECG recordings of 109 healthy subjects above 25 years, with a median of 40 and a 25–75th percentiles of 33–49 years of age. Metrics were computed for the entire recording, for daytime and nighttime periods. They found that the HRF measures increased and the short-term HRV measures decreased with age for all time periods. The non-linear indices were less correlated with age.

The authors also found, in [24], that the word groups W_0 and W_1 decreased significantly with age. However, this decrease was not significant for W_0 in the sleep period.

The W_3 word group significantly increased with aging. W_2 also showed a tendency to increase with age, but less correlated. Overall, W_1 and W_3 were the patterns with stronger associations with age.

Campana et al. [116] showed that AC and DC decreased with age in a population of 166 participants aged 21 to 60. The PRSA metrics were computed for sleep ECG recordings lasting 6.5 to 8.5 hours.

As a summary, these studies indicate that: (1) HRV indices decrease with age, although the decrease of short-term HRV measures after late middle age was not consistent for the studies presented; (2) HRF indices related to increased fragmentation/fluency increased/decreased with aging; and (3) both AC and DC indices decreased with aging.

The present study will offer an unprecedented comparative analysis on the association of HRF, traditional HRV, and PRSA indices with cross-sectional age from young adulthood to late adulthood in three populations. We will further investigate if the newer HRF analysis, which attempts to resolve inconsistency in results obtained using traditional HRV measures, adds value to both HRV and PRSA analyses.

4.3 Methods

For this study, we analyzed two relatively small open-access ECG databases, the Normal Sinus Rhythm RR Intervals Database (NSRdb) [78] and the Fantasia Database [83], and one large database, the Autonomic Aging Database (AAdb) [96]. These databases contained only healthy subjects with no overt disease.

4.3.1 Databases

The three databases mentioned above differ in the recording conditions. The NSRdb contains 24-h recordings in which participants performed their daily life routines; the Fantasia Database contains 2-hour recordings of subjects in resting supine position, while watching the movie "Fantasia" from Disney (to help maintain awakeness); and the AAdb containing recordings of subjects at rest in supine position in a quite and shaded room for a period between 8 to 45 minutes.

Next, we provide a closer description of each of the databases mentioned.

4.3.1.1 The Normal Sinus Rhythm RR Intervals Database

The NSRdb comprises 24-hour ECG holter monitor recordings of 72 healthy subjects aged between 20 and 76 years (mean ± SD: (54±16) years of age). The recordings were sampled at 128 Hz. In subsequent analyses, we treated age as either a continuous or as a binary variable. For the latter case, subjects were divided into two groups, "old" and "young", depending on whether they were ≥ 50 or < 50 years of age. The old group included 46 subjects (22 male), (66±4) (mean ± SD) years of age; the young group included 26 subjects (13 male), (35 ± 7) (mean ± SD) years of age. We independently analyzed the 24-hour,

sleep and awake periods. The sleeping hours were defined as the six continuous hours of lowest average HR; waking hours were defined as the six continuous hours of highest HR. The average HR was calculated using 6-hour moving windows advancing one data point (NN interval) at a time.

4.3.1.2 Fantasia Database

The Fantasia database includes subjects between ages of 21 and 34 ("young") and between 69 and 85 ("old"). The mean ± SD age in these groups were (26 ± 4) and (75 ± 4) years, respectively. The groups included 20 subjects each, as well as equal number of female and male subjects. Only healthy, non-smoking subjects with normal exercise tolerance tests, who were not on medication were admitted to the study. The ECG recordings were acquired with a sampling rate of 250 Hz, during approximately 2 hours, while participants lay supine awake watching a movie.

4.3.1.3 Autonomic Aging Database

The AAdb includes 1039 (650 male) healthy subjects (82 subjects were excluded due to incorrect automatic beat annotations). The database makes available the age group (mostly in bins of 5 years) to which individuals belong, instead of their specific age. To minimize error, we assigned, for each subject, the mean age of the age range of subject's respective age group. We obtained a population with mean ± SD (32 ± 15) years. The population was mainly composed of young and middle age adults, there was only 51 subjects aged above 65 years, as shown in Table 4.1. The ECG recordings were acquired with a sampling rate of 1000 Hz and were on average 19 minutes long, however, there were some recordings with only 8 minutes and others with 45 minutes. During the recording time, subjects were in supine position in a quiet fully shaded room with at controlled temperature of 22 °C.

4.3.2 Heart Rate Dynamical Analysis

For HR dynamical analysis, the NN time series were obtained as described in Section 3.2.

HRF indices measuring the overall degree of HRF, i.e., PIP, PNNLS, PNNSS, and ALS, as well as the percentage of specific patterns of fragmentation, i.e., PAS, W_0, W_1, W_3, W_1^H, W_3^H, W_3^S, and W_3^M, were calculated as described in Sections 2.2.2 and 3.2.

For HRV analysis, we used the following temporal indices: SDNN, RMSSD, SDANN, SDNNI, PNN50. They were computed as described in Section 2.2.1.2.

For PRSA analysis, we computed AC and DC indices as discussed in Section 2.2.3 and 3.2.

Age Range (yrs)	Number of Individuals
$18 \leq$ age ≤ 19	45
$20 \leq$age ≤ 24	402
$25 \leq$age ≤ 29	212
$30 \leq$age ≤ 34	99
$35 \leq$ age ≤ 39	40
$40 \leq$ age ≤ 44	45
$45 \leq$ age ≤ 49	49
$50 \leq$age ≤ 54	50
$55 \leq$ age ≤ 59	16
$60 \leq$age ≤ 64	24
$65 \leq$ age ≤ 69	19
$70 \leq$ age ≤ 74	12
$75 \leq$ age ≤ 79	7
$80 \leq$ age ≤ 84	12
$85 \leq$ age ≤ 92	7
Total	1039

Table 4.1: Age distribution of the population present in the AAdb database.

4.3.3 Statistical Analysis

HR dynamical variables were summarized by their median, 25th and 75th percentile values for all databases.

The HR dynamical indices were compared between old and young groups using either an independent two-sample T-test, Welch's T-test, or Wilcoxon rank-sum test, when the indices for the two groups were normally distributed with equal variances, normally distributed with unequal variances, and non-normally distributed, respectively. Normality and homoscedasticity were tested using Shapiro-Wilk Test and Levene's Test, respectively. In case of paired samples, a paired T-test or a Wilcoxon sign-rank test were used for normally and non-normally distributed sample differences, respectively.

Simple linear regression was used to model the dependence between each calculated HR dynamical index and participants' age ($index = \beta_0 + \beta_1 age$). Spearman's rank and Pearson's product-moment correlation coefficients were used to quantify the strength of the association between HR dynamical indices and age. For the analysis of the AAdb a quadratic term was added to the linear regression model ($index = \beta_0 + \beta_1 age + \beta_2 age^2$). The goodness of fit of this model was evaluated using the correlation coefficient, r, as was presented in Section 2.3.2.2.

Logistic linear regression was used to evaluate how the event of being old was predicted by HR dynamical measures, whenever age was treated as a binary variable. For this analysis normalized odds ratio were used to compare between different indices. AUC

was used to assess the goodness of fit of each model. Likelihood ratio tests were performed to evaluate if the logistic models using one HR dynamical index performed better than the null model (when no independent variable is used, only the intercept regression coefficient).

To evaluate if HRF added value to HRV and PRSA variables, likelihood ratio tests were performed for comparison of logistic models using only one, or one of each, of the HRV and PRSA indices with the respective models where a HRF metric was added.

In these analyses statistical significance was set at a p-value below 0.05 ($p < 0.05$).

4.4 Results

In this Section, we will present the results obtained for each database analyzed, in the following order: NSRdb, Fantasia database, and AAdb.

4.4.1 Changes in Heart Rate Dynamics with the Participants' Age in the NSRdb Population

To analyze the changes in HR dynamics with age in the NSRdb database, we started by testing if each HR dynamical index could be used to distinguish between the two age groups mentioned in Section 4.3.1.1, using 24-hour, awake, and sleep periods. We also provide a comparison between HR dynamical indices between the awake and sleep periods. Next, simple linear regression analysis was used to quantify the dependence of HR dynamical variables with age, also using these three periods. Thus, in the former set of analyses, age is treated as a binary variable (≥ 50 or < 50), while in the latter, age is treated as a continuous variable.

As shown in Table 4.2, for the 24-hour period, PIP, PNNSS, PAS, W_3, W_3^S, W_2^M, and W_3^M were significantly higher, and PNNLS, ALS, W_0, W_1, and W_1^H significantly lower for the older group than the younger one. These results indicate that fragmentation was higher for the older group. Table 4.2 also shows that both PRSA variables, AC and DC, were significantly lower in the older group. Among the HRV variables, SDNN, RMSSD, SDNNI, and PNN50, but not SDNN and SDANN, were significantly lower for older subjects. In Table 4.2 is also visible that HRF and PRSA variables allowed for better separation of younger and older individuals since the interquartile ranges of the two groups for these variables do not overlap.

As can be seen in Table 4.3, for the HRF and PRSA variables, the conclusions obtained for the 24-hour period apply to the awake period since all fragmentation/fluency indices were significantly higher/lower for older subjects in this period.

The HRV variables RMSSD, SDNNI, and PNN50 were significantly lower in the old group, as in the 24h-period, however, in the wake period, SDNN and SDANN were significantly higher in the older group, contradicting the general framework of HRV analysis that correlates higher HRV with better health.

	Variable	NSRdb 24–hour Period		
		Median (25–75th)		p
		Young (N = 26)	Old (N = 46)	
Overall HRF	**PIP (%)**	**59.0 (57.2–64.9)**	**70.1 (65.9–73.5)**	**<0.001**
	PNNSS (%)	**61.1 (56.1–70.8)**	**77.4 (71.9–83.3)**	**<0.001**
	PNNLS (%)	**34.2 (25.0–38.6)**	**18.9 (13.3–24.3)**	**<0.001**
	ALS	**1.8 (1.6–1.9)**	**1.5 (1.4–1.6)**	**<0.001**
Patterns of HRF	**PAS (%)**	**1.5 (1.2–2.1)**	**3.2 (2.7–4.0)**	**<0.001**
	W_0 (%)	6.0 (3.9–7.5)	3.2 (2.1–4.7)	<0.001
	W_1 (%)	**29.6 (23.9–34.3)**	**19.0 (15.1–23.4)**	**<0.001**
	W_3 (%)	**20.2 (16.6–23.7)**	**34.7 (30.8–40.1)**	**<0.001**
	W_3^S (%)	2.6 (1.9–3.5)	4.1 (3.3–4.8)	<0.001
	W_1^H **(%)**	24.0 (18.9–29.1)	13.7 (10.2–17.3)	<0.001
	W_3^H (%)	**5.4 (4.3–6.1)**	**10.7 (8.4–13.0)**	**<0.001**
	W_2^M (%)	9.6 (8.5–10.8)	11.4 (10.4–12.7)	<0.001
	W_3^M (%)	**11.4 (10.0–15.2)**	**20.4 (17.5–22.9)**	**<0.001**
HRV	SDNN (ms)	134.6 (106.8–149.9)	133.6 (116.9–154.9)	0.309
	RMSSD (ms)	33.6 (26.8–43.7)	22.7 (18.2–29.4)	<0.001
	SDANN (ms)	118.0 (94.3–134.3)	125.0 (106.7–146.5)	0.104
	SDNNI (ms)	59.3 (51.5–76.8)	45.5 (39.4–55.7)	<0.001
	PNN50 (%)	9.0 (5.1–19.5)	3.2 (1.2–7.5)	<0.001
PRSA	AC (ms)	14.6 (10.8–17.7)	8.0 (6.1–10.9)	<0.001
	DC (ms)	**13.4 (10.6–17.4)**	**7.7 (5.9–10.3)**	**<0.001**

Table 4.2: Measures of heart rate dynamics reported as median (25–75th) and p-values (p) for the comparison between young and old participants of the NSRdb in the 24-hour period. Values highlighted in bold correspond to measures associated with p-values lower than 0.001 and with non overlapping interquartile ranges.

Considering the sleep period, as is shown in Table 4.4, it is also visible that fragmentation is higher for the old group since most of fragmentation/fluency indices are significantly higher/lower for them. However, for PNNLS, PNNSS, and W_0 indices there was not enough evidence to infer that they had different values for the two age groups. Regarding HRV and PRSA variables, these were all significantly lower for the old group, except for SDANN, which was found not significantly different between the two age groups.

In Table 4.5 we show the results for the comparison of dynamical indices between the sleep and the awake periods for both age groups. The results show that, overall, HRF indices were significantly higher for the awake than the sleep period. The exceptions were PNNLS, PNNSS, and W_0 in the young group. Table 4.5 also shows that most of HRV and PRSA metrics were significantly lower for the awake period in relation to to the

	Variable	NSRdb Awake Period		
		Median (25–75th)		p
		Young (N = 26)	Old (N = 46)	
Overall HRF	**PIP (%)**	**59.8 (55.4–67.3)**	**72.7 (70.4–75.8)**	**<0.001**
	PNNSS (%)	**60.5 (53.3–73.2)**	**82.7 (78.8–88.5)**	**<0.001**
	PNNLS (%)	**33.7 (22.9–39.3)**	**13.1 (9.2–17.7)**	**<0.001**
	ALS	**1.7 (1.5–1.9)**	**1.3 (1.3–1.4)**	**<0.001**
Patterns of HRF	**PAS (%)**	**2.0 (1.5–2.7)**	**4.0 (3.3–4.8)**	**<0.001**
	W_0 (%)	**6.2 (5.1–9.7)**	**2.5 (1.4–3.6)**	**<0.001**
	W_1 (%)	**27.6 (20.7–32.5)**	**14.1 (11.8–18.0)**	**<0.001**
	W_3 (%)	**23.9 (20.0–30.4)**	**42.6 (37.0–46.3)**	**<0.001**
	W_3^S (%)	3.2 (2.4–4.4)	4.7 (3.4–5.6)	0.001
	W_1^H (%)	**18.8 (15.7–26.1)**	**8.1 (6.5–11.3)**	**<0.001**
	W_3^H (%)	**6.7 (5.1–7.9)**	**12.9 (10.5–16.3)**	**<0.001**
	W_2^M (%)	10.1 (9.3–11.0)	11.8 (10.8–12.9)	<0.001
	W_3^M (%)	**13.8 (12.0–16.1)**	**24.7 (21.1–27.0)**	**<0.001**
HRV	SDNN (ms)	76.0 (67.7–99.1)	83.4 (72.9–108.5)	0.050
	RMSSD (ms)	**27.1 (23.4–30.6)**	**17.2 (15.2–23.0)**	**<0.001**
	SDANN (ms)	55.7 (42.9–70.2)	76.1 (60.7–95.2)	<0.001
	SDNNI (ms)	53.6 (45.5–62.7)	37.8 (33.6–45.8)	<0.001
	PNN50 (%)	5.7 (3.4–8.5)	1.1 (0.5–3.4)	<0.001
PRSA	**AC (ms)**	**11.4 (10.0–14.1)**	**5.3 (4.5–7.8)**	**<0.001**
	DC (ms)	**11.1(9.8–13.1)**	**5.1 (4.4–7.0)**	**<0.001**

Table 4.3: Measures of heart rate dynamics reported as median (25–75th) and p-values (p) for the comparison between young and old participants of the NSRdb in the 6-hour awake period. Values highlighted in bold correspond to measures associated with p-values lower than 0.001 and with non overlapping interquartile ranges.

sleep one, except for SDNN in the old group, which presented similar values between the awake and sleep periods; and for SDANN, which presented similar values between sleep and awake periods in the younger group; additionally, in the older group, SDANN was significantly higher in the awake period.

In Table 4.6 we show the differences between HR dynamical indices derived from awake and sleep periods (i.e, $\Delta index = index_{awake} - index_{sleep}$). The absolute differences between HRF indices were significantly larger in the older individuals, except for W_0, W_1, W_1^H, and W_2^M. The differences in HRV indices between awake and sleep periods were significantly larger (in absolute terms) in younger subjects for SDNN and PNN50, and significantly larger in older subjects for SDANN; the change in RMSSD and SDNNI was not significantly different between younger and older subjects. Regarding the differences in AC and DC indices, they were not significantly different between the two age groups.

	Variable	NSRdb Sleep Period		
		Median (25–75th)		p
		Young (N = 26)	Old (N = 46)	
Overall HRF	PIP (%)	56.2 (52.9-60.2)	62.6 (57.2-66.7)	<0.001
	PNNSS (%)	66.7 (54.1-75.6)	71.7 (61.5-76.6)	0.300
	PNNLS (%)	30.2 (23.1-40.6)	25.3 (20.3-33.7)	0.100
	ALS	1.9 (1.7-2.0)	1.7 (1.5-1.8)	<0.001
Patterns of HRF	**PAS (%)**	**0.7 (0.6–1.2)**	**2.0 (1.5–2.8)**	**<0.001**
	W_0 (%)	4.1 (2.8–5.9)	4.3 (2.4–5.7)	0.500
	W_1 (%)	33.8 (29.6–40.5)	26.4 (19.6–32.1)	<0.001
	W_3 (%)	13.4 (10.1–19.6)	23.8 (18.0–28.7)	<0.001
	W_3^S (%)	1.4 (1.0–2.3)	2.7 (1.9–3.6)	<0.001
	W_1^H (%)	29.8 (25.1–36.1)	22.2 (16.0–26.9)	<0.001
	W_3^H (%)	**2.8 (2.2–4.3)**	**6.7 (4.7–9.0)**	**<0.001**
	W_2^M (%)	9.0 (7.9–10.7)	10.9 (8.7–12.8)	0.002
	W_3^M (%)	8.4 (6.0–12.1)	13.7 (10.5–17.3)	<0.001
HRV	SDNN (ms)	90.4 (73.5–122.1)	81.7 (64.1–98.7)	0.020
	RMSSD (ms)	41.8 (34.1–52.2)	31.2 (21.7–43.5)	0.003
	SDANN (ms)	51.5 (40.8–66.4)	53.1 (39.4–65.8)	0.387
	SDNNI (ms)	61.8 (54.4–88.1)	54.0 (45.8–72.4)	0.002
	PNN50 (%)	15.8 (9.2–25.3)	7.5 (1.9–17.0)	<0.001
PRSA	AC (ms)	18.1 (13.1–21.4)	12.2 (8.1–16.6)	<0.001
	DC (ms)	17.1 (14.0–20.6)	11.6 (8.0–14.7)	<0.001

Table 4.4: Measures of heart rate dynamics reported as median (25–75th) and p-values (p) for the comparison between young and old participants of the NSRdb in the 6-hour sleep period. Values highlighted in bold correspond to measures associated with p-values lower than 0.001 and with non overlapping interquartile ranges.

Beginning with the 24-hour period, Table 4.7 and the regression plots in Figure 4.1 allows us to conclude that: (1) fragmentation significantly increased with age; (2) HRV significantly decreased with age by means of RMSSD, SDNNI, and PNN50, but not by means of SDNN and SDANN; and that (3) both PRSA variables significantly decreased with age.

Moreover, it was also possible to infer that correlation with age was stronger for HRF and PRSA variables, than for HRV ones. For HRF and PRSA variables, correlation coefficients varied between 0.43 and 0.71, and -0.61 and -0.64, respectively, whereas, for HRV variables, correlation coefficients varied between -0.36 and -0.51. The strongest correlations with age, $r_p > 0.65$ or $r_s > 0.65$, were all attained by HRF variables, more specifically, W_3 (slope of the regression line, [95% CI]: 0.42 [0.32, 0.52] %/yr), W_3^M (0.23 [0.18, 0.29] %/yr), PIP (0.29 [0.22, 0.37] %/yr), and ALS (-0.009 [-0.012, -0.007] %/yr).

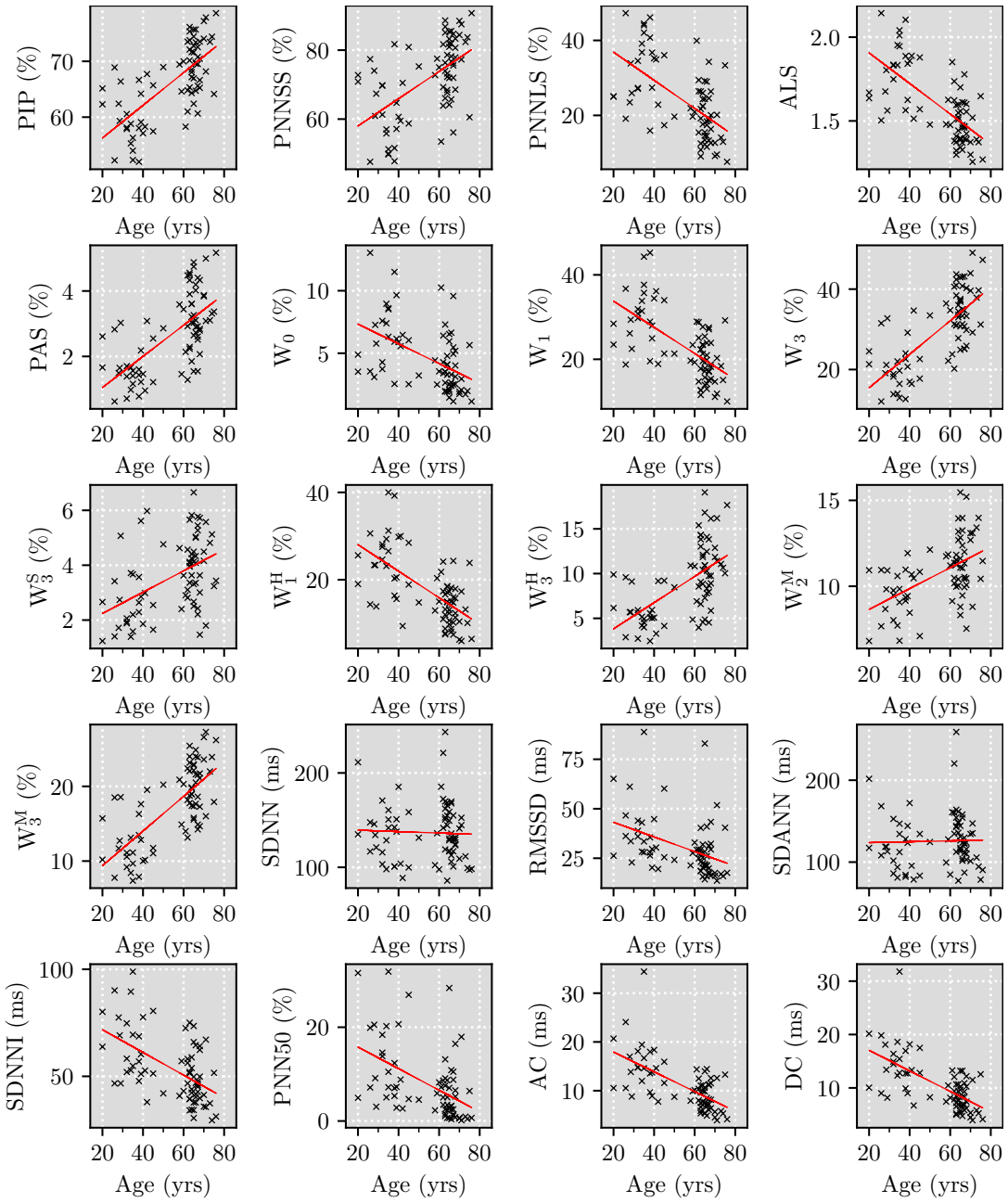

Figure 4.1: Scatter plots of the heart rate fragmentation, traditional heart rate variability, and PRSA indices vs. the participants' age, derived from the analysis of the full 24-hour period of the NSRdb population.

	Variable	Young			Old		
		Awake	Sleep	p	Awake	Sleep	p
Overall HRF	PIP (%)	59.8	56.2	0.020	72.7	62.6	<0.001
	PNNSS (%)	60.5	66.7	**0.400**	82.7	71.7	<0.001
	PNNLS (%)	33.7	30.2	**0.900**	13.1	25.3	<0.001
	ALS	1.7	1.9	0.030	1.3	1.7	<0.001
Patterns of HRF	PAS (%)	2.0	0.7	<0.001	4.0	2.0	<0.001
	W_0 (%)	6.2	4.1	**0.004**	2.5	4.3	<0.001
	W_1 (%)	27.6	33.8	0.004	14.1	26.4	<0.001
	W_3 (%)	23.9	13.4	<0.001	42.6	23.8	<0.001
	W_3^S (%)	3.2	1.4	<0.001	4.7	2.7	<0.001
	W_1^H (%)	18.8	29.8	<0.001	8.1	22.2	<0.001
	W_3^H (%)	6.7	2.8	<0.001	12.9	6.7	<0.001
	W_2^M (%)	10.1	9.0	0.040	11.8	10.9	0.030
	W_3^M (%)	13.8	8.4	<0.001	24.7	13.7	<0.001
HRV	**SDNN (ms)**	76.0	90.4	0.003	83.4	81.7	**0.209**
	RMSSD (ms)	27.1	41.8	<0.001	17.2	31.2	<0.001
	SDANN (ms)	57.7	51.5	**0.867**	76.1	53.1	**<0.001**
	SDNNI (ms)	53.6	61.8	<0.001	37.8	54.0	<0.001
	PNN50 (%)	5.7	15.8	<0.001	1.1	7.5	<0.001
PRSA	AC (ms)	11.4	18.1	<0.001	5.3	12.2	<0.001
	DC (ms)	11.1	17.1	<0.001	5.1	11.6	<0.001

Table 4.5: Measures of heart rate dynamics reported by medians and p-values, p, for the comparison between awake and sleep periods in both young and old participants of the NSRdb population. In bold we highlight the indices that are not concordant with the main change tendency, that is, the HRF metrics that do not decrease and PRSA and HRV metrics that do not increase in sleep relative to the awake period.

For the awake period (cf. Table 4.8), the same conclusions achieved for the 24-hour apply, except that SDANN was positively correlated with age, which, again, contradicts HRV typical interpretation.

For the sleep period (cf. Table 4.9), the same conclusions obtained for the 24-hour period also apply, however, concerning HRF and HRV variables it is observed that: PNNLS, PNNSS, and W_0 were not correlated with age; SDNN was significantly inversely correlated with age, and SDANN was not correlated with age.

For the awake and sleep periods the HR dynamical variables more correlated with age corresponded to fragmentation indices: PNNLS ($r_p = 0.74$) in the awake period, and PAS ($r_s = 0.65$) in the sleep period. The best HRV and PRSA metrics corresponded to SDNNI and DC, respectively.

The correlation between the dynamical indices and cross-sectional age were stronger

Variable		Change in HR dynamics from awake to sleep		
		Median [25, 75th]		p
		Young (N = 26)	Old (N = 46)	
Overall HRF	PIP (%)	4.5 [0.9, 9.0]	9.2 [6.2, 12.4]	<0.001
	PNNSS (%)	-5.5 [-10.7, 8.1]	12.7 [7.5, 18.3]	<0.001
	PNNLS (%)	3.8 [-9.3, 8.1]	-11.8 [-18.0, -8.2]	<0.001
	ALS	-0.1 [-0.3, -0.1]	-0.3 [-0.4, -0.2]	<0.001
Patterns of HRF	PAS (%)	1.3 [0.5, 1.6]	1.6 [1.1, 2.3]	0.009
	W_0 (%)	2.2 [0.7, 4.1]	-1.3 [-2.9, -0.2]	<0.001
	W_1 (%)	-9.6 [-15.8, -1.0]	-11.0 [-15.4, -6.8]	**0.072**
	W_3 (%)	11.5 [3.9, 14.6]	17.6 [12.5, 19.2]	<0.001
	W_3^S (%)	1.6 [1.3, 2.0]	1.7 [0.6, 3.4]	**0.541**
	W_1^H (%)	-12.6 [-18.8, -3.0]	-11.8 [-19.1, -8.1]	**0.478**
	W_3^H (%)	3.5 [1.6, 4.8]	6.2 [3.7, 7.4]	0.004
	W_2^M (%)	0.7 [-0.2, 2.8]	0.8 [0.1, 2.2]	**0.812**
	W_3^M (%)	6.3 [2.4, 7.9]	9.7 [6.7, 11.0]	<0.001
HRV	SDNN (ms)	-14.7 [-30.9, -2.2]	8.1 [-11.4, 32.1]	0.002
	RMSSD (ms)	-14.8 [-26.5,-10.6]	-11.9 [-21.6, -4.4]	**0.104**
	SDANN (ms)	0.0 [-12.4,15.3]	26.0 [5.7, 44.0]	0.001
	SDNNI (ms)	-13.5 [-27.1, -3.1]	-16.0 [-24.1, -5.2]	**0.474**
	PNN50 (%)	-9.3 [-19.8, -6.3]	-6.0 [-12.8, -1.1]	0.012
PRSA	**AC (ms)**	-6.5 [-8.7, -2.3]	-5.9 [-9.2, -3.3]	**0.281**
	DC (ms)	-5.8 [-9.5, -2.7]	-5.7 [-9.4, -2.5]	**0.428**

Table 4.6: Values of the change in heart rate dynamics from awake to sleep period ($index_{awake} - index_{sleep}$) reported as median [25, 75th] and p-values (p) for the comparison of this change between old and young subjects of NSRdb population. In bold we highlight the variables whose change is not significantly different between young and old subjects.

in analyses of the awake period, especially for HRF and PRSA indices. This observation is consistent with the previous finding that the largest difference between old and young groups, for these metrics, were seen for the awake period. Thus, both type of analyses, the one in which age is treated as a binary variable (young *versus* old), and the one in which age is a continuous variable yielded consistent results.

4.4.2 Changes in Heart Rate Dynamics with the Participants' Age in the Fantasia Population

Until now we investigated the use of HRF, HRV, and PRSA indices as aging biomarkers in a population with each subject performing their daily activities. We now analyze subjects that were all performing the same activity, namely, watching a the Fantasia Disney movie in a supine position. This analysis is valuable since it excludes differences in the metrics

	Variable	NSRdb 24-hour Period			
		Pearson		Spearman	
		r_p	p	r_s	p
Overall HRF	**PIP (%)**	0.686	< 0.001	0.648	< 0.001
	PNNSS (%)	0.558	< 0.001	0.551	< 0.001
	PNNLS (%)	−0.596	< 0.001	−0.582	< 0.001
	ALS	−0.678	< 0.001	−0.646	< 0.001
Patterns of HRF	PAS (%)	0.643	< 0.001	0.604	< 0.001
	W_0 (%)	−0.483	< 0.001	−0.515	< 0.001
	W_1 (%)	−0.631	< 0.001	−0.612	< 0.001
	W_3 (%)	0.711	< 0.001	0.653	< 0.001
	W_3^S (%)	0.462	< 0.001	0.426	< 0.001
	W_1^H (%)	−0.633	< 0.001	−0.593	< 0.001
	W_3^H (%)	0.587	< 0.001	0.560	< 0.001
	W_2^M (%)	0.513	< 0.001	0.458	< 0.001
	W_3^M (%)	0.711	< 0.001	0.651	< 0.001
HRV	SDNN (ms)	−0.034	0.743	−0.138	0.248
	RMSSD (ms)	−0.405	< 0.001	−0.463	< 0.001
	SDANN (ms)	0.027	0.823	−0.062	0.265
	SDNNI (ms)	−0.545	< 0.001	−0.524	< 0.001
	PNN50 (%)	−0.482	< 0.001	−0.511	< 0.001
PRSA	AC (ms)	−0.630	< 0.001	−0.613	< 0.001
	DC (ms)	−0.640	< 0.001	−0.617	< 0.001

Table 4.7: Pearson product-moment correlation (r_p) and Spearman rank (r_s) coefficients for the relationships between heart rate fragmentation, traditional heart rate variability, and PRSA indices with cross-sectional age in the 24-hour period of the NSRdb population. The variables highlighted in bold are associated with an absolute value of r_p or r_s greater than 0.650.

caused by differences in activities.

In this database, we performed the analysis using statistical tests to compare the mean/median of the "old" and "young" groups. However, since the age distribution of this population was clearly bimodal, logistic linear regression was used instead of simple linear regression to quantify the relationship between age and each HR dynamical index. It should be noted that we did not restrict the current analysis to comparison statistical tests since logistic regression allows one to compare the performance of dynamical indices.

From the results shown in Table 4.10, for the statistical tests comparing the older and younger subjects,it was possible to infer that fragmentation was higher in older subjects since PIP, PAS, W_3, W_3^S, W_3^H, W_2^M, and W_3^M were significantly higher, and W_1, ALS, and

	Variable	NSRdb Awake Period			
		Pearson		Spearman	
		r_p	p	r_s	p
Overall HRF	**PIP (%)**	0.719	< 0.001	0.636	< 0.001
	PNNSS (%)	0.721	< 0.001	0.672	< 0.001
	PNNLS (%)	−0.735	< 0.001	−0.674	< 0.001
	ALS	−0.728	< 0.001	−0.660	< 0.001
Patterns of HRF	PAS (%)	0.617	< 0.001	0.548	< 0.001
	W_0 (%)	−0.646	< 0.001	−0.657	< 0.001
	W_1 (%)	−0.731	< 0.001	−0.666	< 0.001
	W_3 (%)	0.725	< 0.001	0.645	< 0.001
	W_3^S (%)	0.356	0.002	0.297	0.011
	W_1^H (%)	−0.698	< 0.001	−0.593	< 0.001
	W_3^H (%)	0.573	< 0.001	0.554	< 0.001
	W_2^M (%)	0.508	< 0.001	0.434	< 0.001
	W_3^M (%)	0.733	< 0.001	0.647	< 0.001
HRV	SDNN (ms)	0.111	0.351	0.085	0.479
	RMSSD (ms)	−0.432	< 0.001	−0.464	< 0.001
	SDANN (ms)	0.327	0.005	0.310	0.008
	SDNNI (ms)	−0.540	< 0.001	−0.475	< 0.001
	PNN50 (%)	−0.431	< 0.001	−0.489	< 0.001
PRSA	**AC (ms)**	−0.705	< 0.001	−0.641	< 0.001
	DC (ms)	−0.709	< 0.001	−0.628	< 0.001

Table 4.8: Pearson product-moment correlation (r_p) and Spearman rank (r_s) coefficients for the relationships between heart rate fragmentation, traditional heart rate variability, and PRSA indices with cross-sectional age in the 6-hour wake period of the NSRdb population. The variables highlighted in bold are associated with an absolute value of r_p or r_s greater than 0.700.

W_1^H significantly lower for the older group. However, as in the sleep period of the NSRdb database, PNNLS, PNNSS, and W_0 were not significantly different between the two age groups.

In Table 4.10 is also shown that HRV and PRSA variables were all significantly lower for the old group.

As presented in Table 4.11, for HRF variables a one standard deviation increase in one of the metrics W_3, W_3^S, W_2^M, W_3^M was associated with a 3.3, 77.0, 9.6, 8.6- fold increase in the odds of being old, respectively. The regression models using these variables performed all better than the null model, and the AUC associated with these models were above 0.5, ranging from 0.815 to 0.905. The best HRF performing metric was W_3^S, with a normalized odds-ratio of 77 and an AUC of 0.905, indicating that this fragmentation

	Variable	NSRdb Sleep Period			
		Pearson		Spearman	
		r_p	p	r_s	p
Overall HRF	PIP (%)	0.445	< 0.001	0.448	< 0.001
	PNNSS (%)	0.115	0.336	0.152	0.202
	PNNLS (%)	−0.157	0.189	−0.193	0.104
	ALS	−0.435	< 0.001	−0.415	< 0.001
Patterns of HRF	**PAS (%)**	0.619	< 0.001	0.652	< 0.001
	W_0 (%)	−0.015	0.901	−0.057	0.631
	W_1 (%)	−0.383	< 0.001	−0.376	0.001
	W_3 (%)	0.585	< 0.001	0.562	< 0.001
	W_3^S (%)	0.409	< 0.001	0.474	< 0.001
	W_1^H (%)	−0.424	< 0.001	−0.414	< 0.001
	W_3^H (%)	0.533	< 0.001	0.558	< 0.001
	W_2^M (%)	0.381	< 0.001	0.366	0.002
	W_3^M (%)	0.517	< 0.001	0.507	< 0.001
HRV	SDNN (ms)	−0.262	0.026	−0.345	0.003
	RMSSD (ms)	−0.326	0.005	−0.384	< 0.001
	SDANN (ms)	−0.116	0.333	−0.209	0.078
	SDNNI (ms)	−0.385	< 0.001	−0.389	< 0.001
	PNN50 (%)	−0.419	< 0.001	−0.452	< 0.001
PRSA	AC (ms)	−0.435	< 0.001	−0.447	< 0.001
	DC (ms)	−0.475	< 0.001	−0.487	< 0.001

Table 4.9: Pearson product-moment correlation (r_p) and Spearman rank (r_s) coefficients for the relationships between heart rate fragmentation, traditional heart rate variability, and PRSA indices with cross-sectional age in the 6-hour sleep period of the NSRdb population. The variables highlighted in bold are associated with an absolute value of r_p or r_s greater than 0.500.

pattern was present in old participants, but mainly absent in the younger ones.

In comparison, traditional HRV and PRSA measures were inversely related to old age. HRV variables were associated with AUC's ranging between 0.775 and 0.885. PNN50 was the HRV measure with higher AUC. Regarding PRSA variables, AC and DC yielded models with an AUC of 0.905.

To understand whether HRF added value to HRV and PRSA analysis, likelihood ratio tests were performed to evaluate if each one of HRF variables, individually, added value to models using only one of the HRV or PRSA variables. The results for this analysis are shown in Table 4.12, from which it is possible to infer that PIP, W_2^M, and W_3^M added value to models using either RMSSD, SDANN, SDNNI; PAS and W_3^H added value to models using either SDNN, RMSSD, and PNN50; W_1, W_1^H, and W_1^S added value to SDNNI and

	Variable	Fantasia		
		Median (25–75th)		p
		Young (N = 20)	Old (N = 20)	
Overall HRF	PIP (%)	52.8 (50.7–58.5)	60.8 (57.8–66.5)	0.013
	PNNSS (%)	64.5 (56.2–72.4)	69.4 (60.5–77.8)	0.351
	PNNLS (%)	34.0 (26.7–41.7)	28.3 (20.7–36.8)	0.145
	ALS	2.0 (1.8–2.0)	1.7 (1.6–1.8)	0.032
Patterns of HRF	PAS (%)	0.7 (0.6–1.0)	1.8 (0.7–2.8)	0.010
	W_0 (%)	5.8 (3.1–7.8)	4.9 (2.6–7.7)	0.903
	W_1 (%)	39.7 (26.2–42.3)	25.0 (21.0–30.1)	0.014
	W_3 (%)	8.7 (6.9–12.5)	20.2 (14.9–24.3)	<0.001
	W_3^S (%)	0.2 (0.1–0.4)	0.9 (0.5–1.3)	<0.001
	W_1^H (%)	37.5 (25.5–40.9)	21.5 (14.7–26.7)	0.004
	W_3^H (%)	3.5 (3.0–6.0)	6.6 (4.7–10.5)	0.020
	W_2^M (%)	4.0 (2.9–4.5)	6.9 (5.9–7.8)	<0.001
	W_3^M (%)	3.9 (3.5–5.6)	10.4 (8.4–12.4)	<0.001
HRV	**SDNN (ms)**	92.3 (72.0–101.9)	48.0 (42.9–60.8)	<0.001
	RMSSD (ms)	54.9 (39.2–80.5)	25.1 (18.8–32.6)	<0.001
	SDANN (ms)	34.3 (30.1–38.6)	24.6 (22.9–28.0)	0.002
	SDNNI (ms)	83.0 (61.9–93.4)	39.9 (34.3–49.9)	<0.001
	PNN50 (%)	28.5 (17.5–47.2)	3.9 (0.7–8.0)	<0.001
PRSA	**AC (ms)**	20.5 (16.8–26.0)	8.2 (6.4–11.4)	<0.001
	DC (ms)	21.0 (16.6–25.0)	8.7 (6.3–11.8)	<0.001

Table 4.10: Measures of heart rate dynamics reported as median (25–75th) and p-values (p) for the comparison between young and old participants included in the Fantasia database. Values highlighted in bold correspond to measures associated with p-values lower than 0.001 and with non overlapping interquartile ranges.

SDANN models; and W_3 and W_3^S added value to all HRV variables. However, none of the HRF indices added value to PRSA models.

4.4.3 Changes in Heart Rate Dynamics with the Participants' Age in the AAdb Population

In the previous Sections, we investigated the change in HR dynamical indices with cross-sectional age in two small populations (NSRdb $N = 76$, Fantasia $N = 40$). In this Section, we will analyze a population with 1039 individuals. As mentioned in Section 4.3, the ECG recordings of this population were acquired while participants were at rest in supine position in a fully shaded room.

The visual inspection of the scatter plots regarding the evolution of the HR dynamical indices and age provided indication that the use of a second degree polynomial instead

	Variable	Fantasia			
		OR	95% CI	AUC	LLR p
Overall HRF	PIP (%)	2.43	[1.1, 5.0]	0.72	0.011
	PNNSS (%)	1.47	[0.76, 2.86]	0.602	0.252
	PNNLS (%)	0.61	[0.31, 1.20]	0.648	0.130
	ALS	0.47	[0.23, 0.98]	0.690	0.029
Patterns of HRF	PAS (%)	1.67	[0.73, 3.34]	0.712	0.211
	W_0 (%)	0.96	[0.51, 1.89]	0.550	0.885
	W_1 (%)	0.43	[0.21, 0.89]	0.718	0.013
	W_3 (%)	3.3	[1.4, 7.9]	0.815	0.001
	W_3^S (%)	77.0	[4.2, 1400.0]	0.905	<0.001
	W_1^H (%)	0.38	[0.18, 0.87]	0.750	0.005
	W_3^H (%)	1.22	[0.64, 2.41]	0.688	0.498
	W_2^M (%)	9.6	[2.3, 40.0]	0.875	<0.001
	W_3^M (%)	8.6	[2.4, 31.0]	0.872	<0.001
HRV	SDNN (ms)	0.12	[0.03, 0.41]	0.865	<0.001
	RMSSD (ms)	0.17	[0.05, 0.56]	0.858	<0.001
	SDANN (ms)	0.37	[0.16, 0.86]	0.775	0.007
	SDNNI (ms)	0.11	[0.03, 0.39]	0.875	<0.001
	PNN50 (%)	0.08	[0.02, 0.39]	0.885	<0.001
PRSA	**AC (ms)**	0.06	[0.01, 0.31]	0.905	<0.001
	DC (ms)	0.05	[0.01, 0.24]	0.905	<0.001

Table 4.11: Logistic linear regression analysis of the relationship between heart rate dynamical indices and old age for the Fantasia population. The values presented correspond to the normalized odds ratio (OR), 95% confidence intervals (95% CI), AUC, and the p-value, p, associated with the likelihood ratio test comparing the regression model with a null model containing only the zero-order regression coefficient. In bold are highlighted the variables that yielded regression models with an AUC above 0.9.

of an one degree polynomial was more appropriate for the linear regression analysis of the AAdb population.

In Table 4.13 we show the correlation coefficient, r, for the quadratic relationship between age and each HR dynamical index ($index = \beta_0 + \beta_1 age + \beta_2 age^2$). This table shows that all indices were significantly associated with age through this model. The variables more correlated with age ($r > 0.3$) were W_2^M ($r = 0.399$), W_3^M ($r = 0.411$), PNN50 ($r = 0.349$), and DC ($r = 0.302$).

Considering the plots presented in Figure 4.2, it is visible that fragmentation/fluency metrics tended to progressively decrease/increase from young adulthood to forty/fifty years and then to markedly increase/decrease from this age to late adulthood. However, this pattern was not visible for W_3^S, W_2^M, and W_3^M. These variables seemed to monotonically increase with age, almost linearly. Regarding HRV and PRSA variables, it is

Variable			Fantasia				
			SDNN	RMSSD	SDANN	SDNNI	PNN50
Overall HRF		PIP (%)	0.176	**0.018**	**0.018**	**0.015**	0.139
		PNNSS (%)	0.835	0.176	0.397	0.342	0.409
		PNNLS (%)	0.746	0.140	0.230	0.196	0.375
		ALS (%)	0.407	0.144	0.132	0.116	0.364
Patterns of HRF		PAS (%)	**0.030**	**0.019**	0.148	0.182	**0.015**
		W_0 (%)	0.556	0.459	0.954	0.889	0.886
		W_1 (%)	0.265	0.097	**0.032**	**0.030**	0.270
		$\mathbf{W_3}$ **(%)**	**0.028**	**0.007**	**0.002**	**0.002**	**0.033**
		$\mathbf{W_3^S}$ **(%)**	**0.054**	**0.030**	**<0.001**	**<0.001**	0.197
		W_1^H (%)	0.211	0.082	**0.013**	**0.012**	0.254
		W_3^H (%)	**0.052**	**0.029**	0.338	0.409	**0.024**
		W_2^M (%)	0.106	**0.026**	**<0.001**	**<0.001**	0.502
		W_3^M (%)	0.069	**0.011**	**<0.001**	**<0.001**	0.215

Table 4.12: P-values of the likelihood ratio tests used for the comparison between logistic models of age using a HRV variable and these same models where an HRF variable is added for the participants included in the Fantasia database. Each column corresponds to an HRV variable. Each value in the table corresponds to a likelihood ratio test performed between a model using the HRV variable present in the current column and a model using that HRV variable plus the HRF variable present in the current row. Values inside the table highlighted in bold correspond to p-values below 0.05. Variables highlighted in bold correspond to metrics that improved more than 4 HRV models.

apparent that a decrease from young adulthood to fifty/sixty years of age, is followed by an increase from this age on. Only SDANN did not present this pattern, instead this metric seemed to decrease linearly with age. It is important to note that RMSSD, SDNN, and SDNNI showed a tendency to have similar values for the youngest subjects and the oldest ones, which ill-poses typical HRV interpretation.

As the length of the recordings in this database varied among subjects, we also tested if the changes in each of the HR dynamical indices was correlated with the length of the ECG recordings. Although not shown, we found that only SDANN was associated with the recording length. Specifically, increased SDANN was associated with increased recording length. This is expected since this metric depends on the number of 5-min windows present in the recording.

4.5 Discussion

In summary, from the analysis of the NSRdb, Fantasia, and AAdb databases it is possible to conclude that HRF was higher for older adults than younger ones, and HRV and PRSA indices were generally lower. It was also apparent that HRF and PRSA indices were more

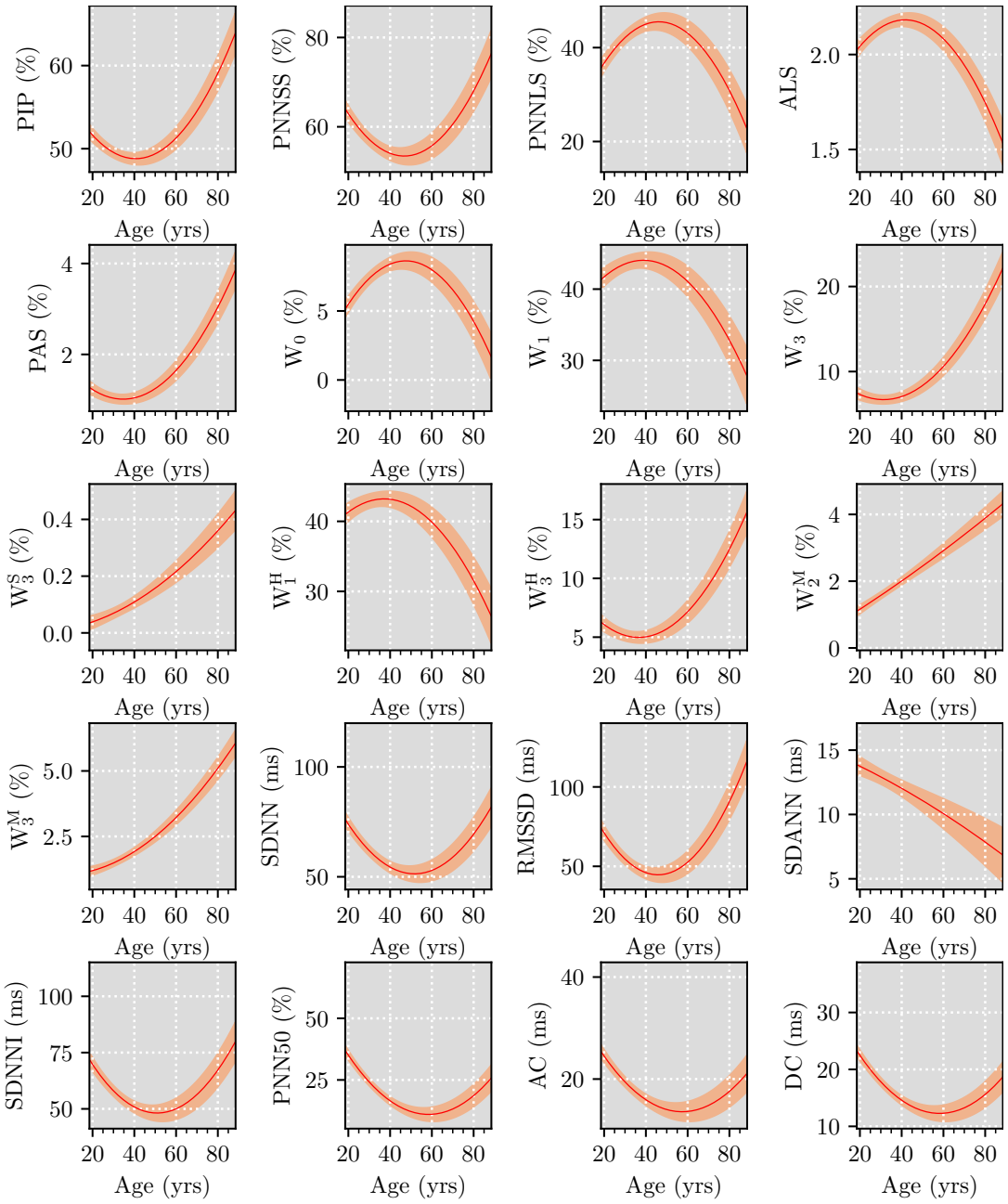

Figure 4.2: Scatter plots of the heart rate fragmentation, traditional heart rate variability, and PRSA indices vs. the participants' age, derived from the analysis of the AAdb population.

AAdb				
Variable			r	p
Overall HRF		PIP (%)	0.197	<0.001
		PNNSS (%)	0.168	<0.001
		PNNLS (%)	0.165	<0.001
		ALS	0.178	<0.001
Patterns of HRF		PAS (%)	0.245	<0.001
		W_0 (%)	0.171	<0.001
		W_1 (%)	0.132	<0.001
		W_3 (%)	0.287	<0.001
		W_3^S (%)	0.257	<0.001
		W_1^H (%)	0.140	<0.001
		W_3^H (%)	0.198	<0.001
		W_2^M (%)	**0.399**	**<0.001**
		W_3^M (%)	**0.411**	**<0.001**
HRV		SDNN (ms)	0.210	<0.001
		RMSSD (ms)	0.199	<0.001
		SDANN (ms)	0.160	<0.001
		SDNNI (ms)	0.204	<0.001
		PNN50 (%)	**0.349**	**<0.001**
PRSA		AC (ms)	0.240	<0.001
		DC (ms)	**0.302**	**<0.001**

Table 4.13: Correlation coefficient (r) and the respective p-value (p) for the polynomial linear regression models ($index = \beta_0 + \beta_1 age + \beta_2 age^2$) used to describe the relationship between age and heart rate dynamical indices in the AAdb population. In bold are highlighted the correlation coefficients greater than 0.3.

related with age than HRV indices.

From the analysis made using the NSRdb database was possible to conclude that, regardless of the period – day, night, and 24-hour –, HRF indices were more associated with aging than PRSA indices and HRV ones, especially the indices W_3^M and W_3. We also noted that the association between age and most of HRF indices was accentuated during the awake period and attenuated during the night one, since in wakefulness older subject were significantly more fragmented, whereas younger subjects were not. The cause of the marked increase in fragmentation in the awake period relative to the sleep one in the older participants is unknown. One might speculate that this inflation of fragmentation in older subjects originates from the accentuation of the decoupling between the SAN and the ANS modulation in the most active moments of the day. This, in turn, might be a consequence of the bluntness of autonomic reflexes, whose effects are more pronounced during more active moments. Another possible explanation for fragmentation to be

higher in the awake period relative to the sleep one in the old might derive from sleep disturbances, which are common in older subjects. We speculate that fragmentation might be spuriously lower in the sleep period due to sleep disturbances. For example, obstructive sleep apnea[1] is responsible for long (> 20 second) oscillations that may lead to a decrease in the frequency of the alteration of HR acceleration sign. These type of oscillations greatly affect PNNLS, W_0, and PNNSS since these metrics increase with oscillations with cycle-lengths superior to 3 s–5 s, depending on the HR.

Regarding HRV indices, PNN50 and SDNNI were the measures whose decrease was more associated with aging. This was also reported in some of the studies [114], [115] presented in Section 4.2. One of HRV indices, SDANN, instead of decreasing, increased with aging. As discussed in Section 2.2.2, this unexpected increase in HRV might be due to non-vagally mediated sinus arrhythmia – fragmentation. Regarding PRSA indices, i.e., DC and AC, they performed similarly. Except for SDNN and SDANN in older participants, and SDANN in younger ones, HRV and PRSA indices were higher in the sleep period. This is consistent with the rise in vagal modulation that is typically observed during sleep [117].

In the Fantasia database, most of HRF indices performed similarly to PRSA and HRV ones. However, W_3^S, DC, and AC were the best indices. As in the sleeping period of the NSRdb, PNNLS, PNNSS, and W_0 were not associated with old age. Although, wakefulness was assumed in the Fantasia database, participants, especially older ones, might have fallen asleep during the recording. Thus, we speculate that the absence of association between age and the mentioned HRF indices might be also due to respiratory sleep disturbances that spuriously decrease these metrics, as was hypothesized for the sleeping period of the NSRdb database.

The analysis of the AAdb database indicates that the changes in fragmentation are described by a decrease from young adulthood to forty/fifty years and an increase from that age period to late adulthood, except for W_3^S, W_2^M, and W_3^M, whose increase was uninterrupted from young adulthood to late adulthood. Except for SDANN, HRV and PRSA indices showed a tendency to decrease from young adulthood to fifty/sixty years of age and to increase from that age period to late adulthood, achieving for RMSSD, SDNNI, and SDNN values greater than in the youngest adults. This paradoxical increase in variability, once more, is hypothesized to be due to the arise of non-vagally mediated short-term HR variations, which is best captured by the HRF measures, as discussed in Section 2.2.2. This observation might be the underlying cause of diminished association of reduced RMSSD with increasing age after the sixth/seventh decade of life reported by some studies mentioned in Section 4.2.

The reason why most of fragmentation indices do not increase monotonically with age between the end of adolescence to middle age is unknown. A similar observation was also made by Hayano et al. [82]. However, they did not suggest any justification for

[1] Obstructive sleep apnea is a syndrome characterized by episodes of complete or partial obstruction of the upper airway, resulting in intermittent hypoxia and transient arousals from sleep.

this phenomena. A possible explanation might derive from the maturation of the ANS system, whereby the synchronization between SAN pacemaker cells and ANS modulation is not fully developed until a certain age in adulthood. Consequently, non-respiratory variations in HR, i.e., short-term variations not due to RSA, might be more prevalent in younger adults, inflating HRF indices. This topic will be further discussed in Chapter 6. However, it could also be the case that younger adults present RSA oscillations with a shorter period due to either shorter PNS response time, or to differences in respiratory rate [118]. To our knowledge the former justification has not been investigated.

It should be noted that the AAdb database included a higher number of younger adults than older ones. Thus, we had access to more diverse genetic/physiological profiles for young adulthood, but not for late adulthood.

5

Changes in Heart Rate Dynamics with Disease

With age the prevalence of cardiovascular diseases increases [119]. AF and CHF are two of the most common cardiovascular diseases in the elderly [120]. The early detection of these diseases, as well as continuous monitoring of their progression is of utmost importance to reduce disease's burden and increase healthspan.

In this Chapter, we investigate how HRF, PRSA, and HRV traditional measures change with the presence of CHF and with AF severity.

5.1 Changes in Heart Rate Dynamics with Atrial Fibrillation Severity

5.1.1 Conceptual Introduction

AF is an evolving epidemic, with an estimated prevalence of 1 % – 2 % in Europe and North America [121], [122], approaching 10 % – 17 % in individuals aged above 85 years [123]. This disease constitutes the most common arrhythmia and is characterized by the very rapid and irregular firing of atrial cells, typically 400 to 600 times per minute, which overrides the slower firing of the SAN. However, the majority of these atrial impulses are not conducted through the AVN, which has some filtering function. Thus, the effective HR, i.e., ventricular rate, is dictated by the unpredictable interaction between the atrial rate and the AVN filtering function [124]. This results in two main manifestations (see Figure 5.1): (1) irregular ventricular rate in the region of 150 pulses per minute, and (2) ineffective atrial contractions [124]. Thus, the cardinal ECG features of AF include: (1) extremely irregular RR intervals, (2) no discernible P-waves that are replaced by irregular *f (fibrillatory) wavelets*, varying continuously in amplitude, polarity, and frequency [41], [125], [126]. The gold standard for AF diagnose is a fibrillation episode lasting more than 30 s [125].

AF may manifest as asymptomatic or as symptomatic, causing palpitations, syncope, and dyspnoea. However, ultimately, this disease can lead to devastating clinical outcomes,

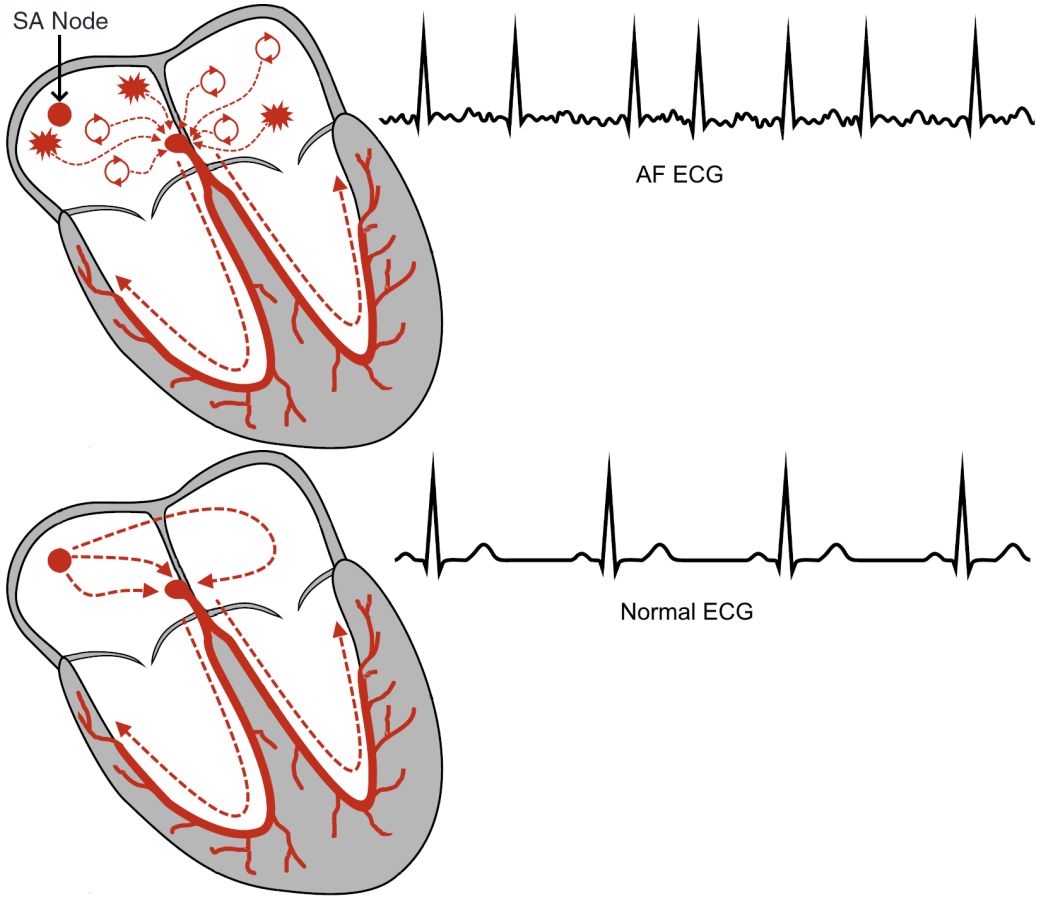

Figure 5.1: Comparison between a normal heart and associated ECG (below) with those of AF patients (above). Red dotted arrows represent the direction of electrical propagation in the heart, star-like red shapes represent triggered ectopic activity, and circular arrows represent reentrant activity in atrial tissue.

such as stroke, CHF, dementia, and even sudden death [126], [127]. Indeed, AF is an independent risk factor for stroke – increasing its risk by five-fold [128]. This is most problematic in asymptomatic AF (or also called "silent" AF or subclinical AF) and in earlier stages of the disease, which often go undetected until a stroke occurs.

Traditionally, patients with AF are divided into three main types, regarding the duration of the fibrillation episode: paroxysmal if it self-terminates within 7 days, persistent if it lasts continuously for more than 7 days, or permanent (chronic) if all treatments fail to reverse the fibrillating status [126]. However, this subtyping of AF patients has been proven to be precarious in the characterization of AF and management guidelines [129]–[131].

Currently, AF has increasingly been seen in a spectrum of atrial disease severity [130], with the underlying phenomenon of *atrial remodeling* [123]. Therefore, a characterization of AF beyond its traditional subtypes, with more insight into the atrial remodeling phenomenon is of paramount importance to readily identify and effectively stratify the risk of AF patients.

For AF to occur there are two requirements: (1) a *trigger* that initiates the arrhythmia, (2) a *vulnerable substrate*, i.e., an altererd atrial tissue, that allows the arrhythmic mechanism to self-sustain [126]. The trigger can be caused by focal ectopic beats that involve the repetitive firing of an ectopic pacemaker, or by reentrant mechanisms (see Figure 5.1). While the first is a problem of abnormal impulse formation, the latter is a problem of impulse conduction (caused by changes in cardiac tissue refractoriness) [41].

The ANS has a significant role in the genesis, maintenance, and progression of AF. Changes in ANS outflow to the heart are thought to alter atrial electrophysiology and increase the susceptibility to atrial arrhythmias. Moreover, AF itself results in substantial shifts in ANS activation that may further promote the maintenance and progression of AF [132].

The mechanism by which ANS dysfunction is associated with AF is still a matter of debate. However, studies have shown that both enhanced sympathetic and parasympathetic outflow, alone or combined, to the heart, seem to promote AF [132]. Enhanced sympathetic activity triggers ectopic activity by increasing automaticity in atrial tissue, whereas enhanced parasympathetic activity promotes reentrant mechanisms in the atrial tissue by shortening the the effective refractory period in regions of the atria [133].

Alterations in SAN integrity might also be associated with AF. SAN dysfunction compromises the ability of the pacemaker to maintain its primacy over other ectopic sources and reentrant activity, undermining the inherent ability of the SAN to prevent atrial arrhythmogenesis [134].

5.1.2 Related Work

We now present a brief overview on the main findings relating changes in HR dynamics and AF.

Agarwal et al. [135] measured the cardiac autonomic function using mean HR, and HRV measures derived from 2-min ECG recordings, such as SDNN, RMSSD, HF, and LF. They concluded that lower overall HRV was independently associated with a higher risk of AF. However, the addition of these measures to major risk scores did not improve their prediction ability. Habibi et al. [136] reported that both higher and lower RMSSD and lower SDNN were independently associated with incident AF. Raman et al. [137] associated with future development of AF increased short-term HRV. To sum up, HRV measures concerning AF were reported higher in [135], [137]–[139], and lower in [137], [140], [141]. The absence of a consensus in the direction of change in HRV measures with AF might be due to the previously discussed "HRV paradox". Nonetheless, these disparate results might be also a reflection of the different ways ANS imbalance associates with AF.

Costa et al. [27] showed that increased HRF was associated with incident AF, whereas conventional HRV and nonlinear indices were not in a three-year follow-up study. Specifically they found that (1) participants with more fragmented dynamics, measured by PIP,

PNNSS, PNNLS, ALS, W_1^H, W_3^M, and W_3^S, had significantly higher risk of developing AF; (2) HRF added value to major cardiac risk assessment indices and to well established risk factors for AF; (3) SDNN, RMSSD, the power of HF, LF bands, and the ratio between LF and HF power, sample entropy and detrended fluctuation analysis were not associated with incident AF; lastly, (4) increased HRF was still associated with augmented AF risk in two high-risk groups, namely those with elevated levels of N-Terminal Pro-B-Type Natriuretic Peptide (NT-proBNP) [1] and those with hypertension.

Chen et al. [142] measured AC and DC to evaluate sympathetic and parasympathetic changes after catheter ablation[2].They found a decline in the absolute values of DC and AC after ablation, suggesting that patients with AF were in a higher DC and a lower AC state before ablation. They hypothesized that these might indicate that AF patients were in a lower sympathetic and a higher parasympathetic modulating state before ablation.

Collectively, these studies indicate that non-vagally mediated short-term HR fluctuations, i.e., fragmentation, are associated with AF and that reduced AC and increased DC might be associated with AF.

Our work is expected to be valuable in this context since, to our knowledge, it is the first study to investigate the association of HR dynamical indices with the severity of AF measured by the time burden of AF.

5.1.3 Methods

For the analysis of the changes in HR dynamics with AF severity, we tested if HRF was higher, and PRSA and HRV indices were lower for AF high burden subjects when compared to low burden ones. We also tested whether the increase in AF burden was correlated with increase/decrease of each one of HR dynamical measures.

5.1.3.1 Database - The Long-Term AF Database

The LTAFdb [84] comprises 84 long-term ECG recordings of subjects with sustained or paroxysmal AF.

The ECG recordings were acquired with a sampling rate of 128 Hz. Participants with less than one consecutive hour of normal sinus rhythm were excluded from the analysis, remaining 50 participants. Recordings' duration varied, but were, typically, 24 to 25 hours long.

Beyond AF, some subjects also presented other minor arrhythmias, such as atrial bigeminy (AB), ventricular tachycardia (VT), supraventricular tachyarrhythmia (SVTA), ventricular trigeminy (T), ventricular bigeminy (B), idioventricular rhythm (IVR), and sinus bardycardia (SBR). In Table 5.1, we summarize the arrhythmias present in the database.

[1] NT-proBNP is chemical released by the myocardium in stretch and is typically increased in structural heart diseases and heart failure.

[2] Catheter ablation is a procedure aimed to treat AF. It uses energy to scar atrial tissue found to be triggering AF.

Arrhythmia	Median (25-75th)			Number of Subjects
	Percentage Time (%)	Number of Episodes	Max Duration	
AF	**13.9 (2.12-27.01)**	**29 (7-96)**	**56 (9-186) min**	**49**
VT	0.003 (0.002-0.009)	2 (1-6)	1.69 (1.54-2.32) s	15
AB	0.222 (0.038-0.601)	25 (5-60)	14 (6-36) s	45
SVTA	0.047 (0.015-0.100)	13 (5-29)	4.1 (2.7-7.2) s	45
T	0.071 (0.017-0.170)	7 (2-20)	13.2 (9.3-18.7) s	19
B	0.168 (0.033-1.435)	14 (3-158)	14.3 (8.5-28.7) s	20
SBR	1.557 (0.119-7.905)	161 (22-417)	35.1 (13.6-344.1) s	29
IVR	0.019	2	8.7 s	1

Table 5.1: Summary of the arrhythmias observed in the Long-term AF Database. This summary presents the median (25-75th) of the percentage time in the arrhythmia, the number of episodes in the recording, the duration of the longest episode, and the number of subjects in the database with the arrythmia. In bold we highlight the summary of the AF arrhythmia.

For subsequent analysis, subjects who presented less than 10% time in AF were considered to have low burden AF, whereas, above or equal to this threshold, were considered to have high burden AF. The low burden group had a median (25^{th}-75^{th}) of 1.70 (0.24-4.25)% percent time in AF, and the high burden group 26.23 (16.60-54.81)%.

The age and gender of participants was unknown, but was assumed that participants were old (aged above 65 years), since AF is more prevalent after this age.

5.1.3.2 Heart Rate Dynamical Analysis

HR dynamical analysis was performed as described in Section 4.3.2.

5.1.3.3 Statistical Analysis

HR dynamical variables were summarized by their median, 25^{th} and 75^{th} percentile values for the two AF burden groups.

The HR dynamical indices were compared between AF high burden and low burden subjects using either an independent two-sample T-test, Welch's T-test, or Wilcoxon rank-sum test, when the indices for the two groups were normally distributed with equal variances, normally distributed with unequal variances, and non-normally distributed, respectively. Normality and homoscedasticity were tested using Shapiro-Wilk Test and Levene's Test, respectively.

Simple linear regression was used to evaluate the change of HR dynamical indices with percent time in AF. Spearman's rank and Pearson's product-moment correlation coefficients were used to quantify the dependence between each of the HR dynamical indices and the percent time in AF.

In these analyses, statistical significance was set at a $p < 0.05$. Borderline significance was considered when $0.10 > p \geq 0.05$.

5.1.4 Results

We will begin by showing the results for the comparison between high and low burden AF subjects, and then present the results for the correlation between AF burden and HR dynamical indices.

In Table 5.2, we show the results for the comparison of the low and high burden AF groups, from which it is possible to conclude that there was a clear tendency for fragmentation to increase with AF burden, since PIP, W_3^H, and PAS were significantly (or borderline significantly) higher for higher AF burden individuals, and PNNLS, ALS, W_1, were borderline significantly lower. W_3^H corresponded to the metric with lower overlap of interquartile ranges.

Regarding PRSA and HRV variables, only RMSSD was borderline significantly higher for higher AF burden individuals.

The scatter plots for the regression analysis are presented in Figure 5.2, and the Pearson and Spearman correlation coefficients are presented in Table 5.3. From the results, it is possible to conclude that PIP, W_3^H, RMSSD, SDANN, SDNNI, and DC were significantly (or at least borderline significantly) positively correlated, and ALS negatively correlated with AF burden.

These observations indicate that there is a tendency for HRF, HRV and DC to increase with the severity of AF.

5.1.5 Discussion

From this study, we found indication that HRF analysis might be useful for risk stratification of AF patients since there seemed to be a trend towards higher fragmentation for higher burden AF. A tendency for short-term HR variations to increase with AF burden was also observed, especially by means of RMSSD and DC. As discussed in Section 5.1.2, the increase in HRV, especially short-term measures, might be justified either by (1) the "HRV paradox", whereby increased amplitude variations of HR are attributed to abnormal sinus arrhythmia – fragmentation –, or by (2) an excessive vagal outflow to the heart that promotes reentrant activity in atrial tissue. If the latter speculation was verified, it could mean that excessive vagal outflow to the heart, and thereby excessive reentrant activity in atrial tissue, is more associated with worst AF cases than excessive sympathetic activity. Conversely, if the former speculation was verified, it could mean that a worsening of the the uncorrelated function between ANS and the SAN complex is linked to worst AF cases, which is typically associated with decreased vagal modulation. Since increased fragmentation was shown to be associated with increased AF burden, we hypothesize the former mentioned justification to explain the increase in RMSSD and DC with AF burden, and not an increase in vagal outflow to the heart.

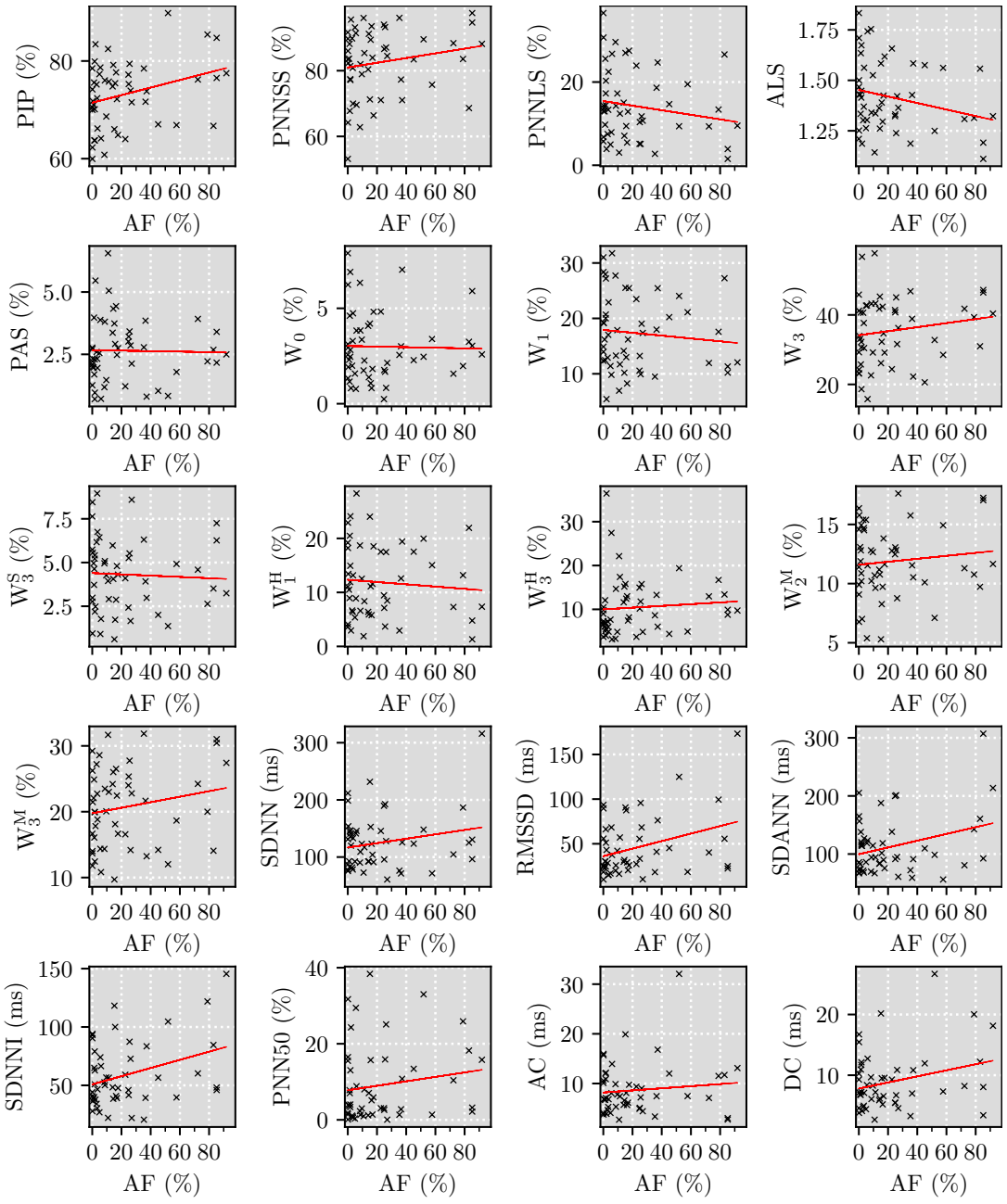

Figure 5.2: Scatter plots of the heart rate fragmentation, traditional heart rate variability, and PRSA indices vs. percent time in atrial fibrillation.

	Variable	LTAFdb		p
		Median (25–75th)		
		AF Low Burden (N = 23)	AF High Burden (N = 27)	
Overall HRF	**PIP (%)**	**71.0 (65.2–75.8)**	**75.5 (71.6–78.1)**	**0.038**
	PNNSS (%)	82.0 (73.6–88.9)	86.6 (78.9–92.2)	0.103
	PNNLS (%)	**14.3 (8.8–21.4)**	**10.7 (6.3–16.8)**	**0.070**
	ALS	**1.4 (1.3–1.6)**	**1.3 (1.3–1.5)**	**0.070**
Patterns of HRF	**PAS (%)**	**2.2 (1.6–2.7)**	**2.9 (2.2–3.6)**	**0.072**
	W_0 (%)	2.9 (2.0–4.2)	2.3 (1.7–3.3)	0.209
	W_1 (%)	17.9 (13.1–25.1)	14.1 (10.9–20.7)	0.064
	W_3 (%)	32.2 (25.0–40.9)	39.3 (31.3–42.8)	0.127
	W_3^S (%)	5.0 (2.9–6.0)	3.9 (2.8–5.1)	0.233
	W_1^H (%)	11.9 (6.6–18.5)	9.4 (6.2–17.5)	0.413
	W_3^H (%)	**6.9 (5.0–9.4)**	**11.8 (8.4–15.1**)	**0.004**
	W_2^M (%)	12.7 (10.2–14.6)	11.3 (9.9–12.9)	0.692
	W_3^M (%)	19.9 (14.4–23.1)	22.8 (16.6–26.3)	0.176
HRV	SDNN (ms)	123.0 (88.6–143.0)	123.1 (92.5–146.8)	0.492
	RMSSD (ms)	**28.5 (21.3–47.1)**	**40.3 (25.4–72.3)**	**0.070**
	SDANN (ms)	114.1 (73.7–121.9)	94.4 (82.0–140.5)	0.446
	SDNNI (ms)	50.2 (38.1–65.7)	48.3 (40.2–84.0)	0.230
	PNN50 (%)	3.6 (1.4–10.9)	5.9 (2.4–15.7)	0.175
PRSA	AC (ms)	7.1 (5.3–10.7)	7.4 (5.4–10.6)	0.423
	DC (ms)	7.2 (5.5–10.6)	7.3 (5.7–10.8)	0.484

Table 5.2: Measures of heart rate dynamics reported as median (25-75th) and p-values (p) for the comparison between AF low burden and high burden participants. Values highlighted in bold correspond to measures associated with p-values lower than 0.1.

As discussed in Section 2.2.2.2, the state of the atrial syncytium, which becomes impaired in AF, plays an important role in the emergence of uncorrelated function between SAN firing and ANS modulation, which generates fragmentation. Thus, not only ANS imbalance, but also the increased impairment of SAN and atrial tissue integrity might be the link between increased AF severity and increased fragmentation.

The tendency of DC to increase was also reported in a study mentioned in Section 5.1.2. They hypothesized it to be caused by an increase in vagal activity. However, associating DC changes with only a branch of the ANS is over-simplistic, as discussed in 2.2.3. Thus, we hypothesize that increased DC may also be a reflection of increased fragmentation.

It should also be noted that the word group W_3^H was the index that better distinguished between high and low burden AF individuals. This can be said to be expected since W_3^H

	Variable	LTAFdb			
		Pearson		Spearman	
		r_p	p	r_s	p
Overall HRF	**PIP (%)**	0.306	0.031	0.279	0.050
	PNNSS (%)	0.187	0.194	0.186	0.196
	PNNLS (%)	−0.172	0.232	−0.181	0.208
	ALS	−0.249	0.082	−0.227	0.113
Patterns of HRF	PAS (%)	−0.021	0.885	0.122	0.397
	W_0 (%)	−0.023	0.876	−0.061	0.672
	W_1 (%)	−0.101	0.486	−0.152	0.293
	W_3 (%)	0.163	0.257	0.170	0.237
	W_3^S (%)	−0.047	0.744	−0.134	0.352
	W_1^H (%)	−0.083	0.568	−0.061	0.672
	W_3^H (%)	0.083	0.569	0.257	0.072
	W_2^M (%)	0.112	0.438	0.011	0.940
	W_3^M (%)	0.185	0.199	0.158	0.272
HRV	SDNN (ms)	0.213	0.138	0.035	0.808
	RMSSD (ms)	0.338	0.016	0.207	0.148
	SDANN (ms)	0.312	0.028	0.100	0.489
	SDNNI (ms)	0.334	0.018	0.180	0.212
	PNN50 (%)	0.157	0.278	0.137	0.343
PRSA	AC (ms)	0.110	0.448	0.017	0.904
	DC (ms)	0.274	0.054	0.097	0.501

Table 5.3: Pearson product-moment correlation (r_p) and Spearman rank (r_s) coefficients for the relationships between heart rate fragmentation, traditional heart rate variability, and PRSA indices with the percent time in atrial fibrillation. The variables highlighted in bold are associated with p-values below 0.1.

corresponds to the most fragmented pattern, which reflects an extremely uncorrelated function between SAN and ANS modulation.

Some major limitations were associated with the present study, which will be highlighted in the following paragraphs. We assumed participants to be all old (aged above 65 years) with similar ages. However, possible effects on HR dynamical indices due to age differences are not excluded. Since increased AF burden might be associated with older subjects, we may not be able to discern changes in HR dynamical measures due to aging or disease's severity.

The number of intervals in the NN time series used to measure each HR dynamical measure varied greatly between subjects, since, as the standard of HR dynamics analysis implies, we could only use the sinus rhythm periods, which in some of the AF subjects were less than 2 hour in total and in others were more than 10 hours. Beyond the varying

number of intervals used, the period of the day where the NN intervals are most concentrated may also vary between subjects. This means that some subjects might have NN intervals occurring predominantly in the sleep period, whereas others may have them more predominantly occurring in the awake period.

Another major problem in this matter, is the continuity of the NN time series. It was referred in Chapter 3 that abnormal beats and arrhythmias were removed from the RR time series, which results in a discontinued NN time series. In normal subjects this might not have a significant impact in the analysis of HR dynamics, since they, typically, do not present large or frequent interruptions of sinus rhythm. However, the subjects of the LTAFdb database present large and frequent interruptions of sinus rhythm, consequently, the higher discontinuity of the NN time series might affect the results of HR dynamics analysis.

5.2 Changes in Heart Rate Dynamics with Congestive Heart Failure

5.2.1 Conceptual Introduction

Congestive Heart Failure (CHF) is a highly prevalent disease, affecting 26 million people worldwide [143]. CHF is a complex clinical syndrome that occurs when the heart is unable to eject enough blood, that is, there is a reduction in stroke volume. This reduction compromises the supply of adequate blood flow and, therefore, oxygen delivery to peripheral tissues and organs [39].

The reduced stroke volume in CHF might have different direct origins, it may either originate from loss of intrinsic inotropy of heart muscle; or from reduced blood filling of the ventricles, i.e., preload, which, for example, can be caused by reduced ventricular compliance [39], i.e., increased "stiffness". In turn, reduced inotropy may be caused by cardiomyopathies and coronary disease, and reduced preload may be caused by tachyarrhythmias (such as AF).

Recalling what was discussed in Section 2.1.4.1, to maintain arterial blood pressure in the context of reduced stroke volume many compensatory mechanisms develop, including autonomic changes, to increase vascular resistance and HR. Thus, overall cardioautonomic changes encompass increased sympathetic activity and decreased parasympathetic activity as a means to increase HR and vasoconstriction [39]. Thus, CHF is associated with a heightening of the sympathetic activity and vagal withdrawal.

5.2.2 Related Work

Many studies have found a consistent association between CHF and diminished short-term and long-term HRV measured by temporal and frequency domain indices [144]–[148].

Regarding AC and DC measures, Hu et al. [36] concluded that DC and AC were independent risk factors for CHF.

To our knowledge, the association between CHF and HRF has not yet been studied. Nevertheless, Wo et al. [149] have reported the presence of what they named "complex patterns", in which unexpected exaggerated short-term variation in HR were observed in advanced CHF patients. This was viewed as a surprising pattern since marked short-term variation should only be caused by enhanced parasympathetic activity, which opposes the general knowledge that CHF is associated with depressed parasympathetic activity. They hypothesized this unexpected result to be caused by a phenomenon (generally seen in normal subjects after intense physical exercise) called "accentuated antagonism", in which an exaggerated effect of vagal stimulation emerges in the presence of high sympathetic tone. However, in light of what has been reported by Costa et al. [23], [24], [80], this abnormal short-term variations might correspond to non-vagally mediated changes – fragmentation –, which might link SAN impairment with CHF. In fact, SAN impairment has been previously reported in prevalent CHF [150].

In the present study, we will discuss the presence of these "complex patterns" by investigating the association between HRF indices and CHF. We also provide a comparative analysis between HRV, HRF, and PRSA indices.

5.2.3 Methods

For the analysis of the changes in CHF, we tested if HRF was higher, and PRSA and HRV indices were lower for CHF subjects from the CHFdb database, when compared to healthy subjects of the NSRdb database. Furthermore, we tested if HRF analysis improved analyses made using PRSA and/or traditional HRV analysis.

5.2.3.1 The Congestive Heart Failure RR Intervals Database

The CHFdb database comprises 44 long-term ECG recordings (20 to 24 hours long) of subjects with CHF, from which 4 subjects were excluded due to having AF. For 29 subjects the ECGs were acquired at a sampling frequency of 128 Hz, and at 250 Hz for the remaining 15 subjects. This population was characterized by an age distribution with mean ± SD of 56 ± 10.

The gender was unknown for most of the subjects.

5.2.3.2 The Normal Sinus Rhythm RR Intervals Database

This database was previously described in Section 4.3.

5.2.3.3 Heart Rate Dynamical Analysis

HR dynamical analysis was performed as reported in Section 4.3.2.

5.2.3.4 Statistical Analysis

HR dynamical variables were summarized by their median, 25^{th} and 75^{th} percentile values for the CHF and healthy groups.

The HR dynamical indices were compared between the two groups using either a independent two sample T-test, Welch's T-test, or Wilcoxon rank-sum test, when the indices for the two groups were normally distributed with equal variances, normally distributed with unequal variances, and non-normally distributed, respectively. Normality and homoscedasticity were tested using Shapiro-Wilk Test and Levene's Test, respectively. We also used these tests to compare the age between the healthy and CHF populations, as a means to exclude differences in HR dynamical indices due to age differences.

Logistic regression analysis was used to evaluate how the presence of CHF was predicted by HR dynamical measures. For this analysis, normalized odds ratio and AUC were used to compare between different indices and assess the goodness of fit of each logistic model, respectively. Likelihood ratio tests were performed to ensure these logistic models performed better than the null model (when no independent variable was used, only the intercept regression coefficient).

To evaluate if HRF added value to PRSA and HRV traditional variables, likelihood ratio tests were performed for comparison of logistic models using only one, or one of both, of HRV and PRSA indices with the respective models where a HRF index was added.

In these analyses, statistical significance was set at a $p < 0.05$.

5.2.4 Results

From the results shown in Table 5.4, for the statistical tests comparing normal healthy subjects and patients with CHF, it is possible to infer that fragmentation was significantly higher in CHF subjects, since the median values of PIP, PNNSS, PAS, W^3, W_3^S, W_3^H, W_2^M, and W_3^M were significantly higher, and those of PNNLS, ALS, W_0, W_1, and W_1^H significantly lower for the CHF population.

All PRSA and HRV traditional measures were significantly lower for the CHF group.

Age was not significantly different between the two populations; therefore, it was possible to conclude that differences measured by the HR dynamical indices were not caused by differences in age.

Table 5.4 also shows that PIP, PNNSS, PNNLS, ALS, W_2^M, SDNN, SDANN, SDNNI, AC, and DC were the measures that best separated the two groups since they were associated with non-overlapping interquartile ranges between healthy and CHF participants.

In Table 5.5, we present the results for the logistic regression analysis. All HRF measures yielded logistic regression models that performed significantly better than the null model. The best HRF performing measures (AUC ≥ 0.84) corresponded to: PIP, PNNSS, PNNLS, ALS, and W_2^M.

A one-standard deviation increase in any of these fragmentation/fluency indices was

	Variable	CHFdb and NSRdb		
		Median (25–75th)		p
		Healthy (N = 72)	CHF (N = 50)	
Overall HRF	**PIP (%)**	**66.8 (60.9–71.8)**	**77.6 (72.8–79.5)**	**<0.001**
	PNNSS (%)	**73.0 (64.1–81.1)**	**90.6 (84.1–95.1)**	**<0.001**
	PNNLS (%)	**22.5 (15.8–29.2)**	**7.7 (3.7–13.1)**	**<0.001**
	ALS	**1.6 (1.4–1.7)**	**1.3 (1.2–1.4)**	**<0.001**
Patterns of HRF	PAS (%)	2.8 (1.6–3.5)	3.5 (2.4–4.0)	0.006
	W_0 (%)	3.9 (2.5–6.1)	1.5 (1.3–3.1)	<0.001
	W_1 (%)	21.8 (17.6–28.5)	12.3 (9.5–18.0)	<0.001
	W_3 (%)	31.1 (22.1–37.0)	44.9 (34.4–48.4)	<0.001
	W_3^S (%)	3.6 (2.5–4.5)	5.1 (3.9–6.3)	<0.001
	W_1^H (%)	15.9 (12.2–23.2)	7.9 (3.9–12.8)	<0.001
	W_3^H (%)	8.9 (5.5–11.2)	11.1 (8.4–13.9)	0.002
	W_2^M (%)	**10.8 (9.5–11.8)**	**13.9 (12.4–15.6)**	**<0.001**
	W_3^M (%)	17.8 (13.1–21.6)	26.5 (20.7–29.9)	<0.001
HRV	**SDNN (ms)**	**134.6 (115.1–153.4)**	**58.7 (43.1–81.4)**	**<0.001**
	RMSSD (ms)	27.5 (20.9–34.1)	14.6 (12.4–21.4)	<0.001
	SDANN (ms)	**123.4 (102.7–144.2)**	**52.6 (38.1–75.9)**	**<0.001**
	SDNNI (ms)	**51.2 (41.6–63.9)**	**24.2 (16.2–32.6)**	**<0.001**
	PNN50 (%)	5.3 (2.5–9.5)	0.9 (0.3–2.7)	<0.001
PRSA	**AC (ms)**	**10.0 (7.4–13.8)**	**3.8 (2.7–5.3)**	**<0.001**
	DC (ms)	**9.4 (6.9–12.8)**	**3.6 (2.6–5.3)**	**<0.001**
Age (yrs)		63.0 (38.8–66.0)	58.0 (51.0–63.0)	0.100

Table 5.4: Measures of heart rate dynamics reported as median (25–75th), and p-values (p) for the comparison between healthy and CHF participants. Values highlighted in bold correspond to measures associated with p-values lower than 0.001 and with non overlapping interquartile ranges.

associated with a 6.20-7.69-fold increase/decrease in the odds of CHF. The AUC associated with the regression models using either one of these variables ranged between 0.84 and 0.86.

In comparison, PRSA and traditional HRV indices were all significantly inversely associated with the presence of CHF. AC, DC, SDNN, SDNNI, and SDANN were associated with higher AUC than the HRF best metrics. These PRSA and HRV traditional metrics were associated with AUC between 0.89 and 0.92.

Nevertheless, from the results obtained for the likelihood ratio tests (cf. Tables 5.6 and 5.7), it was possible to infer that the addition of some HRF variables to logistic regression models using one of HRV or PRSA variables, or even using one of both HRV and PRSA variables, allowed their improvement. The HRF metrics that improved logistic models

	Variable	CHFdb and NSRdb			
		OR	95% CI	AUC	LLR p
Overall HRF	**PIP (%)**	6.2	[3.1, 13.0]	0.852	<0.001
	PNNSS (%)	7.1	[3.4, 15.0]	0.867	<0.001
	PNNLS (%)	0.13	[0.06, 0.28]	0.863	<0.001
	ALS	0.15	[0.07, 0.33]	0.843	<0.001
Patterns of HRF	PAS (%)	1.7	[1.1, 2.6]	0.645	0.012
	W_0 (%)	0.22	[0.11, 0.45]	0.801	<0.001
	W_1 (%)	0.23	[0.12, 0.43]	0.809	<0.001
	W_3 (%)	4.1	[2.3, 7.3]	0.805	<0.001
	W_3^S (%)	2.9	[1.8, 4.7]	0.745	<0.001
	W_1^H (%)	0.23	[0.12, 0.44]	0.796	<0.001
	W_3^H (%)	1.9	[1.2, 2.9]	0.669	0.002
	W_2^M (%)	6.7	[3.3, 14.0]	0.863	<0.001
	W_3^M (%)	5.1	[2.7, 9.6]	0.822	<0.001
HRV	**SDNN (ms)**	0.06	[0.02, 0.17]	0.917	<0.001
	RMSSD (ms)	0.13	[0.05, 0.32]	0.817	<0.001
	SDANN (ms)	0.07	[0.02, 0.17]	0.917	<0.001
	SDNNI (ms)	0.09	[0.03, 0.21]	0.894	<0.001
	PNN50 (%)	0.14	[0.05, 0.39]	0.801	<0.001
PRSA	**AC (ms)**	0.08	[0.03, 0.21]	0.888	<0.001
	DC (ms)	0.07	[0.02, 0.20]	0.885	<0.001
Age (yrs)		1.1	[0.74, 1.6]	0.435	0.656

Table 5.5: Logistic linear regression analysis of the relationship between heart rate dynamical indices and presence of congestive heart failure. The values presented correspond to the normalized odds ratio (OR), 95% confidence intervals (95% CI), area under the ROC curve (AUC), and the p-value, p, associated with the likelihood ratio test comparing the regression model with a null model containing only the zero-order regression coefficient. In bold are highlighted the variables that yielded regression models with an AUC above 0.85.

	Variable	CHFdb and NSRdb					
		SDNN	RMSSD	SDANN	SDNNI	PNN50	DC
Overall HRF	**PIP (%)**	**0.028**	**<0.001**	**0.003**	0.429	**<0.001**	0.537
	PNNSS (%)	**0.013**	**<0.001**	**0.002**	0.144	**<0.001**	0.105
	PNNLS (%)	**0.012**	**<0.001**	**0.002**	0.174	**<0.001**	0.131
	ALS	0.159	**0.010**	**0.041**	0.828	**0.002**	0.923
Patterns of HRF	PAS (%)	0.493	0.995	0.987	**0.019**	**0.888**	**<0.001**
	W_0 (%)	**0.043**	**<0.001**	**0.011**	0.257	**<0.001**	0.245
	W_1 (%)	0.097	**0.005**	**0.017**	0.933	**0.001**	0.273
	W_3 (%)	0.291	**0.012**	0.058	0.383	**0.002**	0.115
	W_3^S (%)	0.272	0.465	0.071	0.909	0.172	0.670
	W_1^H (%)	0.154	**0.028**	**0.028**	0.628	**0.005**	0.105
	W_3^H (%)	0.892	0.249	0.581	0.095	0.211	**0.015**
	W_2^M (%)	**0.011**	**<0.001**	**0.002**	**0.034**	**<0.001**	**0.004**
	W_3^M (%)	0.101	**0.002**	**0.015**	0.942	**<0.001**	1.000

Table 5.6: P-values of the likelihood ratio tests used for the comparison between logistic models of CHF using a HRV or a PRSA variable and these same models where a HRF variable is added for the NSRdb and CHFdb databases. Each column corresponds to a HRV or a PRSA variable. Each value in the table corresponds to a likelihood ratio test performed between a model using the HRV or PRSA variable present in the current column and a model using that variable plus the HRF variable present in the current row. Values inside the table highlighted in bold correspond to p-values below 0.05. Variables highlighted in bold correspond to metrics that improved more than 3 HRV models.

using both PRSA and HRV variables, were PAS, W_1, W_3, W_1^H, W_3^H, and W_2^M. It is notable that PAS improved all HRV + PRSA models.

5.2.5 Discussion

From the study of HR dynamics in CHF, it was possible to conclude that fragmentation significantly increased and AC, DC and traditional HRV measures significantly decreased with the presence of CHF.

Although HRV and PRSA indices were associated with higher AUC values than HRF indices, HRF analysis was found to improve logistic regression models using individually and simultaneously traditional HRV and PRSA analysis. In this matter, we noted that PAS, W_2^M, and W_3^H were the HRF metrics that improved models using one PRSA index, as well as models using both PRSA and HRV indices. This might indicate that these HRF measures are the ones more orthogonally related to most of HRV and PRSA indices in CHF patients.

As discussed in Sections 5.2.1 and 5.2.2, CHF is associated with diminished vagal and increased sympathetic outflow to the heart, thus, the reduction of traditional HRV and PRSA indices might reflect this autonomic imbalance.

	Variable	CHFdb and NSRdb				
		SDNN + DC	RMSSD + DC	SDANN + DC	SDNNI + DC	PNN50 + DC
Overall HRF	PIP (%)	0.333	0.640	0.366	0.414	1.000
	PNNSS (%)	0.136	0.118	0.160	0.119	0.259
	PNNLS (%)	0.135	0.151	0.161	0.139	0.307
	ALS	0.822	1.000	0.841	0.885	0.876
Patterns of HRF	**PAS (%)**	**0.006**	**<0.001**	**0.006**	**0.003**	**<0.001**
	W_0 (%)	0.257	0.291	0.276	0.263	0.443
	W_1 (%)	0.969	0.121	0.856	0.726	**0.040**
	W_3 (%)	0.169	0.064	0.168	0.152	**0.030**
	W_3^S (%)	0.960	0.483	1.000	0.943	0.363
	W_1^H (%)	0.535	0.079	0.474	0.326	**0.040**
	W_3^H (%)	0.058	**0.001**	0.058	**0.043**	**<0.001**
	W_2^M (%)	0.079	**0.001**	0.079	**0.035**	**<0.001**
	W_3^M (%)	0.927	0.956	0.888	0.938	0.798

Table 5.7: P-values of the likelihood ratio tests used for the comparison between logistic models of CHF using both HRV and PRSA variable and these same models where a HRF variable is added for the NSRdb and CHFdb databases. Each column corresponds to a HRV plus a PRSA variable. Each value in the table corresponds to a likelihood ratio test performed between a model using the HRV plus PRSA variable present in the current column and a model using that variables plus the HRF variable present in the current row. Values inside the table highlighted in bold correspond to p-values below 0.05. Variables highlighted in bold correspond to metrics that improved at least one model.

The association between increased/decreased fragmentation/fluency with CHF might indicate the emergence of non-respiratory sinus arrhythmia in this population. We hypothesized this to originate from SAN impairment, which in turn might originate from excessive sympathetic stimulation of the superior pacemaker cells of the SAN. This suggestion aligns with what has been reported by Sanders et al. [150], namely, that patients with CHF showed SAN remodeling with consequent reduced SAN function.

To improve this analysis, we could also have evaluated the differences in HR dynamical measures between awake and sleep periods to draw conclusions about how these periods affect, individually, the used dynamical indices.

6

Changes in Heart Rate Dynamics From Early Childhood to Late Adulthood

The incursion of diseases and deterioration begin early in life. There is increasing evidence that tracking changes in early childhood is not only important to prevent infant mortality, but also to predict diseases and early aging in adulthood [17], [18].

Measuring the maturation of the ANS is a means to track changes in early childhood [14], [151]. In this Chapter, we will investigate if HRF decreases with age in the first years of life, as well as if HRV and AC/DC capacities of the heart increase.

In addition, we will study the evolution of these metrics through all ages, from birth to late adulthood. We expect that between the rise (maturation) and fall (aging) of variability, fluency, and AC/DC capacities of HR it follows a relatively stable phase in adulthood, where these indices reach a relatively stable plateau. Thus, an U-shaped relationship between these HR dynamical measures and age from birth to late adulthood will be evaluated as a candidate to explain the variation of HR dynamical indices with age.

6.1 Introduction

The maturation of the ANS is not limited to the fetal period, instead it continues after birth. Many studies have shown that the two branches of the ANS mature at different rates [14], [151]. Although in fetal life the PNS is the first to structurally appear, it remains relatively unresponsive to the demands of the fetus or newborn [152]. Conversely, the maturation of the SNS occurs steadily throughout gestation and, in the context of a less developed PNS, at birth the SNS is predominant [14]. Nonetheless, during the first months of life there is an active myelination of the vagus nerve [153] with a concurrent progressive increase in its dominance [154].

The normal HR in neonates is much higher when compared to adults, i.e., 120 to 160 bpm *versus* 60 to 100 bpm [155], [156]. This derives from the fact that in the first months of life the maintenance of adequate arterial blood pressure is ensured by a high

HR since the neontal ventricular myocardium has limited capability to increase stroke volume [155]. This is a consequence of the low intrinsic contractility of the ventricular myocardium, i.e, low number of fibrils and a high degree of stiffness [156].

The current knowledge about the maturation of the ANS system from birth to infancy, as well as from infancy to adulthood is limited. It is not yet clear the age at which a fully matured ANS system is attained, nor how this maturation is made in conjugation with the SAN. Most of the work done in this field has been done by HR dynamical analysis.

6.2 Related Work

We now briefly discuss the major studies regarding changes in HR dynamics from early childhood to either adolescence, young adulthood, or late adulthood, using 24-hour ECG recordings.

Finley and Nugent [157] studied 61 individuals aged between 1 month to 24 years of age using frequency domain HRV analysis. They reported a significant increase in HF and LF between 0 to 6 years followed by a decrease until 24 years of age.

Goto et al. [158] evaluated the changes in 60 individuals aged between 3 to 15 years using two HRV frequency domain measures, namely HF and LF, and four HRV time domain measures, namely RMSSD, SDNN, PNN50, and SDANN. They reported an increase in SDNN from 3 to 9 years followed by a decrease from 9 to 15 years; SDANN was shown not to change until the age of 15 years where it decreased; PNN50 and RMSSD were shown to increase from 3 to 6 years and to decrease from 9 to 15 years; HF and LF were shown to increase between 3 to 6 years and then to decrease from 6 to 15 years.

Bobkowski et al. [159] studied 100 subjects aged between 3 to 18 years of age. They found that the power of all frequency bands considered in HRV analysis, as well as SDNN, increased linearly with age without any significant abrupt change.

Cysarz et al. [160] studied 409 individuals aged between 1 to 22 years. They found that SDNN increased during childhood up to age of 9 years, then remain relatively constant until 14 years of age when it increased again until 22 years; LF band was reported to increase only up to 9 years; HF was shown to be constant up to 14 years and then to decrease until the 22 years.

More recently, Garavaglia et al. [161] evaluated data from 700 healthy subjects aged between 1 month and 99 years of age. In this study RMSSD, PNN50, and SDNN were shown to increase until 12 years of age and to decrease thereafter. They reported this change of direction in the magnitude of these variables to be abrupt.

Hayano et al. [82] studied changes in both HRV and HRF using a big dataset containing 3917 subjects. These subjects were aged between 0 to 100 years, however, only ages multiple of 5 were used. They reported an increase in RMSSD until 20 years of age and then a decrease from that age to forty years; thereafter, a plateau phase was reported until 75 years, beyond which RMSSD markedly increased. Regarding fragmentation metrics,

PIP, W_3^M, W_2^M, W_3^S were reported to decrease until 20 years of age and then to stabilize until around thrity to forty years, beyond which these metrics increased. For W_1^H the reverse pattern was observed: an increase until 20 years of age followed by a stable phase and then a marked decrease. W_0 was shown to increase up to 30 years and then to decrease. W_3^H was shown to gradually decrease until middle age, and then to increase with age. No explanation was provided for these patterns of evolution.

Collectively, these studies indicate that there is a tendency for HRF/HRV decrease/increase during infancy until a age around adulthood and adolescence where it starts to decline.

In the present dissertation, we take a closer look on the evolution of HRF measures during infancy, which was not attained by Hayano et al., since they only had access to the ages of 0 (few months), 5, and 10 years. We also investigate the changes in PRSA indices during infancy, which was not previously done to our knowledge.

6.3 Methods

To evaluate the changes in HR dynamical indices from early childhood to infancy, subjects aged between 1 month and 6 years were included from the RR intervals Time Series from Healthy Subjects Database (RRHSdb) [98].

To investigate the evolution of HR dynamical indices from birth to late adulthood all subjects from both RRHSdb and Normal Sinus Rhythm RR intervals Database (NSRdb) [78] databases were included.

6.3.1 RR Interval Time Series from Healthy Subjects Database

The RRHSdb database comprises 147 individuals, 72 males and 67 females (gender data was not available for 8 individuals). In this database there were 71 subjects under one year of age, and only 10 were over 18 years of age. The median (25th-75th) age of subjects aged below or equal to one year was $5(3-8)$ months.

This database provided NN time series instead of the ECG recordings. Above we describe their procedure to obtain these time series. ECG recordings were obtained by Holter monitoring during 24 h with a sampling rate of 128 Hz. Heart beats were automatically detected and classified by the Holter software, and then examined and corrected by two cardiologists. RR time series with more than 8% artifacts were not included, nor those with artifacts longer than 10 s. In the accepted NN time series the segments containing artifacts were removed.

6.3.2 The Normal Sinus Rhythm RR Intervals Database

This database was previously described in Section 4.3.

NSRdb and RRHSdb combined include 198 participants with the age distribution described in Table 6.1.

Age Range (yrs)	Number of Individuals
$0 < age \leq 1$	71
$2 \leq age \leq 7$	24
$8 \leq age \leq 15$	20
$16 \leq age \leq 25$	5
$26 \leq age \leq 30$	5
$31 \leq age \leq 40$	18
$41 \leq age \leq 50$	6
$51 \leq age \leq 64$	21
$65 \leq age \leq 75$	28
Total	198

Table 6.1: Age Distribution of the population included in the NSRdb and RRHSdb Databases.

6.3.3 Heart Rate Dynamical Analysis

HR dynamical analysis was performed as described in Section 4.3.2.

6.3.4 Specific Hypotheses

For the analysis of the changes in HR dynamical indices during early childhood, we tested whether HRF indices decreased and HRV and PRSA indices increased with age between one month to 6 years of life.

Using the full range of ages, we also tested if the relationship between age and each one of the HR dynamical indices was quadratic.

6.3.5 Statistical Analysis

Linear regression analysis was used to quantify the dependence of each calculated HR dynamical index with age in the first years of life. In this analysis, Spearman's rank and Pearson's product-moment correlation coefficients were computed to quantify the association between age and HR dynamical measures.

To evaluate how well an U-shaped function described the relationship of each HR dynamical index and age from birth to late adulthood (1 month to 76 years of age), scatter plots were qualitatively analyzed, and linear regression analysis was performed using a quadratic term (i.e., $W_0 = \beta_0 + \beta_1 age + \beta_2 age^2$). To quantify the goodness of fit of this model, the coefficient of determination, R^2, was used. We also tested if the coefficient associated with the second degree term (β_2) was significantly different from zero.

Statistical significance was set at $p < 0.05$.

Variable		p	r_p
Overall Fragmentation	PNNSS (%)	<0.001	-0.790
	PNNLS (%)	<0.001	0.827
	ALS	0.002	0.874
Patterns of Fragmentation	W_1 (%)	<0.001	0.773
	W_3 (%)	<0.001	-0.808
	W_1^H (%)	0.020	0.853
	W_3^M (%)	<0.001	-0.816

Table 6.2: Evaluation of the independence of HRF indices from mean heart rate when predicting age in early childhood using linear regression models. Values presented correspond to the p-value (p) of the coefficient associated with a HRF index in age linear regression models adjusted for mean heart rate as follows $age = \beta_0 + \beta_1 HRF_{index} + \beta_2 meanHR$, and Pearson coefficients, r_p, for the dependence between a HRF index and mean heart rate.

6.4 Results

From Table 6.3 and the scatter plots presented in Figure 6.1, it is visible that all fragmentation/fluency indices significantly decreased/increased with age from few months of life to infancy. PNNSS, PNNLS, ALS, W_1, W_3, W_1^H, and W_3^M were associated with absolute values of Pearson or Spearman correlation coefficient above 0.700, reflecting a very strong dependence with age. The HRF indices with higher correlation coefficients corresponded to PNNLS ($r_p = 0.801$) and ALS ($r_p = 0.804$).

Regarding HRV and PRSA variables, all indices significantly increased with age. SDNN, SDANN, AC, and DC were associated with Pearson or Spearman correlation coefficient above 0.700. However, none of these dynamical indices yielded greater correlation with age than the PNNLS and ALS indices.

To evaluate if the high correlation values ($r_p > 0.7$) associated with some HRF metrics were not just a byproduct of the changes that occur due to the decrease in the mean HR during this life period, we analyzed the effect of mean HR on the relations between age and HRF indices.

From Table 6.2, we can see that the HRF indices were still associated with regression coefficients significantly different from zero for the models adjusted for mean HR ($age = \beta_0 + \beta_1 HRF_{index} + \beta_2 meanHR$). In this same Table, the Pearson correlation coefficients quantifying the dependence between each HRF index and mean HR are shown. Although the HRF metrics are highly correlated with mean HR, around 20% of the variation in each HRF index could not be explained by the variation in mean HR.

From the scatter plots and regression curves presented in Figure 6.2, it is possible to make some inferences about the evolution of each dynamical index with age. For most of fragmentation indices, i.e., PIP, PNNSS, PNNLS, ALS, PAS, W_1, W_3, W_3^S, W_1^H, W_2^M, and W_3^M, the evolution with the subjects' age seemed to follow an U-shaped relationship

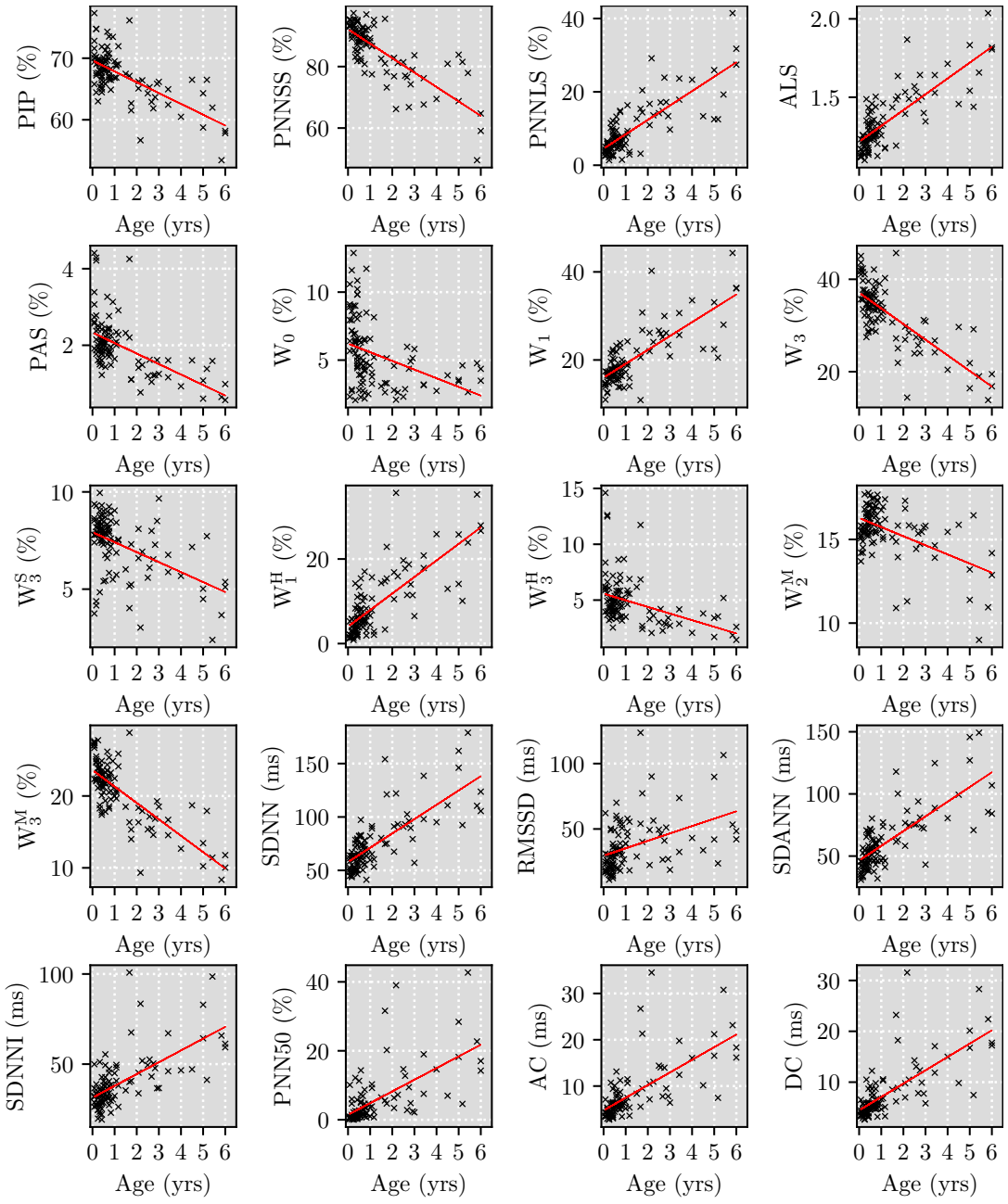

Figure 6.1: Scatter plots of the heart rate fragmentation, traditional heart rate variability, and PRSA indices vs. the participants' age, from early childhood to infancy.

	Variable	RRHdb			
		Pearson		Spearman	
		r_p	p	r_s	p
Overall HRF	PIP (%)	−0.663	< 0.001	−0.511	< 0.001
	PNNSS (%)	−0.789	< 0.001	−0.708	< 0.001
	PNNLS (%)	0.801	< 0.001	0.717	< 0.001
	ALS	0.804	< 0.001	0.751	< 0.001
Patterns of HRF	PAS (%)	−0.558	< 0.001	−0.539	< 0.001
	W_0 (%)	−0.383	< 0.001	−0.511	< 0.001
	W_1 (%)	0.769	< 0.001	0.683	< 0.001
	W_3 (%)	−0.765	< 0.001	−0.685	< 0.001
	W_3^S (%)	−0.493	< 0.001	−0.416	< 0.001
	W_1^H (%)	0.769	< 0.001	0.733	< 0.001
	W_3^H (%)	−0.401	< 0.001	−0.413	< 0.001
	W_2^M (%)	−0.530	< 0.001	−0.164	0.098
	W_3^M (%)	−0.777	< 0.001	−0.694	< 0.001
HRV	SDNN (ms)	0.759	< 0.001	0.701	< 0.001
	RMSSD (ms)	0.419	< 0.001	0.553	< 0.001
	SDANN (ms)	0.755	< 0.001	0.710	< 0.001
	SDNNI (ms)	0.653	< 0.001	0.634	< 0.001
	PNN50 (%)	0.635	< 0.001	0.674	< 0.001
PRSA	AC (ms)	0.689	< 0.001	0.738	< 0.001
	DC (ms)	0.722	< 0.001	0.725	< 0.001

Table 6.3: Pearson product-moment correlation (r_p) and Spearman rank coefficients (r_s) for the relationships between heart rate fragmentation, traditional heart rate variability, and PRSA indices with cross-sectional age from birth to infancy in the RRHdb database. The variables highlighted in bold correspond to the measures with higher correlation coefficients.

described as follows: during the first years of life there is an abrupt decrease in fragmentation, which slows down until around the third to fourth decade of life, where a fragmentation stable minimum is apparently achieved; after the fifth decade, a steep rise in fragmentation occurs until the seventh decade of life.

The other, not mentioned, HRF variables, i.e., W_3^H and W_0, seemed to evolve in another fashion with the subjects' age:

- W_3^H decreases until fifteen years, reaching a minimum at that age. Thereafter, it stays relatively stable until forty years of age, when it starts to rise.
- W_0 dramatically decreases until around fifteen years, reaching a minimum at that age period. However, it showed a tendency to rise from fifteen years to around thirty to forty years of age, falling again through late adulthood. In fact, although

not shown, when a third degree polynomial is used (i.e., $W_0 = \beta_0 + \beta_1 age + \beta_2 age^2 + \beta_3 age^3$), a minimum is observed around fifteen years, as well as maximum around forty years of age.

Regarding traditional HRV and PRSA measures, an U-shaped relationship was as well visible with an apparent maximum also around the third and fourth decade of life. However, there seemed to be a prominent peak at approximately fifteen years of age.

The results for the regression analysis of the second degree polynomial fit are presented in Table 6.4. From this Table, it is possible to conclude that the coefficient of the quadratic term was significantly different from zero for all variables except for W_0.

Regarding HRF variables, the coefficient of determination ranged from 0.336 to 0.599. The variables that were associated with R^2 above 0.5, corresponded to PNNSS, PNNLS, ALS, W_3^S, and W_2^M.

Traditional HRV indices were associated with R^2 ranging between 0.135 and 0.463, being SDNN, and SDANN the variables with higher R^2. AC and DC capacities were associated, respectively, to R^2 of 0.282 and 0.302.

6.5 Discussion

From the results obtained for the relationships between HR dynamical indices and age from birth to infancy, it was possible to conclude that maturation of the ANS is accompanied by a decrease in fragmentation and an increase in both HRV indices and AC/DC capacities.

The increase in HRV and PRSA indices might be due to the increase in vagal predominance, as was discussed in Section 6.1. The increase in HRV metrics is concordant with most of the studies presented in Section 6.2.

We hypothesize that the decrease/increase in fragmentation/fluency measures indicate that at birth the correlated function between SAN and ANS modulation is not yet "well-constructed", giving rise to excessive beat-to-beat fluctuations. Throughout infancy the synchrony between ANS modulation and SAN pacemaker cells might increase causing a decrease in fragmentation. We speculate this synchrony to be ensured by the increase in vagal predominance that occurs throughout infancy.

Higher correlation values with age were observed for most of HRF metrics, when compared to HRV and PRSA indices. This indicates that changes in infancy are best captured by HRF measures.

Regarding the evolution of HR dynamical indices from birth to late adulthood, most of HRF variables were well described by an U-shaped evolution during a lifetime (cross-sectionally estimated), with a minimum (maximum for fluency metrics) around the third and fourth decade of life. This observation is consistent with the results reported by Hayano et al. [82], which were presented in Section 6.2. It is noteworthy that Hayano et al. also reported a distinct behavior for W_3^H and W_0. As the most fragmented pattern,

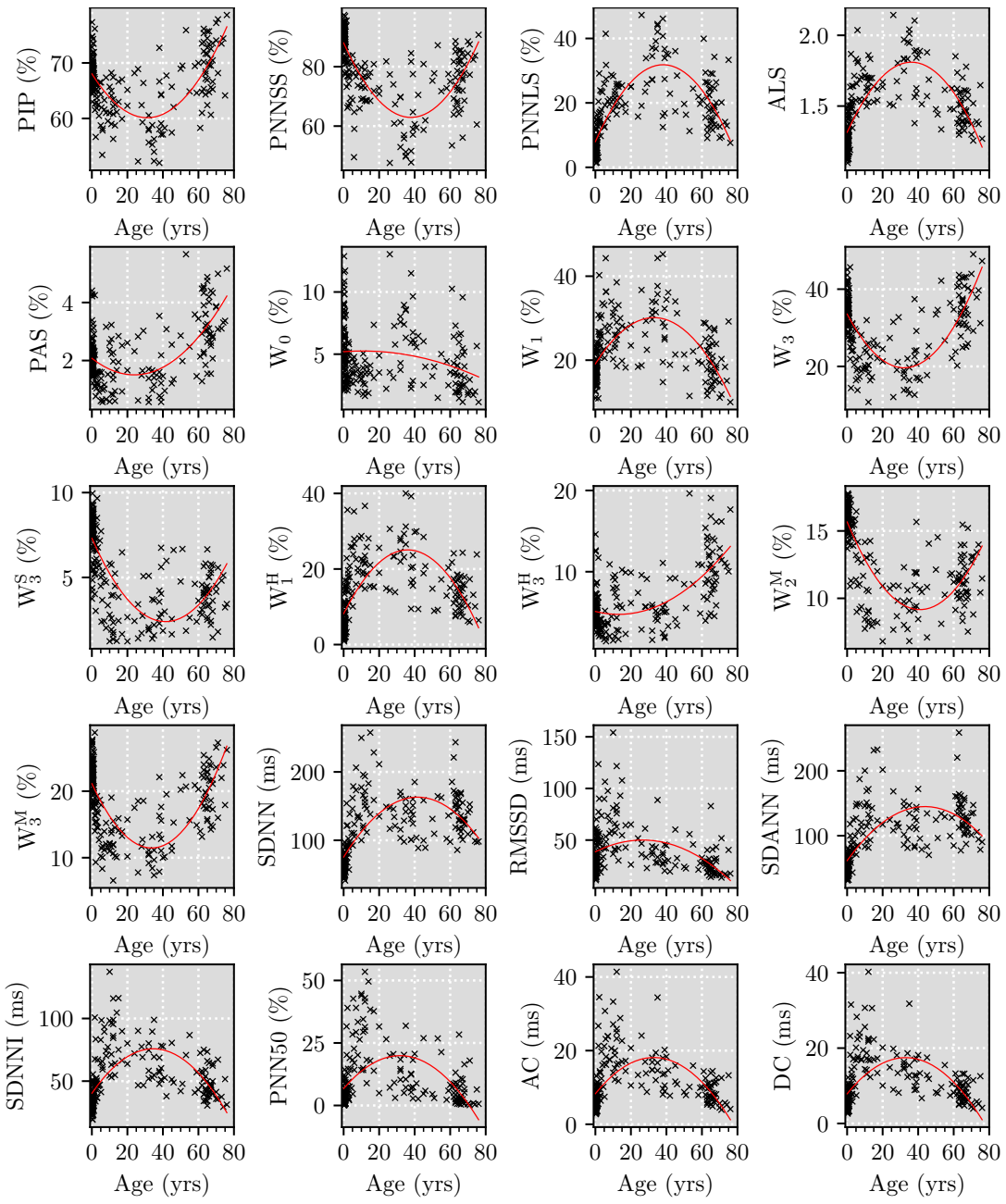

Figure 6.2: Scatter plots of the heart rate fragmentation, traditional heart rate variability, and PRSA indices vs. the participants' age, from early childhood to late adulthood.

	Variable	R^2	p
Overall HRF	PIP (%)	0.396	<0.001
	PNNSS (%)	0.524	<0.001
	PNNLS (%)	0.584	<0.001
	ALS	0.530	<0.001
Patterns of HRF	PAS (%)	0.361	<0.001
	W_0 (%)	0.059	0.241
	W_1 (%)	0.336	<0.001
	W_3 (%)	0.437	<0.001
	W_3^S (%)	0.544	<0.001
	W_1^H (%)	0.432	<0.001
	W_3^H (%)	0.410	<0.001
	W_2^M (%)	0.599	<0.001
	W_3^M (%)	0.450	<0.017
HRV	SDNN (ms)	0.463	<0.001
	RMSSD (ms)	0.135	<0.001
	SDANN (ms)	0.481	<0.001
	SDNNI (ms)	0.334	<0.001
	PNN50 (%)	0.216	<0.001
PRSA	AC (ms)	0.282	<0.001
	DC (ms)	0.302	<0.001

Table 6.4: Polynomial linear regression analysis for the relationship between age and heart rate dynamical indices from birth to late adulthood. Coefficient of determination (R^2) and the p-value (p) associated with the quadratic term. Variables highlighted in bold are associated with an R^2 above 0.5.

W_3^H can be said to reflect extremely uncoordinated function between the SAN and the ANS modulation, thus, its reduction earlier than the other fragmentation metrics may be crucial for the maturation process.

Traditional HRV and PRSA indices also seemed to follow an U-shaped evolution with age; although not so significantly when compared to HRF indices. In general, the fitted polynomial for all HRV and PRSA variables also presented a maximum around the third to fourth decade. However, as mentioned in the results section, a prominent peak was apparent at around 15 years of age for HRV and PRSA measures. This peak was concordant with some studies presented in Section 6.2. One might hypothesize this peak to represent the age of greatest vagal predominance.

Collectively, these results provide indication that the autonomic system, as well as its correlated function with the SAN reach a fully matured state around the third to fourth decade of life.

One might argue that the extension of the maturation process from infancy to adulthood is unexpected or rather odd. However, it should be noted that the maturation of the ANS is not exclusively dependent on well-predetermined physiological events, such as the myelination of the vagus nerve in the first months of life. Instead, it is also highly affected by the development of higher brain areas, such as the cerebral cortex, which does not finish in adolescence. In fact, it was shown that higher brain centers take around 25 years to fully develop [162]. This may explain the results observed in the present study, as well as the ones reported in Section 4.4.3.

As mentioned in Section 6.1, in early childhood mean HR is higher than in adults, thus, typically, to correctly capture high frequency variations in the HR of infants a higher sampling frequency is needed. It has been suggested a minimum of 1000 Hz for sampling the ECG of infants [163], however, 128 Hz was the sampling frequency at which the ECGs of the RRHdb were acquired. An increase in the sampling frequency would probably increase fragmentation, since rapid changes in HR acceleration sign would be better sampled. Thus, the impact of a higher sampling frequency would only favor the tendency observed, i.e., higher fragmentation for infants.

7

Estimation of the Minimum Time Required to Measure Heart Rate Fragmentation Indices

In the present Chapter, we estimate the minimum time required to measure each HRF index by calculating the minimum length time interval that allows the use of HRF for the distinction between young and old individuals in supine resting position. In addition, we estimate the uncertainty associated with measures computed in shorter time intervals when compared to those obtained from the full recording and evaluate the stability of each measure.

7.1 Introduction

To introduce the problem we are addressing we present, in Figure 7.1, the evolution of two HRF indices, i.e., PIP_S and PNNSS, during 2-hour ECG recordings from the Fantasia Database [83], using three different time resolutions. In this example, the HRF indices were computed for two thirds overlapping windows of lengths 5 min, 15 min, and 30 min for a young (bottom row) and an old individual (top row).

Concerning the two plots relative to the PIP_S index shown in Figure 7.1, it is remarkable to note that choosing a 5-minute window from both the young and old subjects, will allow the distinction between the two subjects, for most combinations of windows. This is the case given that most of the PIPs values for these 5-minute windows are above 8% for the old subject, whilst for the young one are below 8%. However, if by chance the only accessible 5-minute window for the old subject was one whose value is below 8%, the distinction between the two subjects could be precluded.

Thus, to establish the minimum time in a quantity that still allows PIPs to separate a healthier subject from an unhealthier one, it is important to quantify the probability associated with the success of PIPs in this task at increasingly shorter window lengths.

Regarding the PNNSS index, as visible in Figure 7.1, it is possible to state that the chance of choosing a 5-minute window that allows the distinction between the young

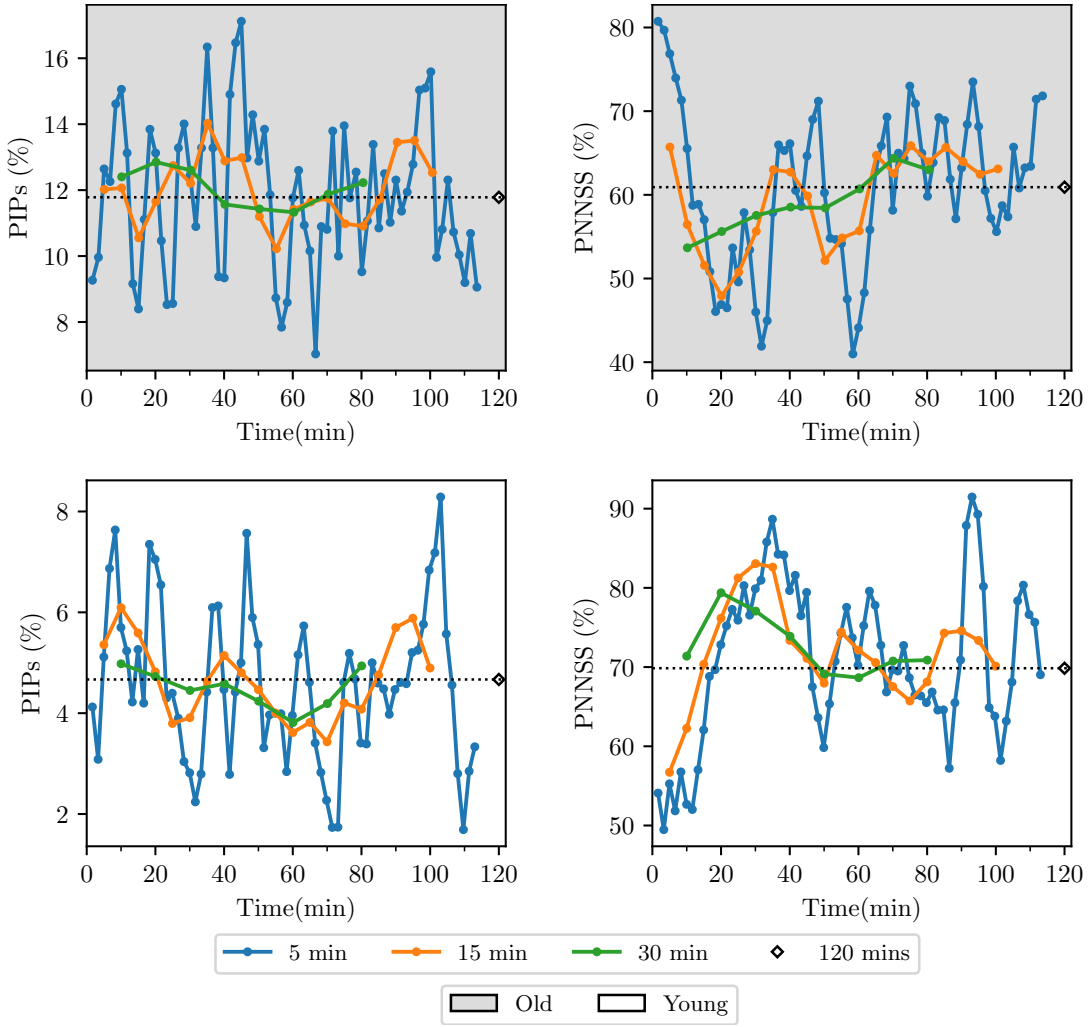

Figure 7.1: Evolution of PIPs (left) and PNNSS (right) in windows of length 5 min (blue), 15 min (orange), and 30 min (green), for an old subject (top row in gray) and a young one (bottom row in white) throughout the full recording time. The dashed horizontal black line represents the full-length metric value.

and old subjects is much lower. This derives from the observation that the two windowed series overlap to a great extent, given that for the old subject most of PNNSS values are between 45% and 75% and for the young one are mostly between 65% and 85%.

Consequently, in this example, it is expected that PIPs might require a lower minimum time to be measured than PNNSS.

Regarding the uncertainty of using a shorter window in relation to the measurement using the full recording, one can say that PIPs windowed values, generally, seem to better approximate to the full length measurement than PNNSS, given that PIP_S windowed measures are closer to full recording measure (in absolute terms). Thus, it is also expected that there is higher uncertainty associated with PNNSS computed in shorter time windows.

To analyze the stability of these metrics, the relative distance between windowed

measures and the full recording measure can be used.

7.2 Methods

In this Section, we describe the population used in this study, the HRF analysis performed, and the procedures used to estimate the minimum time required to measure each HRF index, the associated uncertainty of using shorter window lengths when computing these indices, and the stability of HRF indices.

7.2.1 Population - Fantasia Database

A detailed description of the Fantasia database is provided in Section 4.3.

7.2.2 Heart Rate Fragmentation Analysis

HRF analysis was performed by calculating the following overall fragmentation indices: PIP, PIPs, PIPh, PNNSS, PNNLS, and ALS. The percentage of the following patterns of fragmentation were also computed: PAS, W_0, W_1^H, W_2^H, W_3^H, W_1^S, W_2^S, W_3^S, W_2^M, and W_3^M.

Each HRF index was calculated over the full recording and in moving windows with two thirds of overlap. 60 different time sizes for the windows were used, from 1 minute to 60 minutes in steps of 1 minute.

7.2.3 Statistical Procedures

To estimate the minimum time required to compute a HRF index, we calculated the probability at which the index in a given time interval succeeds in distinguishing young adulthood from late adulthood. To calculate this probability, we observed the statistical procedure illustrated in Figure 7.2.

In this procedure, for each specific time window length, e.g., 30 min, (1) one window was randomly selected from each individual of the young group and the old one, resulting in a set of randomly selected windows for the two groups; (2) the HRF index was computed for all selected windows of the specific time length; (3) a normality test was performed to evaluate if the selected windows were normally distributed for both groups, if so, (4) it was performed an independent two-sampled T-test, otherwise, a Wilcoxon rank-sum test, to compare the randomly selected windows from young and old subjects. This procedure was carried out for window lengths ranging from 1 min to 60 min in 1 min steps, and repeated 1000 times. In the end (5) the probabilities of these statistical tests yielding a p-value below 0.10, and below 0.05 were calculated.

To evaluate the uncertainty and the stability associated with a HRF index, we computed for each considered window length, respectively, the mean SD and mean Coefficient of Variation (CV)[1] of each index, in both young and old groups separately. The SDs and

[1] The CV is a measure of relative dispersion, computed as SD divided by the mean.

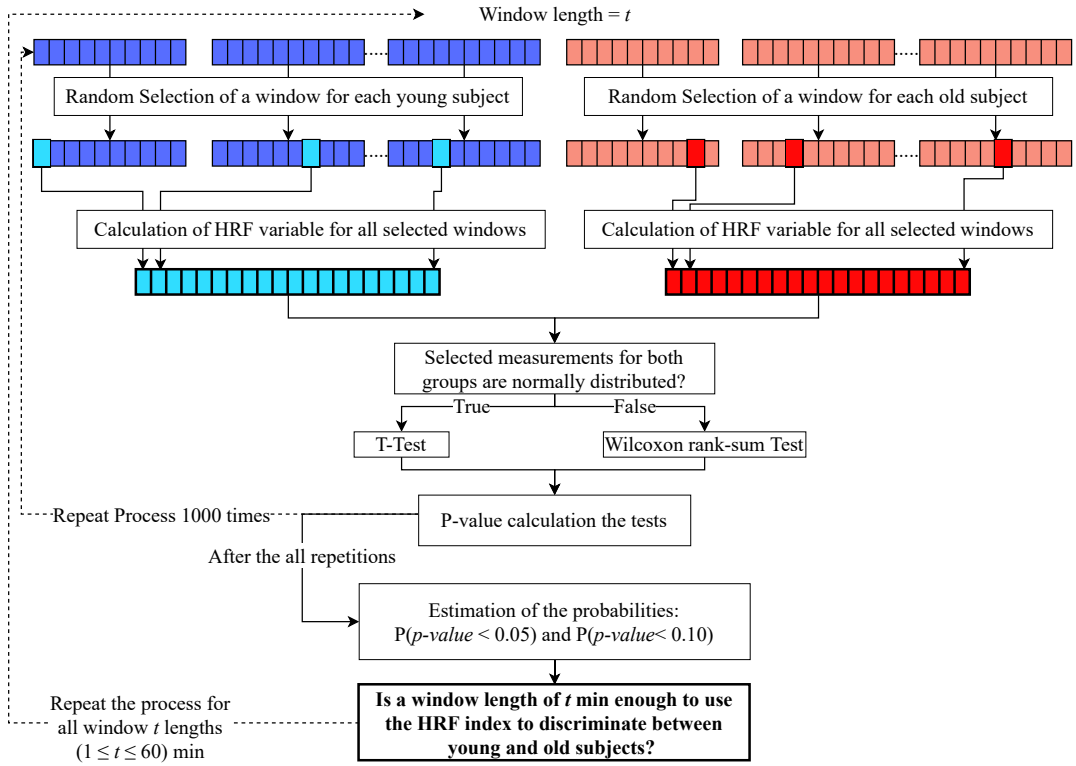

Figure 7.2: Diagram representation of the statistical process used to estimate the minimum time required to use a HRF variable as an aging biomarker. Dashed arrows represent steps that are repeated. The first line of arrays represent the windowed time series for each of the 20 young subjects (left in blue) and for each of the 20 old subjects (right in light red). The second line of arrays represents the random selection of a window from each individual, light blue for the young subjects and darker red for the old subjects. The third line represents all the windows selected for the young subjects (20 windows in the left) and all the windows selected from the old subjects (20 windows in the right).

CVs were calculated for window lengths ranging from 1 minute to 60 minutes (in steps of one minute). This procedure is illustrated in Figure 7.3, where the mean SD and mean CV are being computed for a window length of time t ($1 \geq t \geq 60$) min.

7.3 Results

For the estimation of the minimum time required to measure HRF indices, as shown in the plots of Figure 7.4, it is possible to conclude that PIP_S, W_3^M, W_2^M, W_3^S, and W_3^S required less than 11 minutes to be associated with a probability of one in distinguishing young adulthood from late adulthood with a confidence level above 95%. In particular, PIP_S and W_3^M required 2 minutes, W_2^M 3 minutes, and W_3^S and W_2^S 10 minutes. W_1^H required 10 minutes to distinguish the two groups with a probability of 0.95 with a confidence level of 95%.

For PIP, ALS, PAS, and W_1^S, it is visible that they required much more time to distinguish the two groups with a probability above 0.5 with a confidence level superior to 95%

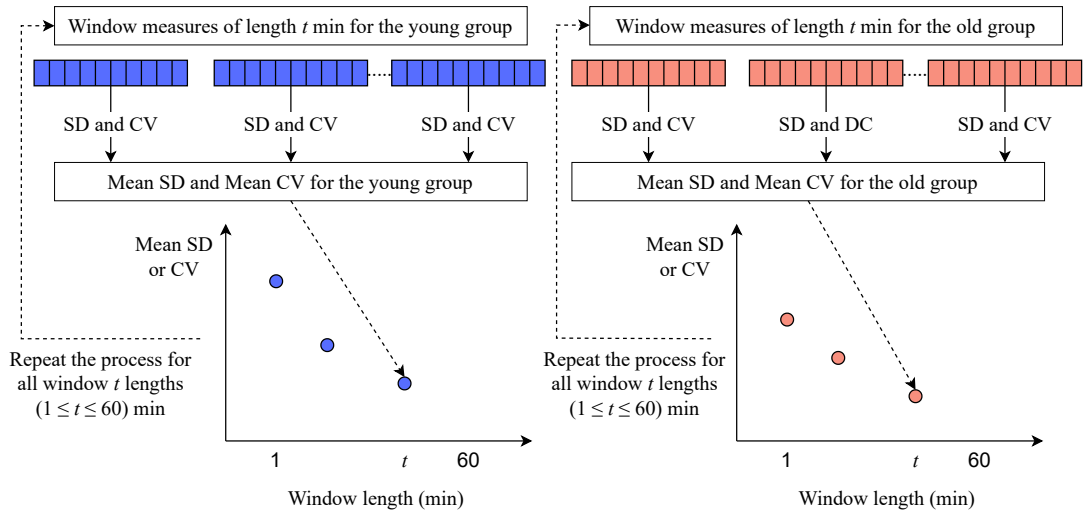

Figure 7.3: Diagram representation of the procedure used to analyze the uncertainty and stability of HRF indices, when computed for shorter window lengths in relation to the metric computed over the full recording length.

and never surpassed a probability of 0.85.

Regarding PNNLS, PNNSS, W_0, and W_3^H, it was not possible to define a minimum time, since they were associated with a very low probability of separating the two groups for all window lengths.

Regarding the evaluation of the uncertainty, in Figure 7.5, we present how mean standard deviation evolves with the window length for each HRF index.

By using both plots presented in Figures 7.4 and 7.5, it is possible to state that, for example, a 1-minute ECG recording is enough to use PIP_S to distinguish between young adulthood and late adulthood with an associated (mean± SD) uncertainty of (6 ± 1)% for an old individual and (4 ± 1)% uncertainty for a younger one.

Regarding the analysis of the stability of HRF indices, Figure 7.6 shows plots relative to the evolution of the mean CV for each HRF metric for both young and older participants. From these plots, it is possible to conclude that most of HRF metrics varied less than 20% in relation to metric computed for the the full recording, after a window length of 20 minutes. The least stable metrics corresponded to PAS, W_0, W_1^S, and W_3^S. Conversely, the most stable metrics corresponded to PIP, PIP_H, ALS, PNNSS, W_2^H, and W_1^H.

7.4 Discussion

We found that, for the HRF variables that were previously shown to significantly separate young subjects from older ones in the Fantasia Database (Section 4.4.2), typically, between 2 minutes to 10 minutes were necessary. This finding might present as very advantageous. The need of relatively short ECG recordings may render easier the design of more reproducible experiments, since it allows the establishment of more controlled

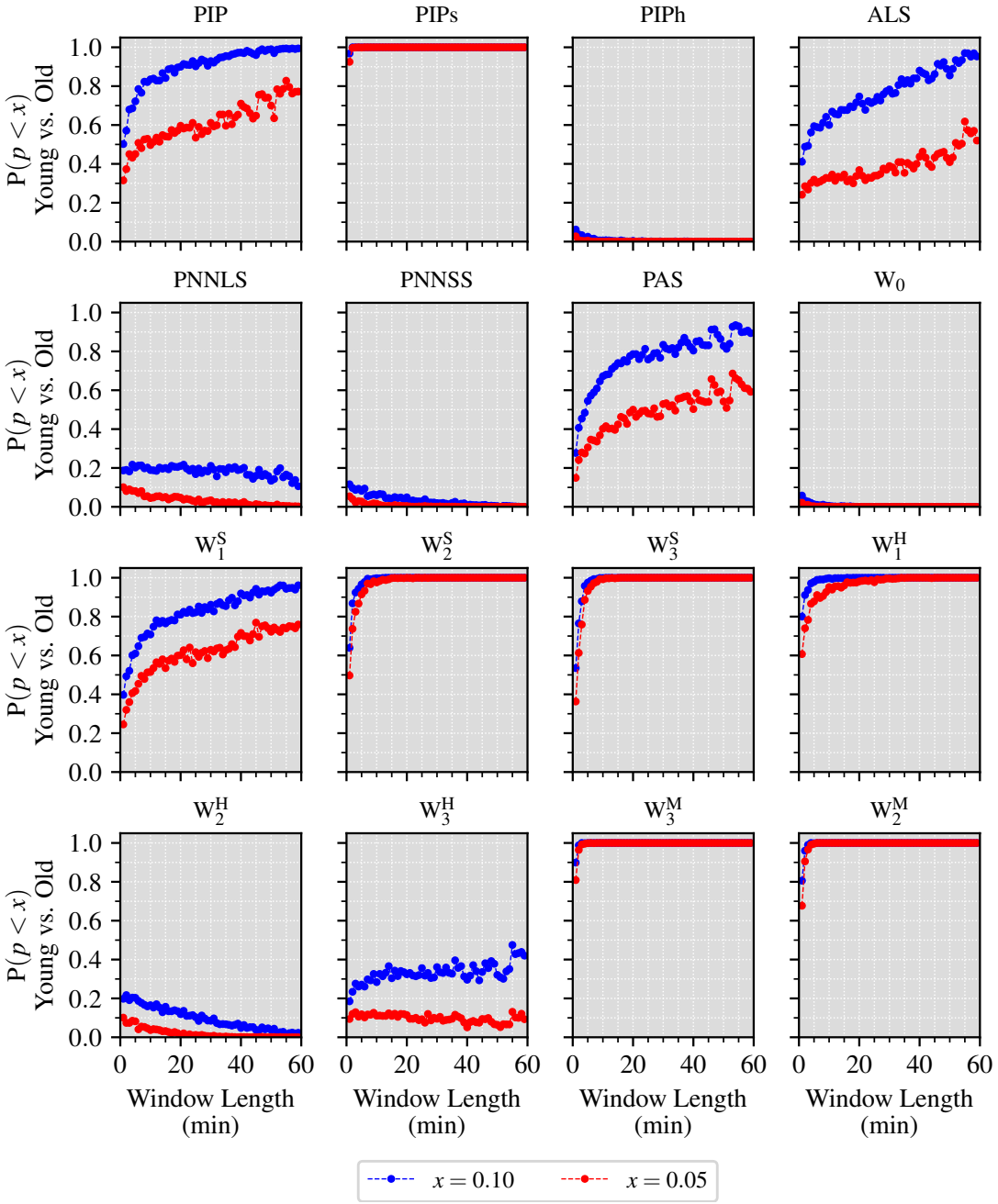

Figure 7.4: Probability associated with the separation of young adulthood from late adulthood with a confidence level above 95% (in red) and above 90% (in blue) using HRF indices along different window lengths.

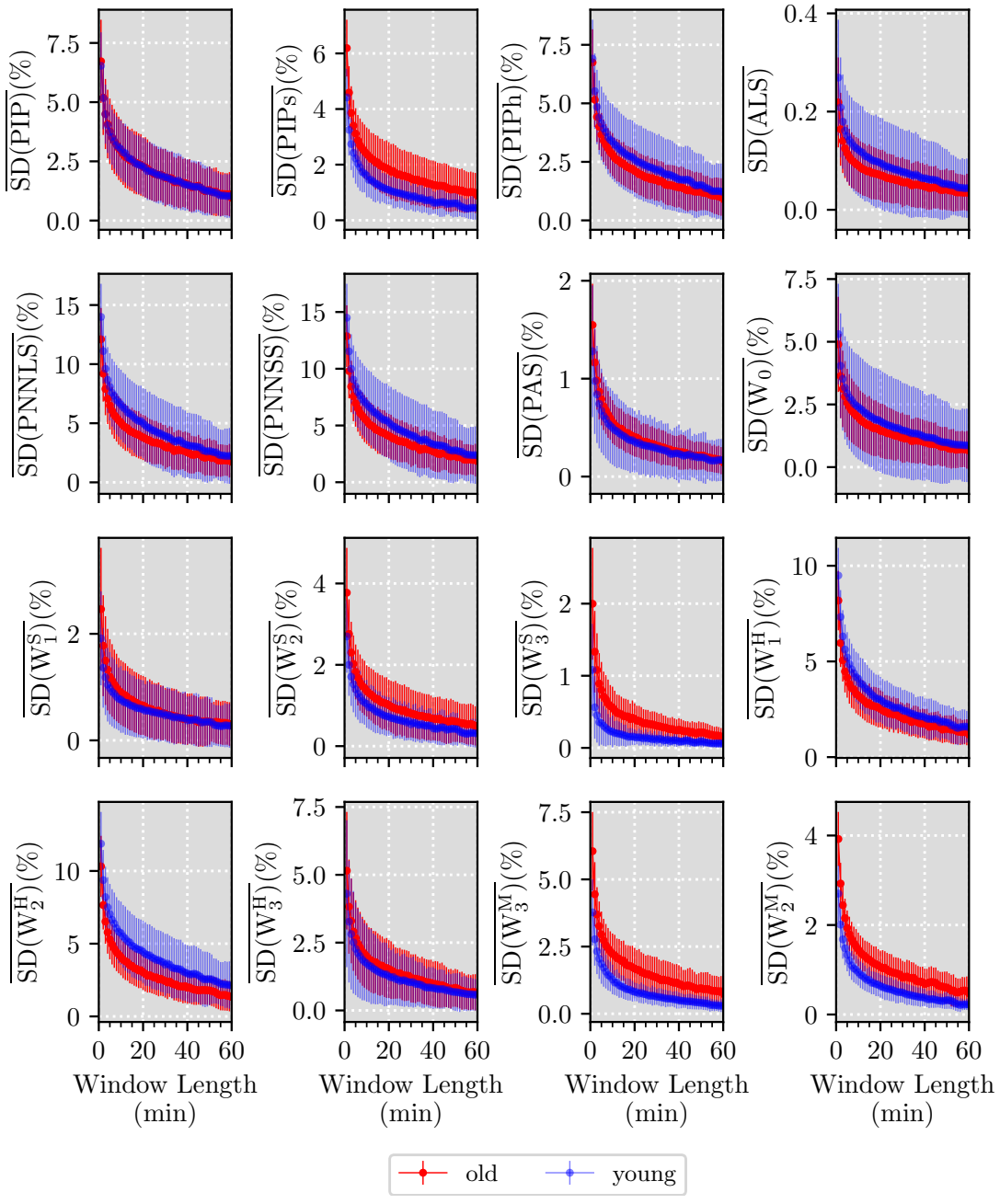

Figure 7.5: Mean standard deviation of each HRF metric for both groups, i.e, old subjects (red) and young subjects in (blue), for increasing window lengths in steps of one minute.

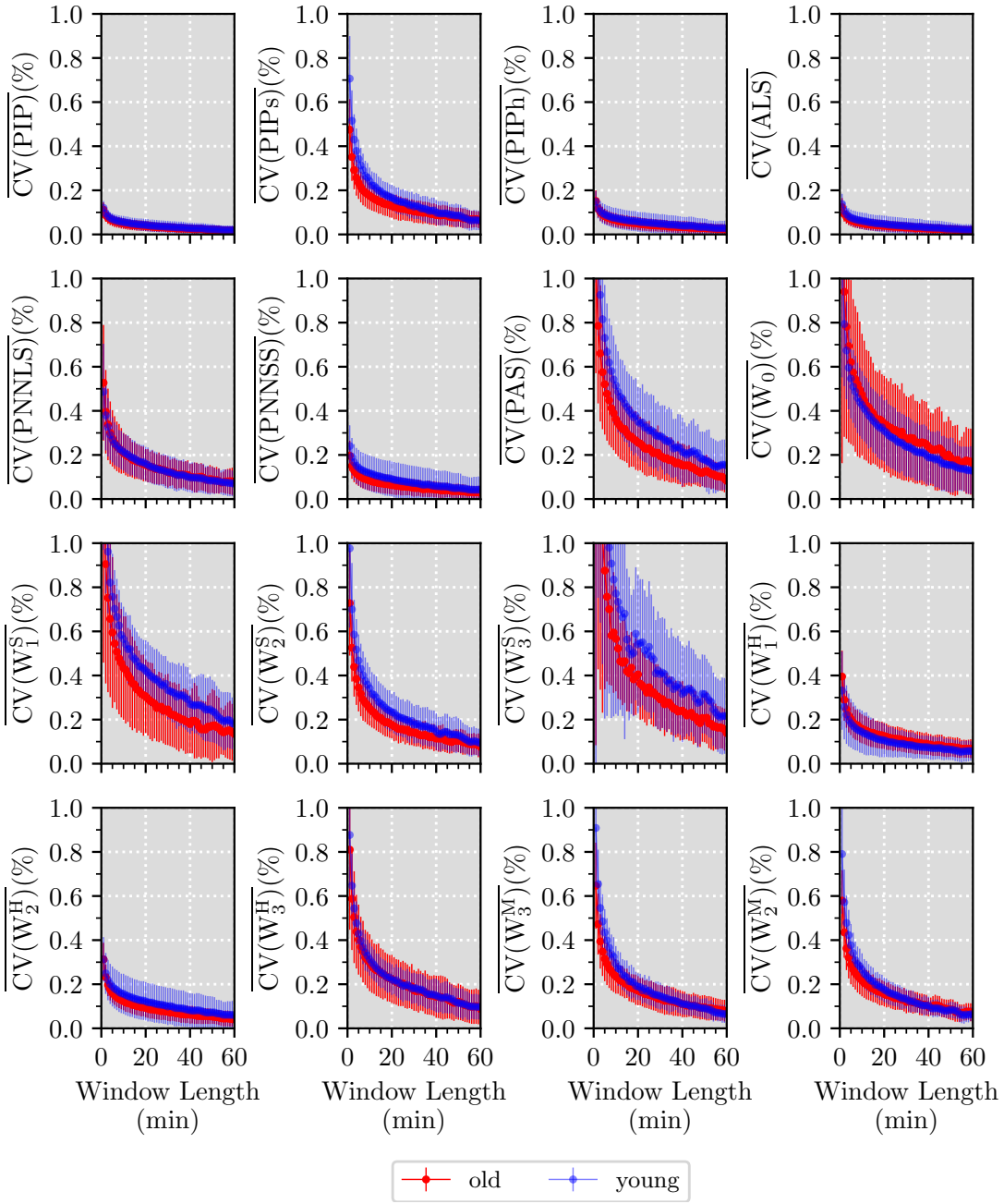

Figure 7.6: Mean coefficient of variation (CV) of each HRF metric for both groups, i.e, old subjects (red) and young subjects in (blue), for increasing window lengths in steps of one minute.

conditions (i.e., with a lower number of confounder factors such as circadian rhythm, respiratory rate, body positioning).

The impossibility to define the minimum time for the metrics PNNLS, PNNSS, W_0, and W_3^H was expected, since in Section 4.4.2 these metrics were shown to be more sparsely associated with age in the Fantasia database.

Although these times were obtained to distinguish between young subjects from older ones in resting conditions, we hypothesize these times to be appropriate for other applications, such as for diagnostic, prediction and risk stratification purposes.

The present study only defines a minimum ECG duration for resting conditions. It should also be valuable to extend this study to different recording conditions, such as in standing, exercising, and sleeping.

The observation that PAS, W_0, W_3^S, and W_1^S corresponded to the least stable HRF metrics in the Fantasia population, might derive from the fact that these metrics all quantify fragmentation patterns that are, typically, less common. In fact, the patterns underlying these metrics were all associated with percentages lower than 6% in the Fantasia database.

8

Conclusion

In the present dissertation, we used traditional HRV, HRF, and PRSA approaches to investigate HR dynamical changes in four different contexts: (1) in aging from adulthood to late adulthood; (2) with AF severity; (3) with prevalent CHF; and (4) in aging from birth to late adulthood, with a closer look in the early development phase. We also proposed minimum ECG recording durations for computation of some HRF metrics in resting conditions.

These evaluations led us to the realization of some key conclusions that we summarize below:

1. Increasing HRF, and decreasing HRV and AC/DC were associated with increasing age from adulthood to late adulthood. However, the results for the analysis of the AAdb indicated an increase of HRV and PRSA indices from late middle age to late adulthood, instead of a decrease.

2. From birth to infancy it was observed a steep decrease in HRF and an increase in HRV and PRSA indices. From infancy to adulthood, HRF was shown to continue to decrease until a plateau phase around the third and fourth decades of life. Regarding HRV and PRSA indices, these were also shown to continue to increase after infancy, although a plateau phase was not so apparent, it seemed that these indices increased only until the end of adolescence and the beginning of adult life.

3. Increased HRF, HRV, and PRSA indices were observed for increasing AF severity.

4. For prevalent CHF, increased HRF and diminished HRV and PRSA indices were observed.

5. We found HRF variables to be more strongly associated with age changes and with AF severity than HRV and PRSA variables. Nonetheless, HRV and PRSA variables were slightly more associated with the presence of CHF than HRF ones.

6. In resting conditions, we estimated around 2 to 10 minutes as minimum ECG duration required for the use of the following HRF metrics for separation of young adulthood from late adulthood: PIP_S, W_2^S, W_3^M, W_2^M, W_3^S, and W_1^H.

The increase in HRF with aging, from adulthood to late adulthood, was hypothesized to be indicative of the progressive deterioration of the correlated function between the SAN and the ANS. Conversely, the general decrease in HRV and AC/DC with aging was thought indicative of the general bluntness of autonomic reflexes. However, the significant increase in some of these metrics from middle age to late adulthood, which could be said to be a sign of health and not a decrease in sensitivity of autonomic reflexes, was speculated to be due to the confounding effect of increased fragmentation, i.e., "HRV paradox".

The concurrent increase in HRF, short-term HRV and DC with AF severity was hypothesized to be caused by an exacerbation of the uncorrelated function between the SAN and the ANS. This exacerbation is thought to derive from increasing loss of SAN and atrial tissue integrity, as well as accentuated autonomic imbalance.

In CHF, the consistent decrease in HRV and both AC and DC capacities was hypothesized to be a consequence of the heightened sympathetic and dampened parasympathetic modulation, typically associated with this disease. The increase in HRF was further thought to be a reflection of these events in conjugation with SAN impairment.

The increase in HRV, AC, and DC from birth to infancy was hypothesized to derive from the increase in vagal predominance with age. The decrease in HRF, in this context, might derive from the progressive formation of a correlated relation between the SAN pacemaker cells and ANS modulation, which might as well be intervened by the increase in vagal predominance.

The observation that the decrease in fragmentation does not stop in the end of infancy, but it extends through adulthood, was hypothesized to derive from the effect of the development of higher brain areas, which take longer to develop, on the ANS modulation of the SAN.

Finally, we anticipated that short-term resting ECG recordings, with lengths of 2 to 10 minutes, might be suitable for disease detection and prognostics.

The overall goal of this dissertation was to advance the current understanding of the properties of HR dynamics and of their changes with aging, AF severity, and cardiovascular disease, specifically CHF. To our knowledge, this work is the first to: 1) investigate the association of HRF and PRSA indices with AF severity; 2) investigate the changes in HRF with cross-sectional age in a population of children under seven years; 3) compare the degrees of HRF of patients with CHF and healthy controls; 4) contrast the performances of different time series analysis methods: HRF, HRV, and PRSA; and 5) investigate the relationship between the length of the ECG recordings and the level of discrimination of two populations attained ("young" *versus* "old").

We concluded that analyses based on assessments of the amplitude of the fluctuations in HR should be taken with caution. In agreement with previous studies [22]–[27], [80]–[82], we found that higher HRV/PRSA values are not necessarily a sign of "better health". To resolve the limitations of these methods, the HRF construct and a set of indices for

its quantification were introduced. Our investigations were supportive of further developing this framework and examine its strengths and limitations in larger databases. We believe this work to be especially relevant at a time when the popularization of wearable technologies provides a unique opportunity for advancing translational time series analysis studies of physiological signals, which in the long-run may constitute an important component of healthspan expansion.

8.1 Future Work

We believe that in order to improve and extend the analyses contained in this dissertation some main future endeavors should be undertaken.

Development of Prediction Models The current dissertation focused on characterizing and interpreting the changes in HR dynamics in diverse contexts. The development of models for predicting aging and diseases based on HR dynamics could further help healthcare providers to prevent early aging and the incursion of diseases. However, it should be noted that this development requires an extensive analysis and data preparation step to ensure meaningful results, specifically, caution should be taken when dealing with data heterogeneity, small datasets, and imbalanced data. As these models would be safety-critical, meaning that their results could potentially have serious consequences, they should also yield interpretable results. Thus, we suggest that methods as linear regression or decision trees could be use in combination with feature selection techniques to ensure the use of sets of meaningful features.

Automatic Beat Classification For computation of heart rate dynamical indices in a fully automated wearable device, heartbeats should be automatically classified. Currently, there exists many available algorithms that address this problem, most of which are based on artificial intelligence methods. However, efforts are still needed to improve the performance of these algorithms [164].

Normative values for Heart Rate Fragmentation Indices for Healthy Individuals A major step for clinical traction of HRF analysis is the establishment of normative values for its indices. Although in the present work we studied these metrics at different ages, we did not design an approach to establish normal values for the ages analyzed, since we mainly focused on relative differences. However, we believe that the AAdb database may be useful for this intent.

Differences of Heart Rate Dynamical Indices between Male and Female Subjects In this dissertation, we did not separate the analysis between male and female subjects due to the small size of the databases or absence of information regarding the sex of the participants. Nevertheless, some studies using traditional HRV have reported significant

differences in their indices between male and female individuals, especially until the age of 50 [165]. These differences have been associated with a higher vagal predominance in women until this age [165]. We believe that it should be valuable to quantify how sex differences affect HRF and PRSA analysis.

Effect of the Sampling Frequency in Heart Rate Fragmentation The databases analyzed in the this dissertation presented different sampling frequencies. The sampling frequency dictates the resolution of the NN intervals of the NN time series, we expect that higher resolution might increase HRF indices, since HR acceleration sign changes might be better captured with higher resolution. However, this effect should be quantified and analyzed.

Application of Fragmentation Analysis to other Physiological Signs HRF is thought to reflect disruptions in the "autonomic-SAN-atrial network". We believe that other physiological signals, such as respiratory rate and blood pressure, might also present fragmentation patterns due to disruption of their control and integrative mechanisms. Thus, the adaptation of fragmentation analysis to the study of the dynamics of these signals might be valuable.

Study of Heart Rate Fragmentation in Other Conditions The strong association between AF and increased HRF indicates that HRF analysis might be meaningful for the study of stroke and dementia, which correspond to two major outcomes of AF. We further believe that a study of the association between all-cause mortality and HRF should be done, given that HRF indices can be thought as measures of integrative physiology. Another disease, which might benefit from HRF analysis is depression. Depression has been linked to low HRV, and it might be valuable to evaluate if high HRF is also associated with this disease.

Association between Heart Rate Fragmentation and Molecular Measures of Aging As we discussed in Section 1.1, markers of biological aging include sophisticated genetic and epigenetic measures, such as DNA methylation patterns and telomere's length. We believe that a study on the correlation of these molecular biomarkers and HRF might be valuable to reinforce the translational value of HRF as a biomaker of aging. If a correlation is demonstrated, the inclusion of HRF indices in composite indices of biological aging should be considered.

Study of the Dynamics of Heart Rate Fragmentation HRF indices are not static measures and, just like HR, they fluctuate over time, having an associated dynamics. Thus, the study of the dynamics of HRF variables might also give access to useful information regarding the physiological state of the ANS and the SAN.

Bibliography

[1] H. Rafalimanana, *World Population Ageing*. 2020, pp. 1–47, ISBN: 9789211483475. [Online]. Available: http://link.springer.com/chapter/10.1007/978-94-007-5204-7%7B%5C_%7D6 (cit. on p. 1).

[2] WHO. "Gho | by category | life expectancy and healthy life expectancy - data by country". (2016), [Online]. Available: https://apps.who.int/gho/data/node.main.688 (visited on 10/04/2021) (cit. on p. 1).

[3] D. W. Belsky, A. Caspi, R. Houts, *et al.*, "Quantification of biological aging in young adults", *Proceedings of the National Academy of Sciences of the United States of America*, vol. 112, no. 30, E4104–E4110, 2015, ISSN: 10916490. DOI: 10.1073/pnas.1506264112 (cit. on pp. 1, 2).

[4] S. S. Khan, B. D. Singer, and D. E. Vaughan, "Molecular and physiological manifestations and measurement of aging in humans", *Aging Cell*, vol. 16, no. 4, pp. 624–633, 2017, ISSN: 14749726. DOI: 10.1111/acel.12601 (cit. on pp. 1, 2).

[5] D. J. Lowsky, S. J. Olshansky, J. Bhattacharya, and D. P. Goldman, "Heterogeneity in healthy aging", *Journals of Gerontology Series A: Biomedical Sciences and Medical Sciences*, vol. 69, no. 6, pp. 640–649, 2014. DOI: 10.1093/gerona/glt162 (cit. on p. 1).

[6] J. Jylhävä, N. L. Pedersen, and S. Hägg, "Biological age predictors", *EBioMedicine*, vol. 21, pp. 29–36, 2017, ISSN: 2352-3964. DOI: https://doi.org/10.1016/j.ebiom.2017.03.046 (cit. on p. 1).

[7] L. Ferrucci, M. Gonzalez-Freire, E. Fabbri, *et al.*, "Measuring biological aging in humans: A quest", *Aging Cell*, vol. 19, no. 2, pp. 1–21, 2020, ISSN: 14749726. DOI: 10.1111/acel.13080 (cit. on pp. 1, 2).

[8] S. Hägg, D. W. Belsky, and A. A. Cohen, "Developments in molecular epidemiology of aging", *Emerging Topics in Life Sciences*, vol. 3, no. 4, pp. 411–421, Jun. 2019, ISSN: 2397-8554. DOI: 10.1042/ETLS20180173 (cit. on p. 2).

[9] C. López-Otín, M. A. Blasco, L. Partridge, M. Serrano, and G. Kroemer, "The hallmarks of aging", *Cell*, vol. 153, no. 6, p. 1194, 2013, ISSN: 10974172. DOI: 10.1016/j.cell.2013.05.039 (cit. on p. 2).

[10] T. Fulop, A. Larbi, J. M. Witkowski, *et al.*, "Aging, frailty and age-related diseases", *Biogerontology*, vol. 11, no. 5, pp. 547–563, 2010, ISSN: 15736768. DOI: 10.1007/s10522-010-9287-2 (cit. on p. 2).

[11] F. Ciccarone, S. Tagliatesta, P. Caiafa, and M. Zampieri, "DNA methylation dynamics in aging: how far are we from understanding the mechanisms?", *Mechanisms of Ageing and Development*, vol. 174, no. October 2017, pp. 3–17, 2018, ISSN: 18726216. DOI: 10.1016/j.mad.2017.12.002 (cit. on p. 2).

[12] R. L. Sprott, "Biomarkers of aging and disease: Introduction and definitions", *Experimental gerontology*, vol. 45, no. 1, pp. 2–4, 2010. DOI: 10.1016/j.exger.2009.07.008 (cit. on p. 2).

[13] M. E. Levine, "Modeling the rate of senescence: Can estimated biological age predict mortality more accurately than chronological age?", *Journals of Gerontology - Series A Biological Sciences and Medical Sciences*, vol. 68, no. 6, pp. 667–674, 2013, ISSN: 2045-2322. DOI: 10.1093/gerona/gls233 (cit. on p. 2).

[14] S. B. Mulkey and A. dú Plessis, "The Critical Role of the Central Autonomic Nervous System in Fetal-Neonatal Transition", *Seminars in Pediatric Neurology*, vol. 28, pp. 29–37, 2018, ISSN: 15580776. DOI: 10.1016/j.spen.2018.05.004 (cit. on pp. 2, 3, 80).

[15] S. B. Mulkey and A. J. du Plessis, "Autonomic nervous system development and its impact on neuropsychiatric outcome", *Pediatric Research*, vol. 85, no. 2, pp. 120–126, 2019, ISSN: 15300447. DOI: 10.1038/s41390-018-0155-0 (cit. on pp. 2, 3).

[16] P. D. Gluckman, M. A. Hanson, and T. Buklijas, "A conceptual framework for the developmental origins of health and disease", *Journal of developmental origins of health and disease*, vol. 1, no. 1, pp. 6–18, 2010. DOI: 10.1017/S2040174409990171 (cit. on p. 2).

[17] Y. Arima and H. Fukuoka, "Developmental origins of health and disease theory in cardiology", *Journal of Cardiology*, vol. 76, no. 1, pp. 14–17, 2020, ISSN: 0914-5087. DOI: doi.org/10.1016/j.jjcc.2020.02.003 (cit. on pp. 2, 80).

[18] D. J. Barker, C. Osmond, P. D. Winter, B. Margetts, and S. J. Simmonds, "Weight in infancy and death from ischaemic heart disease", *The Lancet*, vol. 334, no. 8663, pp. 577–580, 1989. DOI: 10.1016/s0140-6736(89)90710-1 (cit. on pp. 2, 80).

[19] C. Rowe, *Neurosciences*. 10. 2011, vol. 52, ISBN: 9781605353807. DOI: 10.2307/j.ctvw1d7fz.6 (cit. on p. 3).

[20] H. Hotta and S. Uchida, "Aging of the autonomic nervous system and possible improvements in autonomic activity using somatic afferent stimulation", *Geriatrics & Gerontology International*, vol. 10, no. s1, S127–S136, 2010. DOI: https://doi.org/10.1111/j.1447-0594.2010.00592.x (cit. on p. 3).

[21] Guidelines, T. N. American, and Guidelines, "Guidelines Heart rate variability", *European Heart Journal*, vol. 17, pp. 354–381, 1996. DOI: 10.1161/01.CIR.93.5.1043 (cit. on pp. 3, 15, 17–19).

[22] J. Hayano and E. Yuda, "Pitfalls of assessment of autonomic function by heart rate variability", *Journal of Physiological Anthropology*, vol. 38, no. 1, pp. 1–8, 2019, ISSN: 18806805. DOI: 10.1186/s40101-019-0193-2 (cit. on pp. 3, 15, 16, 20, 101).

[23] M. D. Costa, R. B. Davis, and A. L. Goldberger, "Heart rate fragmentation: A new approach to the analysis of cardiac interbeat interval dynamics", *Frontiers in Physiology*, vol. 8, no. MAY, pp. 1–13, 2017, ISSN: 1664042X. DOI: 10.3389/fphys.2017.00255 (cit. on pp. 3, 20, 21, 23, 24, 43, 74, 101).

[24] ——, "Heart rate fragmentation: A symbolic dynamical approach", *Frontiers in Physiology*, vol. 8, no. NOV, pp. 1–14, 2017, ISSN: 1664042X. DOI: 10.3389/fphys.2017.00827 (cit. on pp. 3, 20, 21, 23, 43, 74, 101).

[25] M. D. Costa, S. Redline, R. B. Davis, S. R. Heckbert, E. Z. Soliman, and A. L. Goldberger, "Heart rate fragmentation as a novel biomarker of adverse cardiovascular events: The Multi-Ethnic Study of Atherosclerosis", *Frontiers in Physiology*, vol. 9, no. SEP, pp. 1–14, 2018, ISSN: 1664042X. DOI: 10.3389/fphys.2018.01117 (cit. on pp. 3, 4, 20, 101).

[26] P. K. Stein, P. P. Domitrovich, N. Hui, P. Rautaharju, and J. Gottdiener, "Sometimes higher heart rate variability is not better heart rate variability: Results of graphical and nonlinear analyses", *Journal of Cardiovascular Electrophysiology*, vol. 16, no. 9, pp. 954–959, 2005, ISSN: 10453873. DOI: 10.1111/j.1540-8167.2005.40788.x (cit. on pp. 3, 20, 101).

[27] M. D. Costa, S. Redline, E. Z. Soliman, A. L. Goldberger, and S. R. Heckbert, "Fragmented Sinoatrial Dynamics in the Prediction of Atrial Fibrillation: The Multi-Ethnic Study of Atherosclerosis", *American Journal of Physiology-Heart and Circulatory Physiology*, 2020, ISSN: 0363-6135. DOI: 10.1152/ajpheart.00421.2020 (cit. on pp. 4, 20, 21, 24, 66, 101).

[28] M. D. Costa, S. Redline, T. M. Hughes, S. R. Heckbert, and A. L. Goldberger, "Prediction of Cognitive Decline Using Heart Rate Fragmentation Analysis: The Multi-Ethnic Study of Atherosclerosis", *Frontiers in Aging Neuroscience*, vol. 13, no. August, 2021. DOI: 10.3389/fnagi.2021.708130 (cit. on p. 4).

[29] A. Bauer, J. W. Kantelhardt, A. Bunde, *et al.*, "Phase-rectified signal averaging detects quasi-periodicities in non-stationary data", *Physica A: Statistical Mechanics and its Applications*, vol. 364, pp. 423–434, 2006, ISSN: 03784371. DOI: 10.1016/j.physa.2005.08.080 (cit. on pp. 4, 25).

[30] A. Bauer, J. W. Kantelhardt, P. Barthel, *et al.*, "Deceleration capacity of heart rate as a predictor of mortality after myocardial infarction: cohort study", *Lancet*, vol. 367, no. 9523, pp. 1674–1681, 2006, ISSN: 01406736. DOI: 10.1016/S0140-6736(06)68735-7 (cit. on pp. 4, 25, 26).

[31] J. W. Kantelhardt, A. Bauer, A. Y. Schumann, *et al.*, "Phase-rectified signal averaging for the detection of quasi-periodicities and the prediction of cardiovascular risk", *Chaos*, vol. 17, no. 1, 2007, ISSN: 10541500. DOI: 10.1063/1.2430636 (cit. on pp. 4, 25, 26).

[32] T. Stampalija, D. Casati, M. Montico, *et al.*, "Parameters influence on acceleration and deceleration capacity based on trans-abdominal ecg in early fetal growth restriction at different gestational age epochs", *European Journal of Obstetrics & Gynecology and Reproductive Biology*, vol. 188, pp. 104–112, 2015. DOI: 10.1016/j.ejogrb.2015.03.003 (cit. on pp. 4, 26).

[33] S. M. Lobmaier, N. M. van Charante, E. Ferrazzi, *et al.*, "Phase-rectified signal averaging method to predict perinatal outcome in infants with very preterm fetal growth restriction-a secondary analysis of truffle-trial", *American journal of obstetrics and gynecology*, vol. 215, no. 5, 630–e1, 2016. DOI: 10.1016/j.ajog.2016.06.024 (cit. on pp. 4, 26).

[34] T. Stampalija, D. Casati, L. Monasta, *et al.*, "Brain sparing effect in growth-restricted fetuses is associated with decreased cardiac acceleration and deceleration capacities: A case–control study", *BJOG: An International Journal of Obstetrics & Gynaecology*, vol. 123, no. 12, pp. 1947–1954, 2016. DOI: 10.1111/1471-0528.13607 (cit. on pp. 4, 26).

[35] C. Zou, H. Dong, F. Wang, *et al.*, "Heart acceleration and deceleration capacities associated with dilated cardiomyopathy", *European journal of clinical investigation*, vol. 46, no. 4, pp. 312–320, 2016. DOI: 10.1111/eci.12594 (cit. on pp. 4, 26).

[36] W. Hu, X. Jin, P. Zhang, *et al.*, "Deceleration and acceleration capacities of heart rate associated with heart failure with high discriminating performance", *Scientific Reports*, vol. 6, no. 1, Mar. 2016. DOI: 10.1038/srep23617 (cit. on pp. 4, 26, 74).

[37] D. T. Kaplan and M. Talajic, "Dynamics of heart rate", *Chaos: An Interdisciplinary Journal of Nonlinear Science*, vol. 1, no. 3, pp. 251–256, 1991. DOI: 10.1063/1.165837 (cit. on pp. 6, 8, 16, 18).

[38] F. Shaffer and J. P. Ginsberg, "An Overview of Heart Rate Variability Metrics and Norms", *Frontiers in Public Health*, vol. 5, no. September, pp. 1–17, 2017, ISSN: 2296-2565. DOI: 10.3389/fpubh.2017.00258 (cit. on p. 6).

[39] R. E. Klabunde, *CARDIOVASCULAR PHYSIOLOGY CONCEPTS - Second edition*. 2012, ISBN: 9788578110796 (cit. on pp. 6–9, 15, 73).

[40] Hall and J. Edward, *Guyton and hall textbook of medical physiology thirteenth edition*. 2011, ISBN: 9781416045748 (cit. on pp. 6, 9–11, 13).

[41] A. L. Goldberger, Z. D. Goldberger, and A. Shvilkin, *Goldberger's Clinical Electrocardiography: A Simplified Approach: Ninth Edition*. ELSEVIER, 2017, ch. 13, pp. 122–129, ISBN: 9780323401692 (cit. on pp. 6, 8, 16, 64, 66).

[42] N. Li, B. J. Hansen, T. A. Csepe, *et al.*, "Redundant and diverse intranodal pacemakers and conduction pathways protect the human sinoatrial node from failure", *Science Translational Medicine*, vol. 9, no. 400, eaam5607, 2017. DOI: 10.1126/scitranslmed.aam5607 (cit. on p. 8).

[43] E. A. MacDonald, R. A. Rose, and T. A. Quinn, "Neurohumoral control of sinoatrial node activity and heart rate: Insight from experimental models and findings from humans", *Frontiers in Physiology*, vol. 11, p. 170, 2020, ISSN: 1664-042X. DOI: 10.3389/fphys.2020.00170 (cit. on p. 8).

[44] D. W. Robertson, I. Biaggioni, G. Burnstock, P. Low, and J. F. Paton, *Primer on the Autonomic Nervous System*. 2012, ISBN: 9780123865250. DOI: 10.1016/C2010-0-65186-8 (cit. on pp. 9, 11).

[45] J. S. Shahoud, T. Sanvictores, and N. R. Aeddula, *Physiology, arterial pressure regulation.[updated 2020 sep 6]*, 2021 (cit. on p. 9).

[46] W. Jänig, "Autonomic nervous system", in *Human Physiology*, R. F. Schmidt and G. Thews, Eds. Berlin, Heidelberg: Springer Berlin Heidelberg, 1989, pp. 333–370, ISBN: 978-3-642-73831-9. DOI: 10.1007/978-3-642-73831-9_16 (cit. on p. 10).

[47] L. K. McCorry, "Physiology of the autonomic nervous system", *American journal of pharmaceutical education*, vol. 71, no. 4, 2007. DOI: 10.5688/aj710478 (cit. on pp. 10, 11, 13).

[48] Y. Mizuno-Matsumoto, Y. Inoguchi, S. M. Carpels, A. Muramatsu, and Y. Yamamoto, "Cerebral cortex and autonomic nervous system responses during emotional memory processing", *Plos one*, vol. 15, no. 3, e0229890, 2020. DOI: 10.1371/journal.pone.0229890 (cit. on p. 10).

[49] J. G. Betts, K. A. Young, J. A. Wise, *et al.*, *Anatomy and Physiology*. OpenStax, 2013. [Online]. Available: %7Bhttps://openstax.org/books/anatomy-and-physiology/pages/1-introduction%7D (cit. on pp. 11, 12, 14).

[50] G. E. Billman, H. V. Huikuri, J. Sacha, and K. Trimmel, "An introduction to heart rate variability: Methodological considerations and clinical applications", *Frontiers in physiology*, vol. 6, p. 55, 2015. DOI: 10.3389/fphys.2015.00055 (cit. on p. 13).

[51] C. Borst and J. M. Karemaker, "Time delays in the human baroreceptor reflex", *Journal of the autonomic nervous system*, vol. 9, no. 2-3, pp. 399–409, 1983. DOI: 10.1016/0165-1838(83)90004-8 (cit. on p. 15).

[52] G. J. Tortora and B. H. Derrickson, *Principles of anatomy and physiology*. John Wiley & Sons, 2018 (cit. on p. 15).

[53] F. Shaffer, R. McCraty, and C. L. Zerr, "A healthy heart is not a metronome: an integrative review of the heart's anatomy and heart rate variability", *Frontiers in Psychology*, vol. 5, no. September, pp. 1–19, 2014, ISSN: 1664-1078. DOI: 10.3389/fpsyg.2014.01040 (cit. on p. 15).

[54] O. Monfredi, H. Dobrzynski, T. Mondal, M. R. Boyett, and G. M. Morris, "The anatomy and physiology of the sinoatrial node-A contemporary review", *PACE - Pacing and Clinical Electrophysiology*, vol. 33, no. 11, pp. 1392–1406, 2010, ISSN: 01478389. DOI: 10.1111/j.1540-8159.2010.02838.x (cit. on p. 15).

[55] R. Barbieri, J. K. Triedman, and J. P. Saul, "Heart rate control and mechanical cardiopulmonary coupling to assess central volume: A systems analysis", *American Journal of Physiology-Regulatory, Integrative and Comparative Physiology*, vol. 283, no. 5, R1210–R1220, 2002. DOI: 10.1152/ajpregu.00127.2002 (cit. on pp. 15, 16).

[56] A. Angelone and N. A. Coulter, "RESPIRATORY SINUS ARRHYTHEMIA: A FREQUENCY DEPENDENT PHENOMENON.", *Journal of applied physiology*, 1964, ISSN: 00218987. DOI: 10.1152/jappl.1964.19.3.479 (cit. on p. 16).

[57] F. Yasuma and J. I. Hayano, "Respiratory Sinus Arrhythmia: Why Does the Heartbeat Synchronize with Respiratory Rhythm?", *Chest*, 2004, ISSN: 00123692. DOI: 10.1378/chest.125.2.683 (cit. on pp. 16, 17).

[58] J. A. Hirsch and B. Bishop, "Respiratory sinus arrhythmia in humans: How breathing pattern modulates heart rate", *American Journal of Physiology - Heart and Circulatory Physiology*, 1981, ISSN: 03636135. DOI: 10.1152/ajpheart.1981.241.4.h620 (cit. on p. 16).

[59] M. De Burgh Daly, "Interactions between respiration and circulation", in *Handbook of Physiology*. American Physiology Society, 1986, ch. 3, pp. 529–594, ISBN: 9780470650714 (cit. on p. 16).

[60] J. Hayano, F. Yasuma, A. Okada, S. Mukai, and T. Fujinami, "Respiratory sinus arrhythmia", *Circulation*, vol. 94, no. 4, pp. 842–847, 1996. DOI: 10.1161/01.CIR.94.4.842 (cit. on p. 16).

[61] M. L. Appel, R. D. Berger, J. Saul, J. M. Smith, and R. J. Cohen, "Beat to beat variability in cardiovascular variables: Noise or music?", *Journal of the American College of Cardiology*, vol. 14, no. 5, pp. 1139–1148, 1989, ISSN: 0735-1097. DOI: https://doi.org/10.1016/0735-1097(89)90408-7 (cit. on pp. 16, 18).

[62] A. E. Draghici and J. A. Taylor, "The physiological basis and measurement of heart rate variability in humans", *Journal of Physiological Anthropology*, vol. 35, no. 1, pp. 1–8, 2016, ISSN: 18806805. DOI: 10.1186/s40101-016-0113-7 (cit. on pp. 16, 18–20).

[63] H. M. Stauss, "Heart rate variability", *American Journal of Physiology-Regulatory, Integrative and Comparative Physiology*, vol. 285, no. 5, R927–R931, 2003. DOI: 10.1152/ajpregu.00452.2003 (cit. on pp. 16, 18, 19).

[64] C. M. van Ravenswaaij-Arts, L. A. Kollee, J. C. Hopman, G. B. Stoelinga, and H. P. van Geijn, "Heart rate variability", *Annals of internal medicine*, vol. 118, no. 6, pp. 436–447, 1993. DOI: 10.7326/0003-4819-118-6-199303150-00008 (cit. on pp. 16, 18).

[65] E. H. Hon and S. T. Lee, "ELECTRONIC EVALUATION OF THE FETAL HEART RATE. VIII. PATTERNS PRECEDING FETAL DEATH, FURTHER OBSERVATIONS.", *American journal of obstetrics and gynecology*, 1963, ISSN: 00029378 (cit. on p. 17).

[66] M. M. Wolf, G. A. Varigos, and J. G. Sloman, "Sinus arrhythmia in acute myocardial infarction", *Medical Journal of Australia*, 1978, ISSN: 0025729X. DOI: 10.5694/j.1326-5377.1978.tb131339.x (cit. on p. 17).

[67] A. Murray, D. J. Ewing, I. W. Campbell, J. M. M. Neilson, and B. F. Clarke, "RR interval variations in young male diabetics", *Heart*, 1975, ISSN: 13556037. DOI: 10.1136/hrt.37.8.882 (cit. on p. 17).

[68] D. J. Ewing, C. N. Martyn, R. J. Young, and B. F. Clarke, "The value of cardiovascular autonomic function tests: 10 years experience in diabetes", *Diabetes Care*, 1985, ISSN: 01495992. DOI: 10.2337/diacare.8.5.491 (cit. on p. 17).

[69] G. E. Billman, "Heart rate variability - A historical perspective", *Frontiers in Physiology*, vol. 2 NOV, no. November, pp. 1–13, 2011, ISSN: 1664042X. DOI: 10.3389/fphys.2011.00086 (cit. on p. 18).

[70] A. L. Goldberger, "Complex systems", *Proceedings of the American Thoracic Society*, vol. 3, no. 6, pp. 467–471, 2006, ISSN: 15463222. DOI: 10.1513/pats.200603-028MS (cit. on p. 18).

[71] S. M. Pincus, "Approximate entropy as a measure of system complexity.", *Proceedings of the National Academy of Sciences*, vol. 88, no. 6, pp. 2297–2301, 1991, ISSN: 0027-8424. DOI: 10.1073/pnas.88.6.2297 (cit. on p. 18).

[72] J. S. Richman and J. R. Moorman, "Physiological time-series analysis using approximate and sample entropy", *American Journal of Physiology - Heart and Circulatory Physiology*, 2000, ISSN: 03636135. DOI: 10.1152/ajpheart.2000.278.6.h2039 (cit. on p. 18).

[73] C. K. Peng, S. Havlin, H. E. Stanley, and A. L. Goldberger, "Quantification of scaling exponents and crossover phenomena in nonstationary heartbeat time series", *Chaos*, 1995, ISSN: 10541500. DOI: 10.1063/1.166141 (cit. on p. 18).

[74] S. Akselrod, D. Gordon, F. A. Ubel, D. C. Shannon, A. C. Barger, and R. J. Cohen, "Power spectrum analysis of heart rate fluctuation: A quantitative probe of beat-to-beat cardiovascular control", *Science*, 1981, ISSN: 00368075. DOI: 10.1126/science.6166045 (cit. on p. 18).

[75] J. V. Ringwood and S. C. Malpas, "Slow oscillations in blood pressure via a nonlinear feedback model", *American Journal of Physiology-Regulatory, Integrative and Comparative Physiology*, vol. 280, no. 4, R1105–R1115, 2001. DOI: 10.1152/ajpregu.2001.280.4.R1105 (cit. on p. 18).

[76] M. S. Houle and G. E. Billman, "Low-frequency component of the heart rate variability spectrum: A poor marker of sympathetic activity", *American Journal of Physiology-Heart and Circulatory Physiology*, vol. 276, no. 1, H215–H223, 1999. DOI: 10.1152/ajpheart.1999.276.1.H215 (cit. on p. 18).

[77] B. Pilgram and D. T. Kaplan, "Nonstationarity and 1/f noise characteristics in heart rate", *American Journal of Physiology-Regulatory, Integrative and Comparative Physiology*, vol. 276, no. 1, R1–R9, 1999. DOI: 10.1152/ajpregu.1999.276.1.R1 (cit. on p. 19).

[78] A. L. Goldberger, L. A. Amaral, L. Glass, *et al.*, "Physiobank, physiotoolkit, and physionet: Components of a new research resource for complex physiologic signals", *circulation*, vol. 101, no. 23, e215–e220, 2000. DOI: 10.1161/01.cir.101.23.e215 (cit. on pp. 19, 36, 37, 44, 82).

[79] P. Gomes, P. Margaritoff, and H. Silva, "pyHRV: Development and evaluation of an open-source python toolbox for heart rate variability (HRV)", in *Proc. Int'l Conf. on Electrical, Electronic and Computing Engineering (IcETRAN)*, 2019, pp. 822–828 (cit. on p. 19).

[80] M. D. Costa and A. L. Goldberger, "Heart rate fragmentation: using cardiac pacemaker dynamics to probe the pace of biological aging", *J Physiol Heart Circ Physiol*, vol. 316, pp. 1341–1344, 2019. DOI: 10.1152/ajpheart.00110.2019.-This (cit. on pp. 20, 21, 24, 74, 101).

[81] M. C. De Bruyne, J. A. Kors, A. W. Hoes, *et al.*, "Both decreased and increased heart rate variability on the standard 10- second electrocardiogram predict cardiac mortality in the elderly: The Rotterdam study", *American Journal of Epidemiology*, vol. 150, no. 12, pp. 1282–1288, 1999, ISSN: 00029262. DOI: 10.1093/oxfordjournals.aje.a009959 (cit. on pp. 20, 101).

[82] J. Hayano, M. Kisohara, N. Ueda, and E. Yuda, "Impact of heart rate fragmentation on the assessment of heart rate variability", *Applied Sciences (Switzerland)*, vol. 10, no. 9, 2020, ISSN: 20763417. DOI: 10.3390/app10093314 (cit. on pp. 20, 24, 62, 81, 87, 101).

[83] N. Iyengar, C. K. Peng, R. Morin, A. L. Goldberger, and L. A. Lipsitz, "Age-related alterations in the fractal scaling of cardiac interbeat interval dynamics", vol. 271, no. 4, R1078–R1084, Oct. 1996. DOI: 10.1152/ajpregu.1996.271.4.r1078 (cit. on pp. 22, 27, 36, 44, 91).

[84] S. Petrutiu, A. V. Sahakian, and S. Swiryn, "Abrupt changes in fibrillatory wave characteristics at the termination of paroxysmal atrial fibrillation in humans", *Europace*, 2007, ISSN: 10995129. DOI: 10.1093/europace/eum096 (cit. on pp. 22, 27, 36, 67).

[85] G. Casella and R. L. Berger, *Statistical lnference*. 2002, pp. 1–686, ISBN: 0534243126 (cit. on p. 28).

[86] J. Fox, *Applied regression analysis and generalized linear models*. Sage Publications, 2015 (cit. on pp. 29, 30, 32).

[87] D. W. Hosmer, L. Stanley, and R. X. Sturdivant, *Applied logistic regression*. Wiley New York, 2000 (cit. on p. 32).

[88] G. W. Corder and D. I. Foreman, *Nonparametric statistics: A step-by-step approach*. John Wiley & Sons, 2014 (cit. on p. 33).

[89] S. S. Shapiro and M. B. Wilk, "An analysis of variance test for normality (complete samples)", *Biometrika*, vol. 52, no. 3/4, pp. 591–611, 1965, ISSN: 00063444 (cit. on p. 33).

[90] N. M. Razali, Y. B. Wah, *et al.*, "Power comparisons of shapiro-wilk, kolmogorov-smirnov, lilliefors and anderson-darling tests", *Journal of statistical modeling and analytics*, vol. 2, no. 1, pp. 21–33, 2011 (cit. on p. 33).

[91] H. Levene, *Robust tests for equality of variances*, 1960 (cit. on p. 33).

[92] W. F. Guthrie, *Nist/sematech e-handbook of statistical methods (nist handbook 151)*, 2020. DOI: 10.18434/M32189 (cit. on pp. 34, 35).

[93] H. B. Mann and D. R. Whitney, "On a test of whether one of two random variables is stochastically larger than the other", *The Annals of Mathematical Statistics*, vol. 18, no. 1, pp. 50–60, Mar. 1947. DOI: 10.1214/aoms/1177730491 (cit. on p. 35).

[94] A. Hart, "Mann-whitney test is not just a test of medians: Differences in spread can be important", *BMJ*, vol. 323, no. 7309, pp. 391–393, Aug. 2001. DOI: 10.1136/bmj.323.7309.391 (cit. on p. 35).

[95] R. F. Woolson, "Wilcoxon signed-rank test", Sep. 2008. DOI: 10.1002/9780471462422.eoct979 (cit. on p. 35).

[96] A. Schumann and K. Bär, *Autonomic aging: A dataset to quantify changes of cardiovascular autonomic function during healthy aging*, 2021. DOI: 10.13026/2HSY-T491. [Online]. Available: https://physionet.org/content/autonomic-aging-cardiovascular/1.0.0/ (cit. on pp. 36, 44).

[97] D. S. Baim, W. S. Colucci, E. S. Monrad, *et al.*, "Survival of patients with severe congestive heart failure treated with oral milrinone", *Journal of the American College of Cardiology*, vol. 7, no. 3, pp. 661–670, Mar. 1986. DOI: 10.1016/s0735-1097(86)80478-8 (cit. on p. 36).

[98] I. M. Irurzun, L. Garavaglia, M. M. Defeo, and J. Thomas Mailland, *Rr interval time series from healthy subjects*, 2021. DOI: 10.13026/51YD-D219. [Online]. Available: https://physionet.org/content/rr-interval-healthy-subjects/1.0.0/ (cit. on pp. 36, 82).

[99] P. Virtanen, R. Gommers, T. E. Oliphant, *et al.*, "SciPy 1.0: Fundamental Algorithms for Scientific Computing in Python", *Nature Methods*, vol. 17, pp. 261–272, 2020. DOI: 10.1038/s41592-019-0686-2 (cit. on p. 36).

[100] S. Seabold and J. Perktold, "Statsmodels: Econometric and statistical modeling with python", in *9th Python in Science Conference*, 2010 (cit. on p. 37).

[101] C. Xie, L. McCullum, A. Johnson, T. Pollard, B. Gow, and B. Moody, *Waveform database software package (wfdb) for python*, 2021. DOI: 10.13026/EGPF-2788. [Online]. Available: https://physionet.org/content/wfdb-python/3.4.1/ (cit. on p. 37).

[102] A. J. Demski and M. Llamedo Soria, "Ecg-kit a matlab toolbox for cardiovascular signal processing", *Journal of Open Research Software*, vol. 4, Apr. 2016. DOI: 10.5334/jors.86 (cit. on p. 37).

[103] J. Martinez, R. Almeida, S. Olmos, A. Rocha, and P. Laguna, "A wavelet-based ECG delineator: Evaluation on standard databases", *IEEE Transactions on Biomedical Engineering*, vol. 51, no. 4, pp. 570–581, Apr. 2004. DOI: 10.1109/tbme.2003.821031 (cit. on p. 37).

[104] A. U. Ferrari, A. Radaelli, and M. Centola, "Invited review: Aging and the cardiovascular system", *Journal of Applied Physiology*, vol. 95, no. 6, pp. 2591–2597, 2003. DOI: 10.1152/japplphysiol.00601.2003 (cit. on p. 42).

[105] D. M. Kaye and M. D. Esler, "Autonomic control of the aging heart", *Neuromolecular medicine*, vol. 10, no. 3, pp. 179–186, 2008. DOI: 10.1007/s12017-008-8034-1 (cit. on p. 42).

[106] C. H. Peters, E. J. Sharpe, and C. Proenza, "Cardiac pacemaker activity and aging", *Annual review of physiology*, vol. 82, pp. 21–43, 2020. DOI: 10.1146/annurev-physiol-021119-034453 (cit. on p. 42).

[107] S. M. F. 3rd, J. P. Naughton, and W. L. Haskell, "Physical activity and the prevention of coronary heart disease", *Annals of clinical research*, vol. 3, no. 6, pp. 404–432, 1971 (cit. on p. 42).

[108] I. Shiraishi, T. Takamatsu, T. Minamikawa, Z. Onouchi, and S. Fujita, "Quantitative histological analysis of the human sinoatrial node during growth and aging.", *Circulation*, vol. 85, no. 6, pp. 2176–2184, 1992. DOI: 10.1161/01.cir.85.6.2176 (cit. on p. 42).

[109] T. Shimazu, N. Tamura, and K. Shimazu, "Aging of the autonomic nervous system", *Nihon rinsho. Japanese journal of clinical medicine*, vol. 63, no. 6, pp. 973–977, 2005 (cit. on p. 42).

[110] K. D. Monahan, "Effect of aging on baroreflex function in humans", *American Journal of Physiology-Regulatory, Integrative and Comparative Physiology*, vol. 293, no. 1, R3–R12, 2007. DOI: 10.1152/ajpregu.00031.2007 (cit. on p. 42).

[111] C. M. Masi, L. C. Hawkley, E. M. Rickett, and J. T. Cacioppo, "Respiratory sinus arrhythmia and diseases of aging: Obesity, diabetes mellitus, and hypertension", vol. 74, no. 2, pp. 212–223, Feb. 2007. DOI: 10.1016/j.biopsycho.2006.07.006 (cit. on p. 42).

[112] R. E. De Meersman, "Aging as a modulator of respiratory sinus arrhythmia", *Journal of Gerontology*, vol. 48, no. 2, B74–B78, Mar. 1993. DOI: 10.1093/geronj/48.2.b74 (cit. on p. 42).

[113] M. Reardon and M. Malik, "Changes in heart rate variability with age", vol. 19, no. 11, pp. 1863–1866, Nov. 1996. DOI: 10.1111/j.1540-8159.1996.tb03241.x (cit. on p. 43).

[114] P. K. Stein, R. E. Kleiger, and J. N. Rottman, "Differing effects of age on heart rate variability in men and women", vol. 80, no. 3, pp. 302–305, Aug. 1997. DOI: 10.1016/s0002-9149(97)00350-0 (cit. on pp. 43, 62).

[115] K. Umetani, D. H. Singer, R. McCraty, and M. Atkinson, "Twenty-four hour time domain heart rate variability and heart rate: Relations to age and gender over nine decades", vol. 31, no. 3, pp. 593–601, Mar. 1998. DOI: 10.1016/s0735-1097(97)00554-8 (cit. on pp. 43, 62).

[116] L. M. Campana, R. L. Owens, G. D. Clifford, S. D. Pittman, and A. Malhotra, "Phase-rectified signal averaging as a sensitive index of autonomic changes with aging", vol. 108, no. 6, pp. 1668–1673, Jun. 2010. DOI: 10.1152/japplphysiol.00013.2010 (cit. on p. 44).

[117] E. Vanoli, P. B. Adamson, Ba-Lin, G. D. Pinna, R. Lazzara, and W. C. Orr, "Heart rate variability during specific sleep stages", *Circulation*, vol. 91, no. 7, pp. 1918–1922, Apr. 1995. DOI: 10.1161/01.cir.91.7.1918 (cit. on p. 62).

[118] S. Fleming, M. Thompson, R. Stevens, *et al.*, "Normal ranges of heart rate and respiratory rate in children from birth to 18 years of age: A systematic review of observational studies", *The Lancet*, vol. 377, no. 9770, pp. 1011–1018, Mar. 2011. DOI: 10.1016/s0140-6736(10)62226-x (cit. on p. 63).

[119] J. B. Strait and E. G. Lakatta, "Aging-associated cardiovascular changes and their relationship to heart failure", *Heart Failure Clinics*, vol. 8, no. 1, pp. 143–164, Jan. 2012. DOI: 10.1016/j.hfc.2011.08.011 (cit. on p. 64).

[120] A. Yazdanyar and A. B. Newman, "The burden of cardiovascular disease in the elderly: Morbidity, mortality, and costs", *Clinics in Geriatric Medicine*, vol. 25, no. 4, pp. 563–577, Nov. 2009. DOI: 10.1016/j.cger.2009.07.007 (cit. on p. 64).

[121] J. Kornej, C. S. Börschel, E. J. Benjamin, and R. B. Schnabel, "Epidemiology of atrial fibrillation in the 21st century", *Circulation Research*, vol. 127, no. 1, pp. 4–20, Jun. 2020. DOI: 10.1161/circresaha.120.316340 (cit. on p. 64).

[122] M. Zoni-Berisso, F. Lercari, T. Carazza, and S. Domenicucci, "Epidemiology of atrial fibrillation: European perspective", *Clinical Epidemiology*, p. 213, Jun. 2014. DOI: 10.2147/clep.s47385 (cit. on p. 64).

[123] S. Nattel, B. Burstein, and D. Dobrev, "Atrial remodeling and atrial fibrillation", *Circulation: Arrhythmia and Electrophysiology*, vol. 1, no. 1, pp. 62–73, Apr. 2008. DOI: 10.1161/circep.107.754564 (cit. on pp. 64, 65).

[124] S. Nattel, "New ideas about atrial fibrillation 50 years on", *Nature*, vol. 415, no. 6868, pp. 219–226, Jan. 2002. DOI: 10.1038/415219a (cit. on p. 64).

[125] P. Kirchhof, S. Benussi, D. Kotecha, *et al.*, "2016 ESC guidelines for the management of atrial fibrillation developed in collaboration with EACTS", *European Journal of Cardio-Thoracic Surgery*, vol. 50, no. 5, e1–e88, Sep. 2016. DOI: 10.1093/ejcts/ezw313 (cit. on p. 64).

[126] G. Y. Lip, L. Fauchier, S. B. Freedman, *et al.*, "Atrial fibrillation", *Nature Reviews Disease Primers*, vol. 2, pp. 1–26, 2016, ISSN: 2056676X. DOI: 10.1038/nrdp.2016.16 (cit. on pp. 64–66).

[127] L. Staerk, J. A. Sherer, D. Ko, E. J. Benjamin, and R. H. Helm, "Atrial Fibrillation: Epidemiology, Pathophysiology, Clinical Outcomes", *Circulation Research*, vol. 120, no. 9, pp. 1501–1517, 2017, ISSN: 15244571. DOI: 10.1161/CIRCRESAHA.117.309732 (cit. on p. 65).

[128] P. A. Wolf, T. R. Dawber, H. E. Thomas, and W. B. Kannel, "Epidemiologic assessment of chronic atrial fibrillation and risk of stroke", *Neurology*, vol. 28, no. 10, pp. 973–973, 1978, ISSN: 0028-3878. DOI: 10.1212/WNL.28.10.973 (cit. on p. 65).

[129] D. J. Wilber, C. Pappone, P. Neuzil, *et al.*, "Comparison of antiarrhythmic drug therapy and radiofrequency catheter ablation in patients with paroxysmal atrial fibrillation: A randomized controlled trial", *JAMA - Journal of the American Medical Association*, vol. 303, no. 4, pp. 333–340, 2010, ISSN: 00987484. DOI: 10.1001/jama.2009.2029 (cit. on p. 65).

[130] L. Y. Chen, M. K. Chung, L. A. Allen, *et al.*, "Atrial fibrillation burden: Moving beyond atrial fibrillation as a binary entity: A scientific statement from the american heart association", *Circulation*, vol. 137, no. 20, e623–e644, 2018. DOI: 10.1161/CIR.0000000000000568 (cit. on p. 65).

[131] K. T. Nguyen, E. Vittinghoff, T. A. Dewland, *et al.*, "Electrocardiographic predictors of incident atrial fibrillation", *The American Journal of Cardiology*, vol. 118, no. 5, pp. 714–719, Sep. 2016. DOI: 10.1016/j.amjcard.2016.06.008 (cit. on p. 65).

[132] D. Linz, A. D. Elliott, M. Hohl, *et al.*, "Role of autonomic nervous system in atrial fibrillation", vol. 287, pp. 181–188, Jul. 2019. DOI: 10.1016/j.ijcard.2018.11.091 (cit. on p. 66).

[133] O. F. Sharifov, V. V. Fedorov, G. G. Beloshapko, A. V. Glukhov, A. V. Yushmanova, and L. V. Rosenshtraukh, "Roles of adrenergic and cholinergic stimulation in spontaneous atrial fibrillation in dogs", vol. 43, no. 3, pp. 483–490, Feb. 2004. DOI: 10.1016/j.jacc.2003.09.030 (cit. on p. 66).

[134] N. Li, B. J. Hansen, T. A. Csepe, *et al.*, "Redundant and diverse intranodal pacemakers and conduction pathways protect the human sinoatrial node from failure", *Science Translational Medicine*, vol. 9, no. 400, pp. 1–27, 2017, ISSN: 19466242. DOI: 10.1126/scitranslmed.aam5607 (cit. on p. 66).

[135] S. K. Agarwal, F. L. Norby, E. A. Whitsel, *et al.*, "Cardiac Autonomic Dysfunction and Incidence of Atrial Fibrillation", *Journal of the American College of Cardiology*, vol. 69, no. 3, pp. 291–299, 2017, ISSN: 07351097. DOI: 10.1016/j.jacc.2016.10.059 (cit. on p. 66).

[136] M. Habibi, H. Chahal, P. Greenland, *et al.*, "Resting Heart Rate, Short-Term Heart Rate Variability and Incident Atrial Fibrillation (from the Multi-Ethnic Study of Atherosclerosis (MESA))", *American Journal of Cardiology*, 2019, ISSN: 18791913. DOI: 10.1016/j.amjcard.2019.08.025 (cit. on p. 66).

[137] D. Raman, F. Kaffashi, L. Y. Lui, *et al.*, "Polysomnographic Heart Rate Variability Indices and Atrial Ectopy Associated With Incident Atrial Fibrillation Risk in Older Community-Dwelling Men", *JACC: Clinical Electrophysiology*, vol. 3, no. 5, pp. 451–460, 2017, ISSN: 2405500X. DOI: 10.1016/j.jacep.2016.09.001 (cit. on p. 66).

[138] H. Mori, R. Kato, Y. Ikeda, *et al.*, "Analysis of the heart rate variability during cryoballoon ablation of atrial fibrillation", *Europace*, vol. 20, no. 8, pp. 1259–1267, 2018, ISSN: 15322092. DOI: 10.1093/europace/eux225 (cit. on p. 66).

[139] H. S. Friedman, "Heart rate variability in atrial fibrillation related to left atrial size", *American Journal of Cardiology*, vol. 93, no. 6, pp. 705–709, 2004, ISSN: 00029149. DOI: 10.1016/j.amjcard.2003.11.052 (cit. on p. 66).

[140] J. Perkiömäki, O. Ukkola, A. Kiviniemi, *et al.*, "Heart rate variability findings as a predictor of atrial fibrillation in middle-aged population", *Journal of Cardiovascular Electrophysiology*, vol. 25, no. 7, pp. 719–724, 2014, ISSN: 15408167. DOI: 10.1111/jce.12402 (cit. on p. 66).

[141] S. K. Agarwal, F. L. Norby, E. A. Whitsel, *et al.*, "Cardiac Autonomic Dysfunction and Incidence of Atrial Fibrillation: Results From 20 Years Follow-Up", *Journal of the American College of Cardiology*, vol. 69, no. 3, pp. 291–299, 2017, ISSN: 15583597. DOI: 10.1016/j.jacc.2016.10.059 (cit. on p. 66).

[142] Z. Chen, Y. Yang, C. Zou, *et al.*, "Low heart deceleration capacity imply higher atrial fibrillation-free rate after ablation", vol. 8, no. 1, Apr. 2018. DOI: 10.1038/s41598-018-23970-7 (cit. on p. 67).

[143] S. S. Virani, A. Alonso, E. J. Benjamin, *et al.*, "Heart disease and stroke statistics—2020 update: A report from the american heart association", *Circulation*, vol. 141, no. 9, Mar. 2020. DOI: 10.1161/cir.0000000000000757 (cit. on p. 73).

[144] J. P. Saul, Y. Arai, R. D. Berger, L. S. Lilly, W. S. Colucci, and R. J. Cohen, "Assessment of autonomic regulation in chronic congestive heart failure by heart rate spectral analysis", vol. 61, no. 15, pp. 1292–1299, Jun. 1988. DOI: 10.1016/0002-9149(88)91172-1 (cit. on p. 73).

[145] J. Nolan, A. D. Flapan, S. Capewell, T. M. MacDonald, J. M. Neilson, and D. J. Ewing, "Decreased cardiac parasympathetic activity in chronic heart failure and its relation to left ventricular function.", vol. 67, no. 6, pp. 482–485, Jun. 1992. DOI: 10.1136/hrt.67.6.482 (cit. on p. 73).

[146] G. Casolo, E. Balli, T. Taddei, J. Amuhasi, and C. Gori, "Decreased spontaneous heart rate variability in congestive heart failure", vol. 64, no. 18, pp. 1162–1167, Nov. 1989. DOI: 10.1016/0002-9149(89)90871-0 (cit. on p. 73).

[147] M. G. Kienzle, D. W. Ferguson, C. L. Birkett, G. A. Myers, W. J. Berg, and D. Mariano, "Clinical, hemodynamic and sympathetic neural correlates of heart rate variability in congestive heart failure", vol. 69, no. 8, pp. 761–767, Mar. 1992. DOI: 10.1016/0002-9149(92)90502-p (cit. on p. 73).

[148] P. F. Binkley, E. Nunziata, G. J. Haas, S. D. Nelson, and R. J. Cody, "Parasympathetic withdrawal is an integral component of autonomic imbalance in congestive heart failure: Demonstration in human subjects and verification in a paced canine model of ventricular failure", vol. 18, no. 2, pp. 464–472, Aug. 1991. DOI: 10.1016/0735-1097(91)90602-6 (cit. on p. 73).

[149] M. A. Woo, W. G. Stevenson, D. K. Moser, and H. R. Middlekauff, "Complex heart rate variability and serum norepinephrine levels in patients with advanced heart failure", vol. 23, no. 3, pp. 565–569, Mar. 1994. DOI: 10.1016/0735-1097(94)90737-4 (cit. on p. 74).

[150] P. Sanders, P. M. Kistler, J. B. Morton, S. J. Spence, and J. M. Kalman, "Remodeling of sinus node function in patients with congestive heart failure", vol. 110, no. 8, pp. 897–903, Aug. 2004. DOI: 10.1161/01.cir.0000139336.69955.ab (cit. on pp. 74, 79).

[151] J. Karin, M. Hirsch, and S. Akselrod, "An estimate of fetal autonomic state by spectral analysis of fetal heart rate fluctuations", vol. 34, no. 2, pp. 134–138, Aug. 1993. DOI: 10.1203/00006450-199308000-00005 (cit. on p. 80).

[152] S. W. Porges, *The polyvagal theory: neurophysiological foundations of emotions, attachment, communication, and self-regulation (Norton Series on Interpersonal Neurobiology)*. WW Norton & Company, 2011 (cit. on p. 80).

[153] P. M. Pereyra, W. Zhang, M. Schmidt, and L. E. Becker, "Development of myelinated and unmyelinated fibers of human vagus nerve during the first year of life", vol. 110, no. 1-2, pp. 107–113, Jul. 1992. DOI: 10.1016/0022-510x(92)90016-e (cit. on p. 80).

[154] J. L. Segar, "Ontogeny of the arterial and cardiopulmonary baroreflex during fetal and postnatal life", vol. 273, no. 2, R457–R471, Aug. 1997. DOI: 10.1152/ajpregu.1997.273.2.r457 (cit. on p. 80).

[155] C. M. J. Tan and A. J. Lewandowski, "The transitional heart: From early embryonic and fetal development to neonatal life", vol. 47, no. Suppl. 5, pp. 373–386, Sep. 2019. DOI: 10.1159/000501906 (cit. on pp. 80, 81).

[156] A. Sharma, S. Ford, and J. Calvert, "Adaptation for life: A review of neonatal physiology", vol. 15, no. 3, pp. 89–95, Mar. 2014. DOI: 10.1016/j.mpaic.2014.01.002 (cit. on pp. 80, 81).

[157] J. P. Finley and S. T. Nugent, "Heart rate variability in infants, children and young adults", vol. 51, no. 2, pp. 103–108, Feb. 1995. DOI: 10.1016/0165-1838(94)00117-3 (cit. on p. 81).

[158] M. Goto, M. Nagashima, R. Baba, *et al.*, "Analysis of heart rate variability demonstrates effects of development on vagal modulation of heart rate in healthy children", vol. 130, no. 5, pp. 725–729, May 1997. DOI: 10.1016/s0022-3476(97)80013-3 (cit. on p. 81).

[159] W. Bobkowski, M. E. Stefaniak, T. Krauze, *et al.*, "Measures of heart rate variability in 24-h ECGs depend on age but not gender of healthy children", vol. 8, May 2017. DOI: 10.3389/fphys.2017.00311 (cit. on p. 81).

[160] D. Cysarz, M. Linhard, F. Edelhäuser, *et al.*, "Unexpected course of nonlinear cardiac interbeat interval dynamics during childhood and adolescence", vol. 6, no. 5, M. Breakspear, Ed., e19400, May 2011. DOI: 10.1371/journal.pone.0019400 (cit. on p. 81).

[161] L. Garavaglia, D. Gulich, M. M. Defeo, J. T. Mailland, and I. M. Irurzun, "The effect of age on the heart rate variability of healthy subjects", vol. 16, no. 10, A. Barbuti, Ed., e0255894, Oct. 2021. DOI: 10.1371/journal.pone.0255894 (cit. on p. 81).

[162] S. Sharma, Arain, Mathur, *et al.*, "Maturation of the adolescent brain", *Neuropsychiatric Disease and Treatment*, p. 449, Apr. 2013. DOI: 10.2147/ndt.s39776 (cit. on p. 90).

[163] D. F. Dickinson, "The normal ECG in childhood and adolescence", *Heart*, vol. 91, no. 12, pp. 1626–1630, Dec. 2005. DOI: 10.1136/hrt.2004.057307 (cit. on p. 90).

[164] P. deChazal, M. O'Dwyer, and R. Reilly, "Automatic classification of heartbeats using ECG morphology and heartbeat interval features", *IEEE Transactions on Biomedical Engineering*, vol. 51, no. 7, pp. 1196–1206, Jul. 2004. DOI: 10.1109/tbme.2004.827359 (cit. on p. 102).

[165] J. Koenig and J. F. Thayer, "Sex differences in healthy human heart rate variability: A meta-analysis", *Neuroscience & Biobehavioral Reviews*, vol. 64, pp. 288–310, May 2016. DOI: 10.1016/j.neubiorev.2016.03.007 (cit. on p. 103).